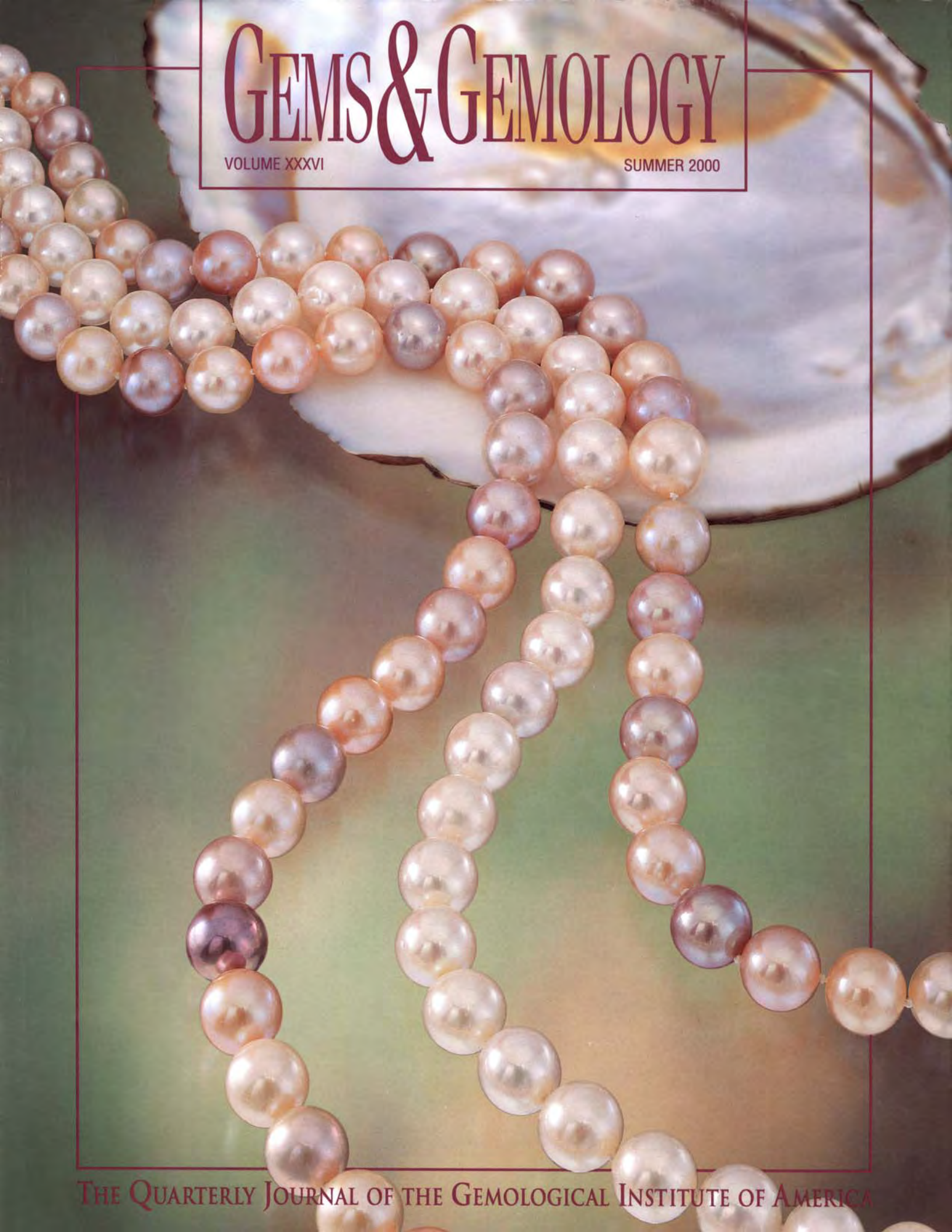

GEMS & GEMOLOGY

VOLUME XXXVI SUMMER 2000

THE QUARTERLY JOURNAL OF THE GEMOLOGICAL INSTITUTE OF AMERICA

GEMS & GEMOLOGY
SUMMER 2000 VOLUME 36 NO. 2


pg. 102


pg. 111

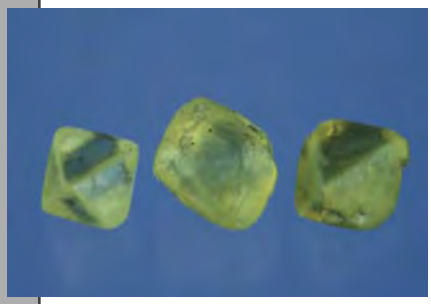
pg. 129

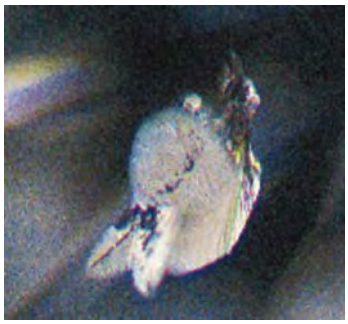
pg. 142

Not Invented Here

Earlier this year, we had an interesting discussion with some prospective authors. Their paper had just come back from review, and they were concerned that none of the reviewers understood what they wanted to achieve, as all of the comments related to what the reviewers felt was best for the *G&G* reader. In the course of our discussion, they asked a number of questions about the review system, our role as editors, their rights as authors, and our understanding of "what the reader wants."

I realized then that many knowledgeable members of the gemological community still do not understand the peer-review system or the critical role that a professional journal plays in the development of a science such as gemology. I'd like to take this opportunity to explain the peer-review system in general, *G&G*'s system in particular, and the benefits of peer review to the trade as well as to the academic community.

Peer review: Not invented here

The editorial peer-review system adopted by *G&G* in 1981 actually started hundreds of years ago. Its origins have been traced back to at least 1752, when the Royal Society of London established a "Committee on Papers" to review the articles submitted to *Philosophical Transactions*. Even before then, the concept of submitting papers or information for review by valued colleagues had become integral to the growth of scientific knowledge.

Today, virtually all respected scientific journals have some form of peer-review system, and all legitimate branches of science have a peer-reviewed journal through which research and other developments are presented. At GIA in 1981, Richard Liddicoat and the Board of Governors felt strongly that the only way gemology could move forward as a science was to have a well-respected, peer-reviewed journal. The integrity of the jewelry trade—just like the integrity of medicine, law, and other professions—requires a firm basis in the professional literature.

What does this mean for the gemologist?

This means that you, the reader, may not always get the literary style that you prefer, and authors may not get to say quite as much as they would like, but the science and the trade will get the information they *need*. Every *G&G* manuscript is sent to at least three members of the Editorial Review Board or other subject specialists for evaluation. On the basis of these reviews, the editorial staff makes a decision as to whether the paper should be accepted outright, revised, or rejected. Often, revised articles are sent for re-review. Although the decision of the editors is final, in almost all cases it is consistent with the consensus of the reviewers. And what do the reviewers look for? Originality of the information. A thorough understanding of previous work on the topic. Accuracy of the scientific method. Soundness of the results and discussion. Appropriateness of the article for the *G&G* audience.

As is the case with most scientific journals, *G&G* does not pay reviewers or authors. Serving as a referee is considered a professional obligation by some, a privilege by others. For example, a diamantaire who was asked to review a recent treatment article said that, as busy as he was, he felt he must do it. His business had benefited so much from articles such as the ones on fluorescence and "cut" in diamonds that he wanted to reciprocate.

The members of our Editorial Review Board come from prominent universities, such as Harvard and the California Institute of Techology in the U.S., as well as from leading gemological laboratories. Others are prominent researchers in their own right. Their recommendations are not always popular with authors, but they invariably result in a better article, a stronger contribution to the literature in a scientific field that—in many respects—is still in its infancy. Rather than "censor" the content of the articles, the reviewers ensure that the research conducted and data provided are of the highest quality.

With few exceptions, articles for *G&G* are not solicited. We do make every effort, though, to provide a variety of articles with information you need to function effectively as a laboratory gemologist, a gem dealer, a retailer, a scientist, an appraiser—in this rapidly evolving field. Not just any information, but well- researched, thoroughly evaluated information. It is not always perfect. In time, it may change. Yet only by constant questioning and testing, can a science move forward, the advances of each researcher building on the foundations laid earlier by their colleagues.

Likewise, only by accepting the need for, and results of, the scientific method can an industry operate effectively and efficiently in today's world. By replacing rumor and innuendo with fact and proof, scientific journals provide a measure of integrity and confidence that cannot be purchased at any price.

Alice S. Keller
EDITOR, akeller@gia.edu

LETTERS

New Spectral Evidence for GE POL Diamond Detection

We have read with interest the article titled "Spectroscopic Evidence of GE POL HPHT-Treated Natural Type IIa Diamonds," by David Fisher and Raymond Spits from De Beers, in the Spring 2000 issue of *Gems & Gemology*. We congratulate the authors on this excellent work.

This letter is to advise your readers that our team has reached both comparable and complementary results to those of Fisher and Spits. The SSEF Swiss Gemmological Institute is using a Renishaw Raman microspectrometer operated with an argon-ion 514.5 nm laser in conjunction with a cryogenic sample stage. While our preliminary results published in *Revue de Gemmologie* (No. 138/139, 1999, pp. 2–11) and *Journal of Gemmology* (Vol. 27, No. 2, 2000, pp. 73–78) were based on room-temperature Raman measurements, we now have analyzed 21 GE POL diamonds and 31 untreated type IIa diamonds at liquid nitrogen temperature. Our results confirm the criterion based on the ratio of 637/575 nm luminescence proposed by Fisher and Spits.

We introduce here a new and related criterion that, when combined with the 637/575 ratio, can be used to further confirm the identification of GE POL diamonds. It is based on the shape of the 637 nm peak in type IIa diamonds: The *full width at half maximum* (FWHM; figure 1) of this peak is at or below 11 cm^{-1} in untreated diamonds, while that of GE POL diamonds is at or above 13 cm^{-1} (figure 2), as determined by J.-P. Chalain using a standard computer program. This criterion was applicable for 20 of the 21 GE POL samples and 21 of the 31 untreated diamonds; the remaining stones did not show any 637 nm peak. The FWHM of the peak is a measure of the residual strain in the diamonds, and the implication of this difference is that the HPHT processing increases the strain slightly (A. T. Collins, pers. comm., 2000).

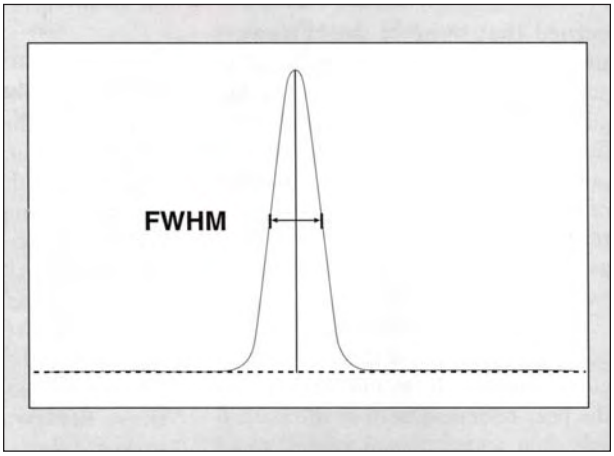

Figure 1. The full width at half maximum (FWHM) of a peak is the measurement of its width at a position equal to half its height. For the current photoluminescence study, FWHM is expressed in cm^{-1}.

Figure 2. The FWHM of the 637 nm luminescence peak measured at liquid nitrogen temperature is at or above 13 cm^{-1} in GE POL diamonds, while that of untreated type IIa diamonds (both colorless and brown) is at or below 11 cm^{-1}.

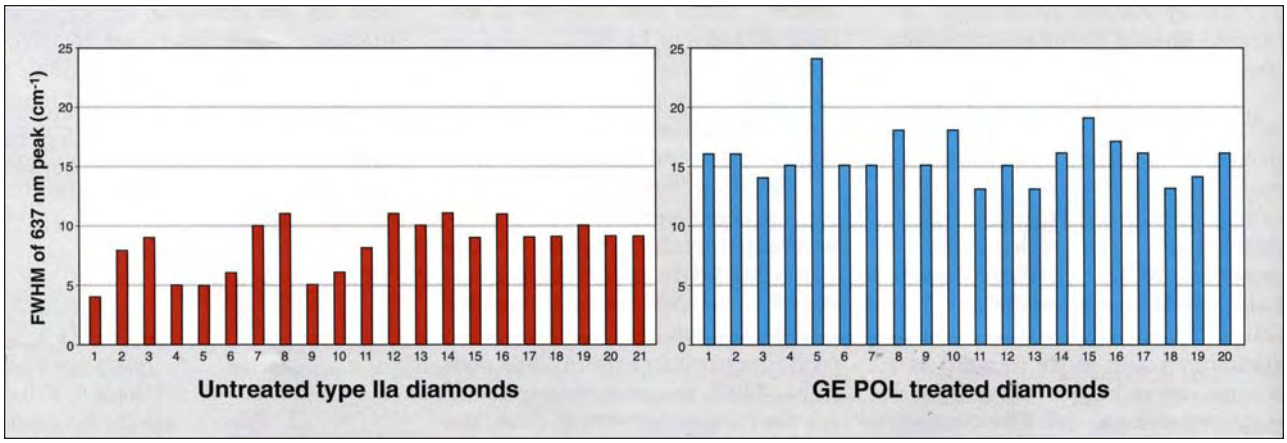

We feel that these results, together with further spectroscopic features, confirm the ability of a well-equipped gemological laboratory to identify GE POL diamonds.

Dr. H. A. Hänni, FGA
Professor, University of Basel, Director of SSEF
J.-P. Chalain, DUG
Director of SSEF Diamond Department
Dr. E. Fritsch
Professor, University of Nantes

What Is "Natural"?

On reading the article on emerald enhancement in the Winter 1999 issue (by S. F. McClure, T. M. Moses, M. Tannous, and J. I. Koivula, pp. 176–185), I was horrified to see the statement "Conclusion . . . NATURAL EMERALD" on the new GIA Gem Trade Laboratory "Emerald Report." This statement, printed in bold lettering, is misleading, contradicts information in finer print, and damages credibility.

A "reasonable person" may have no knowledge about gem treatments, but will believe she understands what is meant by a *natural* item. To the public, the declaration of an item as natural means that the condition of the object is as natural as the object's origin.

If the question arises as to whether a lady's hair is natural, the issue is not just whether it grew on her (or any other human's) head, but whether the curls and/or the color are artificially altered. Everyone understands that cutting a lady's hair does not preclude it from being termed *natural* because cutting of hair, to make it easier to wear and to show it to best advantage, is entirely expected. It is also expected that most gems will be cut to make them easier to wear and show them to their best advantage, so cut gemstones can be called "natural" if they are not treated.

Wording that distracts attention from treatment with the excuse of emphasizing the origin of the untreated raw material—which is no longer untreated, so does not qualify as natural—is misleading even if done innocently. At worst it could be deliberate misrepresentation.

Of course the word *natural* can correctly apply in a more limited way when it is referring to a particular characteristic of an object, rather than to the object itself. An example would be the natural origin of a ruby that has been heat treated. This should not be called "natural ruby" because it is only one aspect that is natural, not the entire stone.

Appropriate identification statements for items that are not completely natural in origin and condition would include: "heat treated ruby, natural origin," "clarity enhanced emerald, natural origin," and "cultured black pearl, natural color."

Richard H. Cartier, FGA, FCGmA
Toronto, Ontario, Canada
richardcartier@home.com

In Reply

Although Mr. Cartier has raised some interesting points, we feel his interpretation of the word *natural* is too strict.

The wording of the conclusions on Identification Reports (e.g., "Natural Ruby. Evidence of heat treatment is present.") has been used for decades at the GIA Gem Trade Laboratory, and I believe similar wording is used by most major labs that issue identification reports on gem materials. We have had very few comments, if any, regarding the interpretation of the conclusions on the hundreds of thousands of Identification Reports we have issued over the years. We know that many of these Reports end up in the hands of consumers, also with virtually no confusion.

GIA's fundamental mission for nearly seven decades has been to educate jewelers and to provide gemological research in support of our industry—ultimately protecting the consumer. We would not compromise these beliefs with misleading conclusions on our Laboratory Reports.

Thomas M. Moses
GIA Gem Trade Laboratory
New York

Photo Enhancement?

The photographs by Maha Tannous in the recent article on color-change garnets (K. Schmetzer and H.-J. Bernhardt, Winter 1999, pp. 196–201) are truly outstanding.

Besides merely solving the problem of different colored backgrounds resulting from the use of fluorescent and incandescent light sources—which has vexed all previous photographers—it was solved in a manner which duplicated every single reflection from every single facet.

Such an accomplishment truly deserves the accolades of all who have struggled with gemstone photography. I believe an explanation of the camera, film, and lighting techniques used to accomplish these data would surely be a contribution to gemology.

W. Wm. Hanneman, Ph.D.
Hanneman Gemological Instruments
Poulsbo, Washington

In Reply

Okay, Dr. Hanneman, you caught us—not the photographer, Ms. Tannous, but the *Gems & Gemology* staff. We did replace the color in the garnet image that we had for incandescent lighting to illustrate fluorescent lighting. Nor is this the first time we have modified an image to show our readers the *actual* color of the stone.

The problem is very basic: The cameras, films, lights, and processing equipment available cannot always capture the distinctive color of a gem material. For example, many synthetic emeralds routinely appear blue when photographed, regardless of who photographs them. We add

Continued on page 188

CHARACTERISTICS OF NUCLEI IN CHINESE FRESHWATER CULTURED PEARLS

By Kenneth Scarratt, Thomas M. Moses, and Shigeru Akamatsu

*There has been considerable debate in the gem trade concerning the nucleation procedures being used to grow large round Chinese freshwater cultured pearls (FWCPs). Of particular concern are claims that most of these cultured pearls are nucleated by reject mantle-tissue-nucleated FWCPs, and that such a product would be difficult to separate from normal tissue-nucleated cultured pearls and in some cases from natural pearls. However, field research indicates that many Chinese growers are currently using larger mussels (*Hyriopsis cumingi*), combined with new tissue-insertion techniques, to grow larger, better-shaped FWCPs. For this study, X-radiographs of approximately 41,000 Chinese freshwater cultured pearls from dozens of farms were examined, and 10 samples were sectioned. All showed evidence of mantle tissue nucleation only; the presence of a bead, whether shell or a tissue-nucleated FWCP, would be identifiable by distinctive features seen in the X-radiograph.*

ABOUT THE AUTHORS

Mr. Scarratt is laboratory director at the AGTA Gemological Testing Center, New York; Mr. Moses is vice president of Identification Services at the GIA Gem Trade Laboratory, New York; and Mr. Akamatsu is former manager of the Pearl Research Laboratory and currently general manager, Sales Promotion Department, at K. Mikimoto & Co. Ltd., Tokyo, Japan.

Please see acknowledgments at the end of the article.

Gems & Gemology, *Vol. 36, No. 2, pp. 98–109*

China is producing an estimated 600 to 1,000+ metric tons of freshwater cultured pearls (FWCPs) annually, of which totally round FWCPs larger than 8 mm represent a fraction of a percentage point ("China starts pearling revolution," 2000; Xie Shaohe, pers. comm., June 2000). Typically, Chinese FWCPs are tissue nucleated; that is, they are composed almost entirely of nacre, without the internal bead used to produce saltwater cultured pearls. However, since the appearance over the past several years of large (10+ mm) near-spherical freshwater cultured pearls from China, in a variety of colors (see cover and figure 1), the trade has been rife with rumors about how they are grown. Pearl dealers, industry authors, and some gemologists have suggested that the implant made to grow these cultured pearls is more than tissue alone.

Most recently, articles in the trade press (see, e.g., Matlins, 1999–2000a and b, 2000; Ward, 2000) have claimed that the vast majority of large FWCPs currently being described as "non-nucleated" *are* bead nucleated, with the largest sizes obtained by multiple insertions and reinsertions of nuclei formed from low-quality, all-nacre freshwater cultured pearls. The main concerns expressed in these publications have been that cultured pearls produced in such a manner require shorter growing times than are typically claimed for tissue-nucleated FWCPs, and that they are indistinguishable from normal tissue-nucleated cultured pearls—and in some cases from natural pearls—on X-radiographs. Similar claims about the reuse of tissue-nucleated FWCPs to produce large round FWCPs in China have also appeared in the professional literature (Rinaudo et al., 1999).

Matlins based her assertions on an examination of two Chinese FWCPs that had been sawn in half (A. Matlins, pers. comm., February 2000). However, neither these specific samples, nor descriptive photographs or X-radiographs of them, have yet been made publicly available. Ward's most

Figure 1. Attractive large, round Chinese freshwater cultured pearls have entered the gem market in recent years. These 9–10 mm Chinese mantle tissue–nucleated FWCPs are courtesy of Honora, New York. Photo © Harold & Erica Van Pelt.

recent analysis of the situation is based largely on his observations of changes in the Chinese product and on interviews with a number of pearl dealers (Ward, 2000). Following their introductory statements about the use of tissue-nucleated cultured pearls as nuclei in large round Chinese FWCPs, Rinaudo and her colleagues used a number of sophisticated techniques to study a strand of Chinese FWCPs. However, their paper does not present a clear conclusion with regard to the nucleation process determined for these samples.

The present study was conducted to address these issues and provide a better understanding of the identification of tissue-nucleated cultured pearls. Accordingly, this article: (1) reports on how Chinese FWCPs have been produced in the past, (2) describes new techniques being used to cultivate freshwater pearls in China, (3) investigates the possible use of rounded tissue-nucleated cultured pearls as the nuclei for Chinese FWCPs currently in the U.S. market, and (4) discusses whether such bead-nucleated cultured pearls could be identified nondestructively by X-radiography.

THE NUCLEATION OF FRESHWATER CULTURED PEARLS IN CHINA

Historical Background. Kunz and Stevenson (1908) reported that bead-nucleated freshwater cultured pearls were being produced in China at least as early as 1900, with cultured blister pearls widespread in the 13th century. We have seen samples of almost-whole Chinese FWCPs with shell bead nuclei that date back to the 18th century (figure 2). It is interesting to note that the bead nuclei shown in figure 2 were inserted into the mollusk together and connected by a fine thread. Carl V. Linne used a similar method in Sweden in 1761 (Webster, 1994), but he employed a "T" shaped metal holder to help keep the shell beads away from the shell itself in order to obtain near-whole cultured pearls (figure 3).

Commercial freshwater pearl cultivation in China, however, dates back only to the late 1960s and early 1970s, when tremendous quantities of small, irregularly shaped "rice" or "Rice Krispie" FWCPs entered the market. Although these "Rice Krispie" cultured pearls dominated Chinese production through the 1980s—in 1984, for example, 49

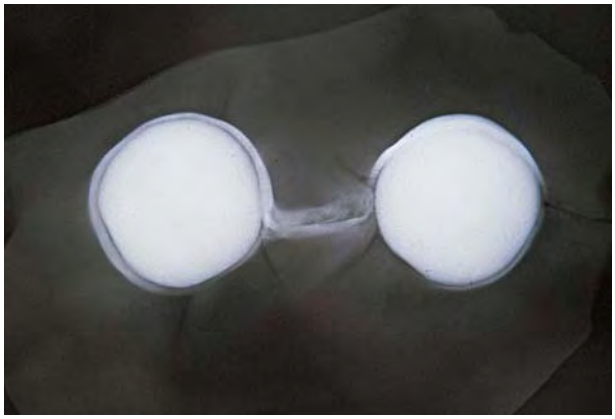

Figure 2. This X-radiograph shows two cultured pearls that were grown with a shell bead nucleus by the Chinese in the 18th century. The bead nuclei appear as opaque white spheres that are separated from the nacre overgrowth by a black line corresponding to an organic layer. Note the narrow nacre-coated thread that passes over the top of the bead on the right (inside the cultured pearl) and joins it to the cultured pearl on the left. Specimen recovered by Fred Woodwood from British Museum (Natural History) surplus.

tons were imported into Japan alone—eventually Chinese pearl farmers began to realize the importance of quality as well as quantity. Gradual changes in technology and, most importantly, in the mussel used, resulted in the production of greater quantities of larger and more lustrous round, near-round, and baroque cultured pearls in a variety of colors.

Figure 3. This X-radiograph of pearls cultured by Carl V. Linne in 1761 reveals two shell beads that are strung together with thread (as in the Chinese example in figure 2). The cultured pearls are separated from the shell surface by two T- shaped metal posts. In this manner, Linne produced cultured pearls that were almost entirely coated with nacre. Specimen loaned to Fred Woodwood by the Linaeus Society, London.

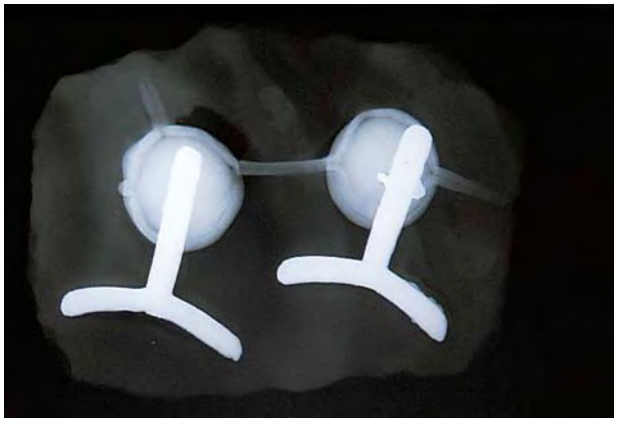

Current Practices. Saltwater cultured pearls are grown by the insertion of a bead with a piece of mantle tissue (to provide the epithelial cells that produce nacre) into the gonad of the oyster. However, Chinese "rice" pearls and their successors typically have been grown by nucleation with mantle tissue only in the mantle of the mussel.

Tissue Nucleation. The basic technique used today is similar to that described by Crowningshield (1962) for Japanese tissue-nucleated cultured pearls and observed by one of the authors (KS) in 1989 during a visit to a pearl-culturing farm in Yangxin, China, about 170 km southwest of Wuhan (Jobbins and Scarratt, 1990). At Yangxin, the parent mussel, then *Cristaria plicata*, was subjected to culturing when it reached 8 cm long. Some mussels were sacrificed for their mantle tissue: A strip (or graft) approximately 1.5 to 2 cm wide was taken from the outer edge of the mantle, and then sliced lengthwise and crosswise to make numerous pieces of flat tissue, each about 1 mm square (figure 4). At that time, 40 "squares" of tissue were inserted into the mantle of each host mussel, yielding 40 cultured pearls (figure 5). (Typically, only one bead is inserted into the gonad of a saltwater oyster.)

Co-author KS has identified three significant improvements made in the quality of the Chinese FWCP over the last several years: surface smoothness, roundness of shape, and size. The first, improving surface quality, was accomplished by changing from the *C. plicata* mussel (which, though abundant and easy to grow quickly, produces a cultured pearl with many wrinkles and other surface irregularities) to the *Hyriopsis cumingi* (figure 6). Also known as the "triangle mussel" (*san jiao bang* in Chinese) because of its shape, this mollusk yields a better product with a very smooth surface.

The second improvement, production of a more spherical cultured pearl, required the development of a new insertion technique. Although it is difficult to generalize about pearl culturing in China, because there are literally hundreds of small independent farms, one of the authors (SA) has observed a number of changes during his visits to Chinese pearl farms in recent years. One of these is the use of newly modified tissue. Some farms are using larger and thicker pieces of mantle tissue (about 4 mm × 4 mm) from sacrificed *H. cumingi* mollusks. They

Figure 4. The basic tissue-nucleation technique involves slicing a strip of mantle tissue into small squares (shown here on the glass slide below the left hand of the operator) and then carefully inserting them into the mantle of a mussel. This photo was taken at a pearl culturing farm in Yangxin, China, in 1989 by Kenneth Scarratt.

roll the tissue into a round shape and then place it in a mantle pocket, thus facilitating the cultivation of a round pearl. Mr. Yip of Evergreen Pearls Co. Ltd. has also stated (Sheung, 1999) that the new culturing techniques use fewer but larger ("the size of a soya bean") mantle-tissue nuclei.

The third improvement, in size, was accomplished with a longer cultivation period and the use of younger mussels. In the case of an 8 mm FWCP, at least six years are needed. When the pearl cultivator starts tissue nucleation with a larger mussel, it will grow too old to produce a large pearl during the cultivation period required. Therefore, many pearl farmers have changed to using younger (about one and a half years old) mussels as hosts. The FWCPs grow larger along with their hosts.

Another factor, though probably unintentional, in the greater size of the Chinese FWCPs is the move from one pearl farm to another during cultivation. It takes approximately two years to cultivate a 4 mm tissue-nucleated pearl and, as noted above, at least six years for one over 8 mm. In need of funds to pay double-digit interest rates, one farmer will sell his four-year-old, six-year-old, or even older

Figure 5. This C. plicata *mussel at the Yangxin farm yielded several near-spherical cultured pearls during the 1989 visit. Photo by Kenneth Scarratt.*

mussels to another farmer, who will move them to his lake or pond for further growth (and larger product). In some cases, the second farmer will resell them to a third. The change in environment (e.g., water temperature and water conditions) stimulates the mussels, causing them to secrete more nacre. The change in environments may also have some impact on the internal growth structure of these cultured pearls, such as changes in color from growth in one pond to growth in another.

Bead Nucleation. Although considerable research has been done into bead nucleation of freshwater cultured pearls in China, historically there have been difficulties with rejection of the bead (Crowningshield, 1962) and high mussel mortality.

Figure 6. The use of the Hyriopsis cumingi*, or "triangle," mussel by Chinese farmers in recent years has contributed to the cultivation of larger freshwater cultured pearls with better surface quality.*

Figure 7. These round Chinese freshwater cultured pearls are representative of the samples examined for this study. The largest white FWCPs shown are 10–11 mm in diameter. Photo by Elizabeth Schrader.

One of the authors (KS) observed first-hand the problems associated with bead nucleation of FWCPs at a pearl farm on the banks of Ho Tay in Hanoi, Vietnam, in 1992 (Bosshart et al., 1993). In the procedure used, a freshwater shell bead was implanted along with a piece of mantle tissue into the mantle of *C. plicata* mollusks. Although the success rate was said to be three nucleated, nacre-coated pearls out of every six to eight beads implanted, X-radiographs of 15 FWCPs obtained at the time of the visit revealed a bead nucleus in only two of the samples (see X-radiographs published in Bosshart et al., 1993). The remainder were grown from the tissue implanted at the same time as the bead (tissue nucleated), which indicates that the beads had been ejected early in the 18 to 24 month growth period.

In recent years, however, at least one large Chinese cultivator is said to have been successful with bead-nucleated freshwater pearls: Xie Shaohe of Shaohe Pearl in Chenghai, Guangdong Province ("China producing nucleated rounds," 1995; "China starts pearling revolution," 2000). In 1998, Doug Fiske of GIA Education visited one of Mr. Xie's pearl-culturing farms during the preparation of the new GIA Pearls course. He observed that, in three-year-old *H. Cumingi* mussels that measured about 12 cm (4.7 inches) from dorsal to ventral edge, nucleators inserted pieces of mantle tissue along with two to four round shell beads (up to 6 mm) in the mantle of each valve (D. Fiske, pers. comm., March 2000). Mr. Xie, a marine biologist, claimed that much of his early success was due to the development of exceptionally strong mussels and carefully choosing the size of the bead ("China producing nucleated rounds," 1995).

Mr. Xie was interviewed by Dr. Taijin Lu of GIA Research in late June 2000, at which time Mr. Xie confirmed that he was producing "a few hundred kilograms" annually of freshwater bead-nucleated cultured pearls, a very small portion of which are 10+ mm round FWCPs. He explained that approximately four to eight small shell beads (*not* reject tissue-nucleated FWCPs) are inserted into the outer (mantle) portion of the animal, with a single large (over 8 mm) bead inserted deep into the inner portion. The bead-culturing process takes approximately five to seven years: three to four years to grow the mussels, and two to three years to cultivate the pearls. The maximum size he produces is 14–15 mm. The nacre thickness ranges from 0.5–2.0 mm. The mortality of the mussel with bead nucleation continues to be a problem. Also, he estimates a bead rejection rate of about 20%, although James Peach of the United States Pearl Company feels the rejection rate for some bead nucleation operations could exceed 50% (pers. comm., 2000). In his conversation with Dr. Lu, Mr. Xie confirmed that most of his product was sold within China, although the largest, highest-quality pearls are distributed through a Hong Kong company, which we believe to be Man Sang Jewellery Company. Man Sang indicated that they do distribute "Shaohe pearls," but neither they nor Mr. Xie were able to provide any samples for our research.

MATERIALS AND METHODS

For this study, two of the authors (KS and TM) borrowed 791 strands (in traditional hank lengths) of Chinese FWCPs from the New York-based company Honora, which specializes in the Chinese product. These cultured pearls were represented to be recent production from dozens of farms in China. We also purchased two strands of 8 mm Chinese FWCPs, and individual larger samples, for possible destructive testing. In total, we examined approximately 41,000 Chinese-grown FWCPs. A variety of shapes and colors were included, in sizes ranging from 4 to 11 mm (see figure 7 and table 1). Thus, the samples included both the larger cultured pearls

that are claimed to be bead nucleated, and the smaller ones that could be used as nuclei. All were believed to be tissue nucleated.

We studied all of these samples by X-radiography, using the standard technique: First, the cultured pearls were placed in close contact with a fine-grained X-ray sensitive film and exposed to a beam of X-rays generated by a Faxitron X-ray unit for 20 to 30 seconds at 80 to 90 kV and 3 ma. Then the X-radiographs were examined at 10× magnification with various types of background lighting to ensure that no details were missed. Darker areas on X-radiographs represent greater exposure of the film to X-rays. In cultured pearls, such dark areas correspond to cavities or organic material, because these more easily allow passage of the X-rays than the crystalline aragonite or calcite of which the nacre is composed.

Ten Chinese FWCPs (8–12 mm) were sawn in half with a standard rotary gemstone saw. Each half was examined with a gemological microscope and various lighting techniques.

To supplement this research, KS and TM reviewed their previous records of pearls examined over the past 25 years, placing particular emphasis on those from the past six years.

TABLE 1. Chinese freshwater cultured pearls studied for this report.

	Number of strands	Size (mm)
	16	10–11
	2	8
	129	7–8
	81	6.5+
	56	6–6.5
	322	5.5–6
	187	4–4.5
Total:	793	

RESULTS

X-Radiography. Accurate interpretation of pearl X-radiographs requires considerable expertise. It is important to understand that while the image is two-dimensional, the structures seen actually occur at varying depths within the pearl. Several X-radiographs are commonly taken of a given sample to gain a three-dimensional "picture" of the interior from different angles. Therefore, we have used line drawings to illustrate some of the features seen in the X-radiographs.

The X-radiographs in figures 8–11 are typical of the Chinese FWCPs in our sample. The gray tube-like features that run through each sample and are aligned along the strand are drill holes. Also visible in each sample is a faint gray shadow that starts at the rim and diminishes in intensity as it approaches the center; these should be ignored, as they are aberrations of the printing process (they are not on the original X-radiographs). Relevant growth structures are discussed below and in the figure legends.

All tissue-nucleated cultured pearls contain a characteristic elongate cavity that appears dark in the X-radiographs (figure 8). This cavity, which

Figure 8. These X-radiographs of Chinese FWCPs (10–11 mm) show characteristics typical of tissue nucleation. On the left, large twisted cavities related to the original tissue implant are evident in the top row, second from left, and bottom row, center. In the image on the right, the original tissue implant is represented by ovoids. Note that the tissue-related cavity is not apparent in all of the FWCPs illustrated here, although all were found to have such a cavity. It is important to take several X-radiographs of pearls, from different directions and often at different exposures, to reveal the distinguishing features. A single strand may require seven or eight X-radiographs.

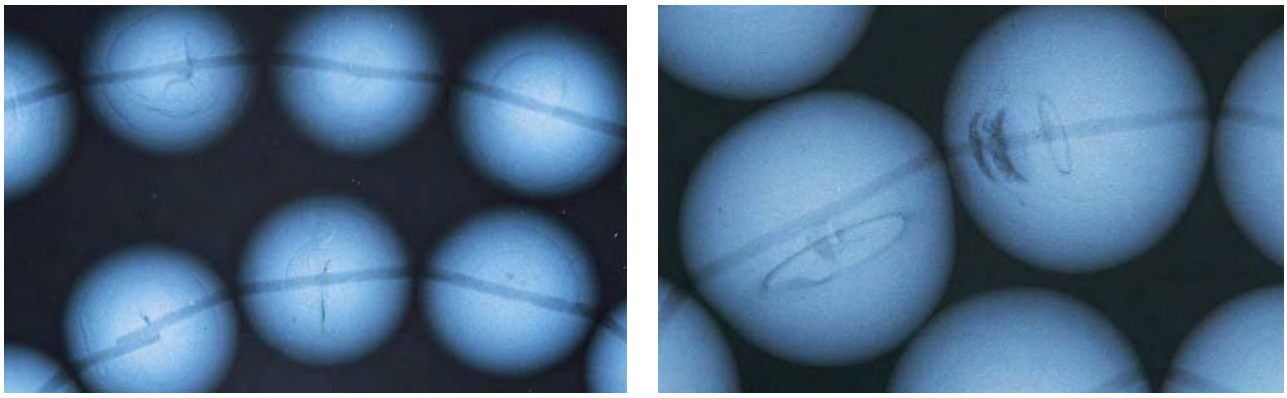

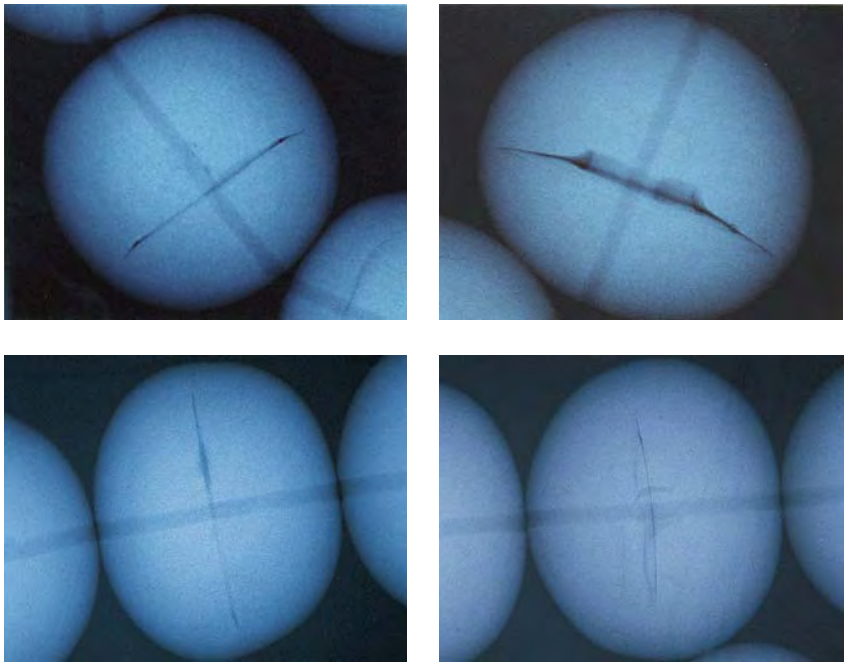

Figure 9. These X-radiographs of Chinese freshwater cultured pearls (10–11 mm) show a single dark line that relates to the tissue implant. Top left, the off-center implant line that crosses the FWCP on this X-radiograph takes up approximately 80% of the diameter of the entire sample. Top right, this off-center thick, dark implant line takes up approximately 90% of the sample's diameter. Bottom left, this centrally located implant line takes up 80%–90% of the diameter. Bottom right, the centrally located thick dark line takes up approximately 70% of the sample's diameter.

often has the appearance of an apple core, is related to the original tissue implant; it is typically, but not always, located at or near the center of the cultured pearl (figure 9). In some samples, it appears that two implants (i.e., tissue nuclei) are responsible for the growth of each cultured pearl (figure 10). Concentric growth structures, which also typically are seen in tissue-nucleated cultured pearls, are revealed by the presence of organic zones that are more transparent to X-rays than the adjacent crystalline zones (see, e.g., figure 11). Both the various types of implant structures and related organic zones are also illustrated in the line drawings shown in figure 12.

In more than 50% of the larger (7–11 mm) cultured pearls we examined, X-radiography revealed that the tissue-related structure occupied 60% to 99% of the host's diameter (see, e.g., figures 9 and 10), which contradicts the use of any kind of bead. The concentric growth structures—in this case having as a common core a line rather than a central point—appear to evolve from the core implant structure (see, in particular, figure 11).

For the most part, the cavities and other growth structures associated with the tissue implant in the larger samples were proportionately larger than those observed in the smaller (less than 6 mm) specimens. Importantly, none of the samples showed any growth features (such as a uniform organic layer surrounding a potential bead) that are indicative of a "bead" nucleus—whether a shell bead, a polished

Figure 10. The Chinese freshwater cultured pearls illustrated here all revealed a double implant structure on their X-radiographs. In the FWCP on the far left, the doubled tissue implants are revealed by two dark near-parallel lines. In the FWCP in the center, the tissue implants can be recognized by two dark ovoid structures; note that these implant-related structures take up at least 80% of the diameter of the sample. On the far right, the two dark lines relating to the tissue implants take up more than 90% of the sample's diameter.

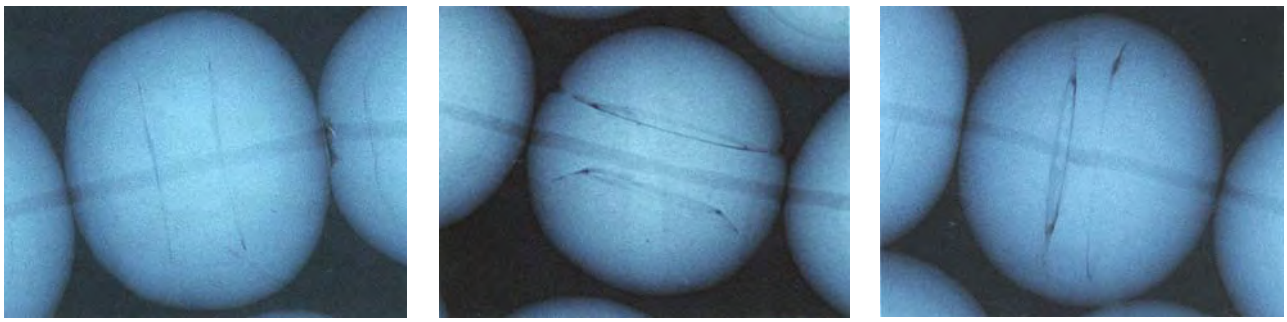

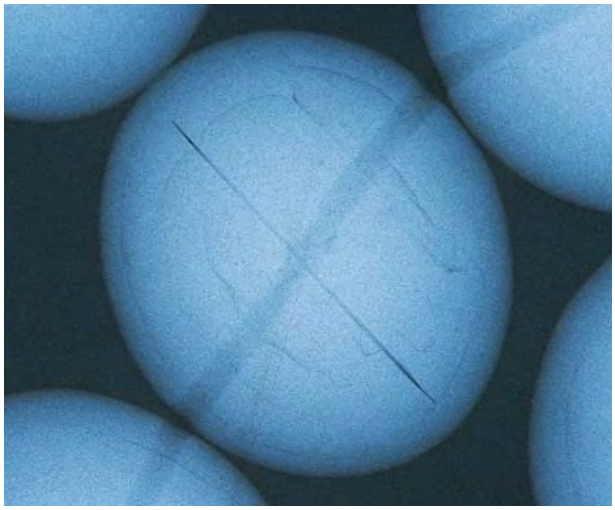

Figure 11. Concentric rings, related to the growth of this 10–11 mm Chinese FWCP, can be seen circling the elongate implant line in the center and a smaller implant "core" to the right. Note, however, that the central implant line takes up approximately 80% of the diameter of this FWCP, crossing some of the concentric lines, so the presence of a bead or cultured pearl nucleus would be impossible.

round tissue-nucleated cultured pearl, or an unfashioned tissue-nucleated cultured pearl.

Over the years, both KS and TM have recorded X-radiographs of cultured pearls with unusual nuclei. Some of these, because they are unlike almost any other samples we have examined, appear to be the result of experimentation by the growers. Figure 13 reveals a large saltwater cultured pearl that contains three nuclei: two shell beads and one tissue-nucleated cultured pearl. Note that the X-radiograph clearly shows an organic layer (revealed as a black line) that separates the tissue-nucleated cultured pearl from

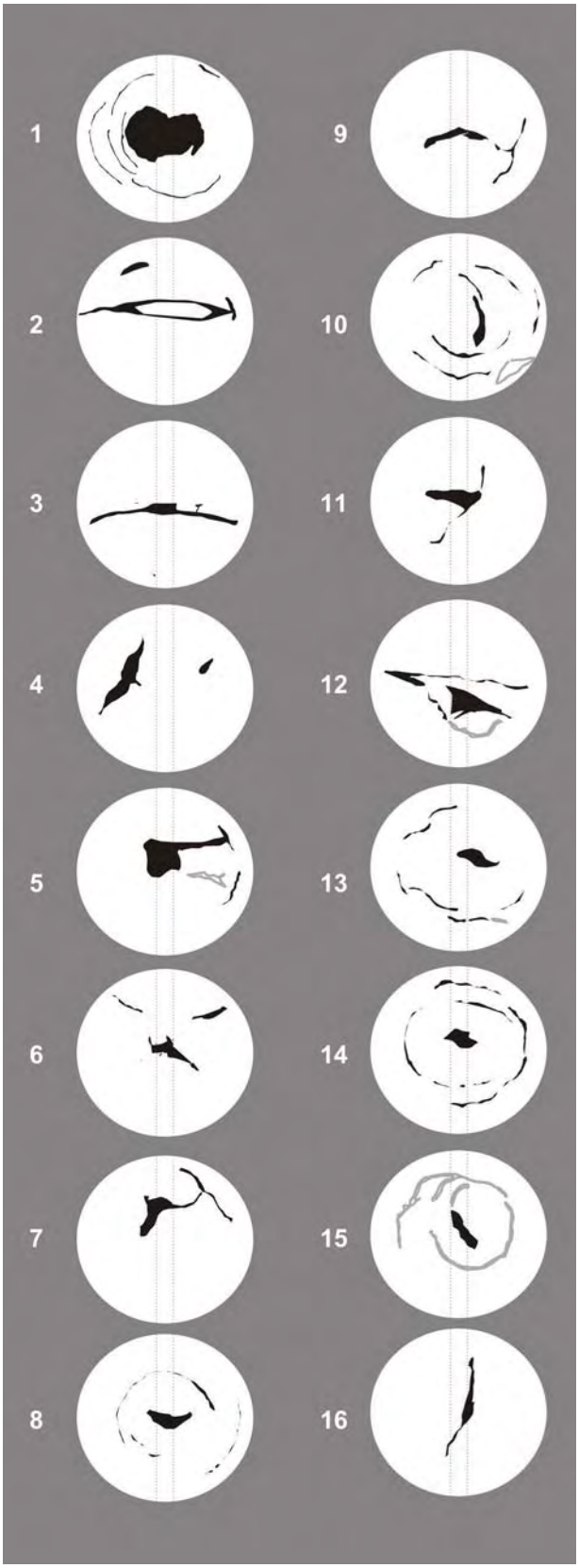

Figure 12. These line drawings illustrate details of the X-radiographic images that were recorded for some of the 10–11 mm Chinese FWCPs examined for this study. The various dark structures inside the white circles (which indicate the cultured pearls themselves) represent the normal cavities seen within tissue-nucleated cultured pearls and related "growth rings." Note that the implant-related cavities are very large in many instances (1, 2, 3, 4, 5, 7 on the left; 9, 11, 12, and 16 on the right); some are centrally located, whereas many are positioned off-center. There was no evidence of any form of bead in any of the cultured pearls examined for this study. Rather, it appears that large pieces of mantle tissue were used as the implants.

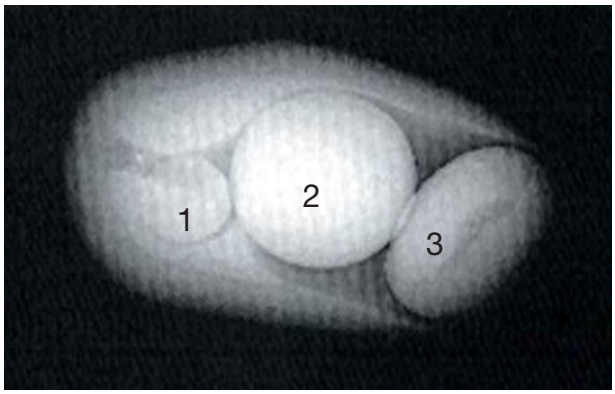

Figure 13. This X-radiograph shows an atypical single cultured pearl that has three solid nuclei: two shell beads (1 and 2) and one tissue-nucleated cultured pearl (3).

the cultured pearl overgrowth. In the Summer 1988 Lab Notes section of *Gems & Gemology*, Bob Crowningshield reported on the X-radiograph of a cultured pearl that had been nucleated with a wax bead. Most recently, in March 2000, one of the authors (TM) X-radiographed a necklace that revealed several unusual beads (figure 14). These examples represent what is only a small number of such cultured pearls that the authors have encountered in their laboratory experiences, and illustrate the effectiveness of radiography in identifying different kinds of nuclei.

Figure 14. The necklace shown in this X-radiograph revealed a variety of unusual features (bottom row, from the left): (1) a bead-nucleated cultured pearl, with the bead clearly visible at the bottom right and a large cavity evident to the left and above; (2) a cultured pearl in which the mollusk surrounded the bead with a large amount of organic matter that deteriorated and resulted in the bead becoming loose—multiple drill holes in the bead testify to the various attempts made to drill the cultured pearl; and (3) a cultured pearl with two bead nuclei, one (on the right) a normal shell bead (again showing multiple drill holes) and the other (on the left) a tissue-nucleated cultured pearl.

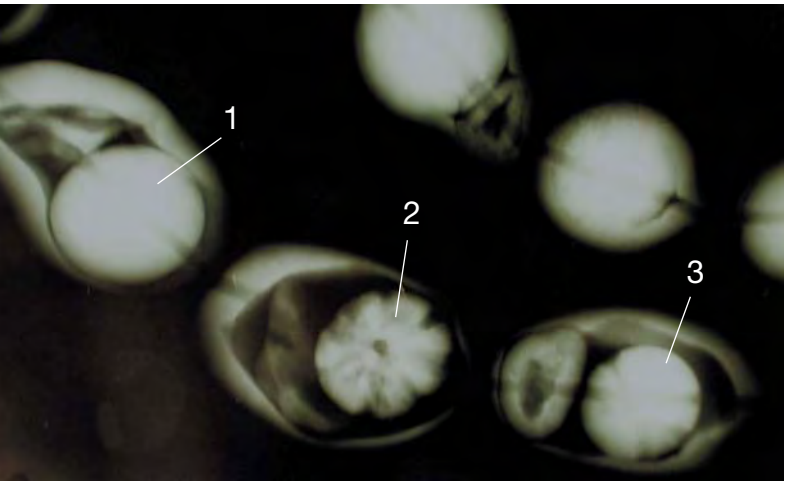

Sawn Chinese Freshwater Cultured Pearls. The sawn samples include one that measured approximately 12 mm (figure 15 left) and nine others that ranged from 8 to 10 mm (see, e.g., figure 15 right). In all cases, the growth structures observed were those normally expected for this kind of cultured pearl, that is, concentric, often randomly spaced ring arrangements. No signs of any kind of bead nucleation were seen. It is notable that only slight indications of a tissue implant cavity may be evident in sawn samples (see figures 15 and 16). This could be due to: (1) removal of the cavity by sawing through it, or (2) an off-center location of the cavity. Thus, there are distinct advantages to the different perspectives that can be achieved with X-radiography.

As with the interpretation of X-radiographs, the interpretation of growth structures in a sawn sample also requires caution. It is important to remember that some features in natural freshwater pearls can resemble those seen in Chinese freshwater cultured pearls, or those expected for cultured pearls nucleated by reject tissue-nucleated cultured pearls. See, for example, the thin sections of American natural freshwater pearls shown in figure 17, which were made by Basel Anderson during his original study of natural versus cultured pearls, probably in the 1930s. The freshwater pearl on the left in figure 17 shows a distinct color variation within its growth structure that might be misinterpreted as progressively larger tissue-nucleated FWCP "beads" (as described in Roskin, 2000, and Ward, 2000). The natural freshwater pearl in the center of figure 17 also contains growth features that could easily be misinterpreted as a "bead" implant: Some growth rings are continuous, while others are broken, and the outer portion is a different color and contains more organic matter than the inner section. The pearl on the far right in figure 17 reveals structures similar to those seen in many Chinese-grown tissue-nucleated FWCPs (especially those that don't show the tissue implant structures when sectioned). Note

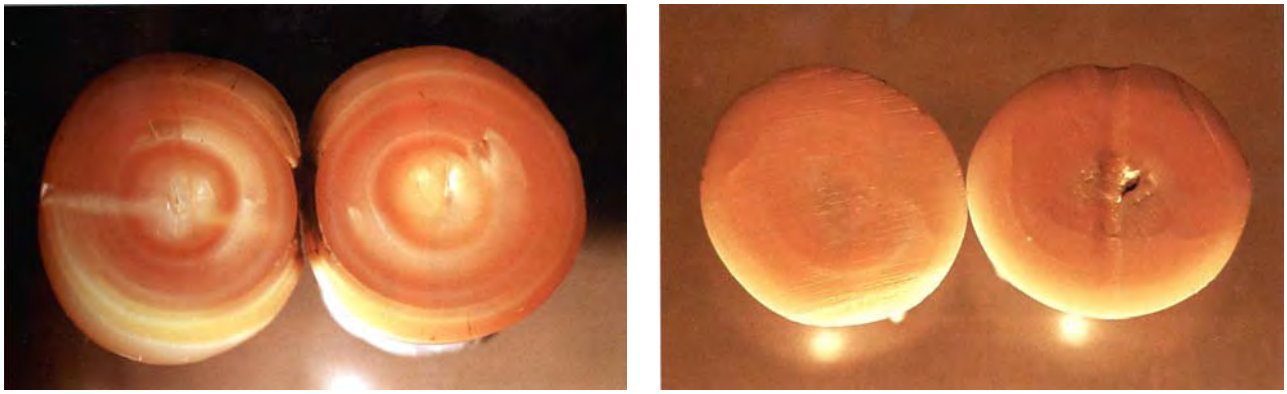

Figure 15. The concentric growth structures in these 12 mm (left) and 8.5 mm (right) Chinese FWCPs that have been sawn in two are entirely normal for tissue-nucleated freshwater cultured pearls. No indications of a solid nucleus of any type were seen. Photos by Kenneth Scarratt.

(e.g., at the 10 o'clock position) that certain growth "indentations" extend from the surface of the pearl to the point where the entire structure changes. Such indentations were seen running from the edge all the way to the center of some of the Chinese tissue-nucleated freshwater cultured pearls examined for this study.

DISCUSSION

The recent reports in the trade literature that tissue-nucleated freshwater cultured pearls are being used as "nuclei" to produce most of the recent large round Chinese FWCPs appear to be based on growth structures observed in pearls that have been cut in half (see, e.g., Matlins, 1999–2000a, 2000; Roskin, 2000; Ward, 2000). Specifically, Matlins (1999–2000a, p. 5) refers to the presence of "several different colorations of nacre rings, each different 'color zone' indicating where there has been a reinsertion."

In our experience, and again as illustrated in figure 17, *all* natural and cultured pearls have internal growth structures that correspond to periods of slower or interrupted growth, changes in the material being deposited (crystalline or organic), and/or resumption in growth. In particular, the growth structures shown in figure 17 (left) are similar to those described by Matlins.

Our research also contradicts the claims that nonspherical tissue-nucleated cultured pearls are polished into round nuclei and then inserted into freshwater mollusks as nuclei for most larger round FWCPs (see, e.g., Matlins, 2000; Ward, 2000). If, for example, an oval tissue-nucleated FWCP was polished to a round shape, the finished bead would exhibit surface banding where the nonspherical concentric growth layers are cross-cut by the polishing process (figure 18). Also, the internal growth structures of the bead would no longer align themselves with the exterior shape.

To test this idea, we polished several oval- and drop-shaped Chinese FWCPs into spheres. As expected, the concentric growth layers appeared as bands on the surface of the rounded beads (see figure 18C). If this polished bead were reinserted into another mollusk, the growth features seen in figure 18D should result and be readily apparent on an

Figure 16. In this sawn half of a known tissue-nucleated cultured pearl, note the slight dark line toward the center of the cross section. This is all that may be seen of the tissue implant when this type of cultured pearl is cut in half. X-radiography would have revealed more detail.

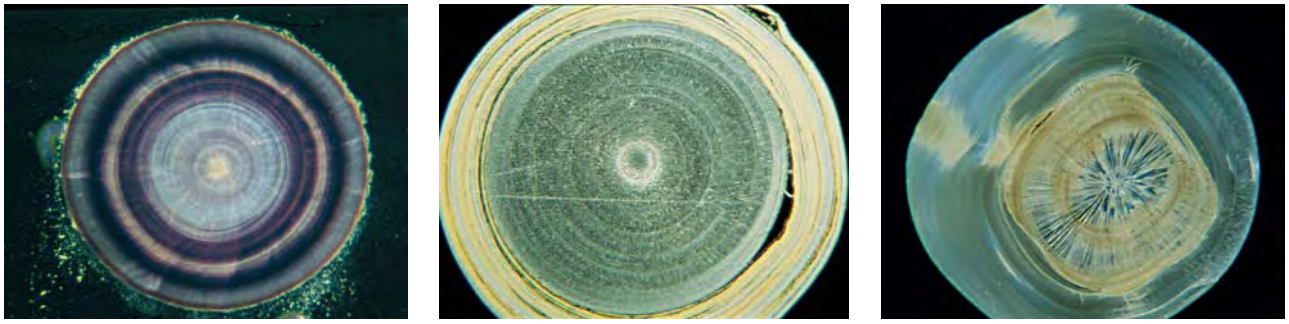

Figure 17. All three thin sections of American natural freshwater pearls show color variations and structural features related to changes in the aquatic environment as the pearls grew. Note especially the dramatic appearance of the central pearl, which could easily be interpreted as having a bead nucleus composed of another natural pearl, whereas the pearl on the left has an appearance similar to that described for FWCPs that reportedly have been nucleated with progressively larger tissue-nucleated cultured pearls. The structures in the thin section on the right are very similar to those observed in many Chinese FWCPs.

X-radiograph. Specifically, the internal growth structures of the cultured pearl nucleus would be misaligned with respect to one another and to the overgrowth, and they would not be concentric. Also, the tissue implant–related cavity would be small in relation to the fully grown (10–12 mm) cultured pearl. Moreover, the reinserted bead would have to be accompanied by a piece of tissue, and we found no evidence of this in any of the cultured pearls examined. Finally, a dark ring (corresponding to a thin organic layer) surrounding the "nucleus" would be expected.

None of the 41,000 Chinese FWCPs examined for this study, or any of those examined in the authors' laboratories over the past six years, revealed unusually small internal cavities together with misaligned or nonconcentric growth banding. As can be seen from figures 8–12, the growth structures normally recorded are concentric, or at least aligned with discernible abnormal growth that is related to other growth structures throughout the sample (e.g., the tissue-implant line). The authors have not examined any Chinese FWCPs that could have been grown by a production technique similar to that described by Matlins and Ward.

Rather, our observations are consistent with the new methods for tissue-nucleated freshwater pearl cultivation in China that were discussed in

Figure 18. (A) This line drawing shows a cross-section of an idealized oval tissue-nucleated freshwater cultured pearl. (B) If the idealized oval FWCP in "A" were to be made round, the inner circle scribed over the line drawing here would be the likely result, with growth features as illustrated in "C" (i.e., they would no longer be concentric with the outer surface). (D) If the rounded tissue-nucleated cultured pearl in "C" were to be inserted into a mollusk and further nacre was deposited, examination of the internal structure, either by radiography or by sectioning, would reveal the rounded tissue-nucleated FWCP in the center as having a structure alien to the overgrowth.

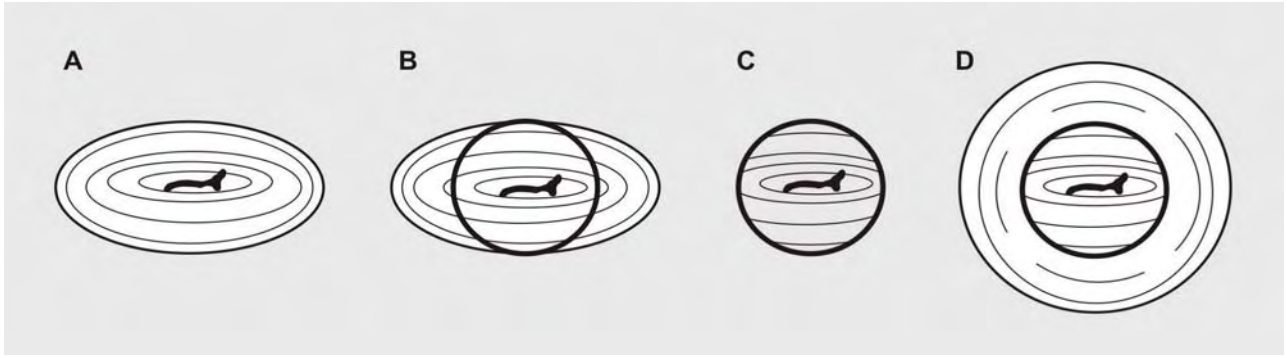

the "Current Practices" section above: For the most part, the cavities that correspond to the mantle tissue inserts are large relative to the pearls' cross sections, which suggests the use of larger implants in larger mussels. The fact that these large tissue-related structures are not always centrally located further rules out any form of bead nucleation.

CONCLUSIONS

Over the last six years, two of the authors (KS and TM) have examined a sizable number of large Chinese FWCPs, taken X-radiographs to study their internal growth characteristics, and even cut several specimens in half to examine the growth characteristics directly. At no time have they observed any evidence to suggest the nucleation process described by Matlins (2000) or Ward (2000). Similar examinations by gemologists in other leading laboratories have led to the same conclusion (H. Hänni, S. Kennedy, C. Smith, N. Sturman, and M. Superchi, pers. comms., February 2000). This is consistent with the experience of co-author SA, who has visited many Chinese pearl-culturing operations over the past few years, and communicated with several leading dealers. Indeed, all evidence points toward the predominance in the marketplace of a simple tissue-aided nucleation process to produce large, round FWCPs.

X-radiography of approximately 41,000 Chinese freshwater cultured pearls in the U.S. market revealed growth characteristics consistent with normal tissue-nucleated cultured pearls. In particular, the tissue-implant structure was large relative to the entire FWCP, not small as one would expect if a reject tissue-nucleated FWCP bead had been used. They are consistent with current tissue-nucleated pearl cultivation practices in China, that is, the use of larger mussels and larger, modified pieces of tissue to promote the growth of larger, rounder pearls. Microscopic examination of several large samples that were sawn in half confirmed the presence of concentric rings but no evidence of any type of bead.

Although it is known that there are commercial operations for the shell bead nucleation of FWCPs, and it is possible that some experimental Chinese FWCPs have been grown using beads of smaller freshwater cultured pearls, they are the exception rather than the rule. If such bead-nucleated cultured pearls became common in the future, they would be readily identifiable by routine X-radiography.

Acknowledgments: The authors gratefully acknowledge the input from colleagues at gemological laboratories around the world, including Dr. Margherita Superchi of CISGEM, Milan, Italy; George Bosshart and Christopher Smith of the Gübelin Gem Lab, Lucerne, Switzerland; Prof. Dr. Henry Hänni of the SSEF Gemmological Laboratory, Basel, Switzerland; Steven Kennedy of the Gemmological Association of Great Britain Gem Trade Laboratory, London; Nick Sturman of the Gems & Pearl Testing Laboratory of Bahrain; and Tay Thye Sun of the Far East Gem Lab, Singapore. Special thanks go to Joel Schechter of Honora, New York, for loaning the large number of cultured pearls used in this investigation, and to Fran Mastoloni of Frank Mastoloni Sons Inc., New York, for polishing the oval- and drop-shaped cultured pearls into round beads. We also thank Doug Fiske, Dr. Taijin Lu, and Akira Hyatt of GIA for their assistance. Maha Tannous of GIA is responsible for the photo reproduction of all the original X-radiographs.

REFERENCES

Bosshart G., Ho H., Jobbins E.A., Scarratt K. (1993) Freshwater pearl cultivation in Vietnam. *Journal of Gemmology*, Vol. 23, No. 6, pp. 326–332.

China producing nucleated rounds. (1995) *Jewellery News Asia*, No. 129, pp. 56, 58.

China starts pearling revolution (2000) *Jewellery News Asia*, No. 186, p. 62.

Crowningshield R. (1962) Fresh-water cultured pearls. *Gems & Gemology*, Vol. 10, No. 9, pp. 259–273.

Crowningshield R. (1988) Gem Trade Lab notes: A rare cultured pearl. *Gems & Gemology*, Vol. 24, No. 2, pp. 114–116.

The GIA *Pearls* course. (1999) Gemological Institute of America, Carlsbad, CA.

Jobbins E.A., Scarratt K. (1990) Some aspects of pearl production with particular reference to cultivation at Yangxin, China. *Journal of Gemmology*, Vol. 22, No. 1, pp. 3–15.

Kunz G.F, Stevenson C.H., (1908) *The Book of the Pearl*. The Century Co., New York.

Matlins A. (1999–2000a) Large Chinese freshwater cultured pearls. *Cornerstone, Journal of the Accredited Gemologists Association*, Winter, pp. 1, 3, 5.

Matlins A. (1999–2000b) Pearl treatments. *Pearl World*, December/ January–March, pp. 1–10.

Matlins A. (2000) Chinese freshwaters: The whole story. *Professional Jeweler*, Vol. 3, No. 2, p. 28.

Rinaudo C., Digennaro M.A., Navone R., Chatrain C. (1999) Investigations about the structure of freshwater cultured pearls, *Zeitschrift der Deutschen Gemmologischen Gesellschaft*, Vol. 48, No. 3, pp. 147–156.

Roskin G. (2000) Are freshwater Chinese pearls being misrepresented? *Jewelers Circular-Keystone*, Vol. 171, No. 3, March, pp. 36–37.

Sheung B. (1999) Chinese freshwater begins new era. *Jewellery News Asia*, No. 5, May 1999, pp. 92–99.

Ward F. (2000) China's amazing new pearls. *Lapidary Journal*, Vol. 54, No. 1, pp. 26–32.

Webster R. (1994) *Gems, Their Sources, Descriptions and Identification*, 5th ed. Rev. by P.G. Read, Butterworth-Heinemann, Oxford, England, 521 pp.

RUBY AND SAPPHIRE FROM JEGDALEK, AFGHANISTAN

By Gary W. Bowersox, Eugene E. Foord, Brendan M. Laurs,
James E. Shigley, and Christopher P. Smith

This study provides detailed mining and gemological information on the Jegdalek deposit, in east-central Afghanistan, which is hosted by elongate beds of corundum-bearing marble. Some facet-grade ruby has been recovered, but most of the material consists of semitransparent pink sapphire of cabochon or carving quality. The most common internal features are dense concentrations of healed and nonhealed fracture planes and lamellar twin planes. Color zoning is common, and calcite, apatite, zircon, mica, iron sulfide minerals, graphite, rutile, aluminum hydroxide, and other minerals are also present in some samples. Although the reserves appear to be large, future potential will depend on the establishment of a stable government and the introduction of modern mining and exploration techniques.

ABOUT THE AUTHORS

Mr. Bowersox (MrGary77@aol.com) is president of GeoVision, Inc., Honolulu, Hawaii, and has been active in Afghanistan since 1972. Dr. Foord (deceased) was a research geologist-mineralogist with the U.S. Geological Survey, Denver, Colorado. Mr. Laurs is senior editor of Gems & Gemology, *and Dr. Shigley is director of GIA Research, at GIA in Carlsbad, California. Mr. Smith (cps@gemkey.com) is director of the Gübelin Gem Lab, Lucerne, Switzerland.*

Please see acknowledgments at the end of the article.

Gems & Gemology, *Vol. 36, No. 2, pp. 110–126*

The gem mines of Afghanistan are some of the oldest in the world. The lapis lazuli mines at Sar-e-Sang, in the Badakhshan region, have been worked for at least 6,500 years (see, e.g., Wyart et al., 1981). Today, Afghanistan continues to be an important source of various gem minerals—including emerald, ruby, sapphire, aquamarine, tourmaline, and spodumene (see, e.g., Bowersox and Chamberlin, 1995). Yet relatively little is known about many of the gem localities.

This article reports on the only known source of ruby in Afghanistan: the Jegdalek region. A historical review, the geology, mining methods, and current production of gem corundum (figure 1) from Jegdalek are given below, together with the results of our research on the gemological properties of this material.

BACKGROUND

Although most of the records of the Ministry of Mines and Industry have been destroyed by the rocket attacks and bombs that have plagued Kabul since 1979, we were able to glean a fair amount of information from the literature. The geographic location of Afghanistan among several powerful neighbors (i.e., China, Iran, Pakistan, Uzbekistan, Tajikistan, and Turkmenistan; figure 2) has resulted in a long history of turmoil. Additionally, invasions by the Greeks (327 BC), Mongols (1227), British (1838–1919), and Russians (1979–1988), among others, destroyed and/or displaced portions of the Afghan population. However, these major invasions also influenced gem exploration and production, as gems were sought to trade for weapons. In addition, throughout history, Afghan mining areas have been the objects of tribal wars and banditry (see, e.g., Wood, 1841). In 1992, the senior author experienced nightly rocket attacks when he visited the ruby mining area.

The Jegdalek mines have been worked for more than 700 years. During the 1200s, wealthy Muhammadan merchants sold rubies to Kublai Khan and other famous historical fig-

Figure 1. Although the Jegdalek region of Aghanistan has produced ruby and sapphire for more than 700 years, relatively little is known about these deposits. The 32.22 ct ruby in this 18K gold pendant is from Jegdalek, as are the 0.94 ct ruby and 1.31 ct sapphire in the ring. The stones were carved by Bart Curren in the Glyptic Illusion style, and the jewelry was manufactured by Gregg Crawford; ring courtesy of Jewelry Box Antiques, Kansas City, Missouri. Photo © Harold & Erica Van Pelt.

ures. These merchants reportedly could tell the difference between ruby and spinel (Bretschneider, 1887). For most of the last 100 years, the mines were owned and operated sporadically by the Afghan government. Shortly after the 1979 invasion, the Soviets ran the Jegdalek mines for five to six months. Today, they are exploited solely by local tribal people year-round.

LOCATION AND ACCESS

The Jegdalek mines are located approximately 60 km (37 miles) east-southeast of Kabul, and can be reached by two routes from Kabul, in approximately four to six hours by four-wheel-drive vehicle (again, see figure 2). Jegdalek also can be reached from Jalalabad by two different routes of approximately eight hours each. However, the southern route has not been used for the last several years because of land mines. The route via Sorobi on the war-torn Kabul/Jalalabad road still can be negotiated by vehicle. At Sorobi, the road turns south onto a Jeep trail. As it approaches the mining area, the trail alternates between dirt track and streambed, which makes the drive very slow.

The coordinates of the Jegdalek mines are 34°26′N, 69°49′E (Orlov et al., 1974; Shareq et al., 1977). This was verified by the senior author, using a GPS (Ground Positioning System) instrument, during his survey in 1996. At that time, the deposit was being worked from 34°25′98″ N, 69°49′80″ E to 34°26′19″N, 69°49′08″E, at elevations ranging from 1,550 m (5,100 feet) to 2,000 m (6,550 feet).

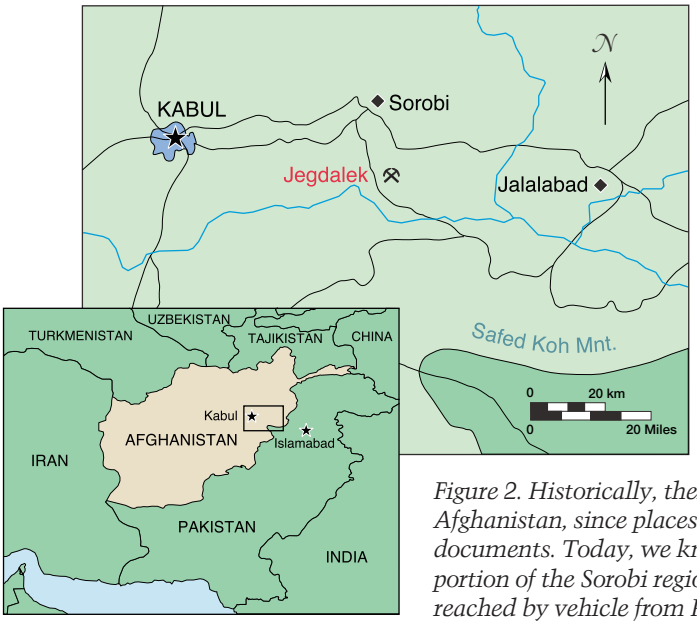

Figure 2. Historically, there was confusion over the location of the ruby deposits in Afghanistan, since places, names, and transliterations were gleaned from historical documents. Today, we know that the Jegdalek mining area is found in the southern portion of the Sorobi region, 60 km (37 miles) east of Kabul. The mines can be reached by vehicle from Kabul in about four to six hours.

REGIONAL GEOLOGY

The Jegdalek deposit is located within the continental collision zone between the Asian and

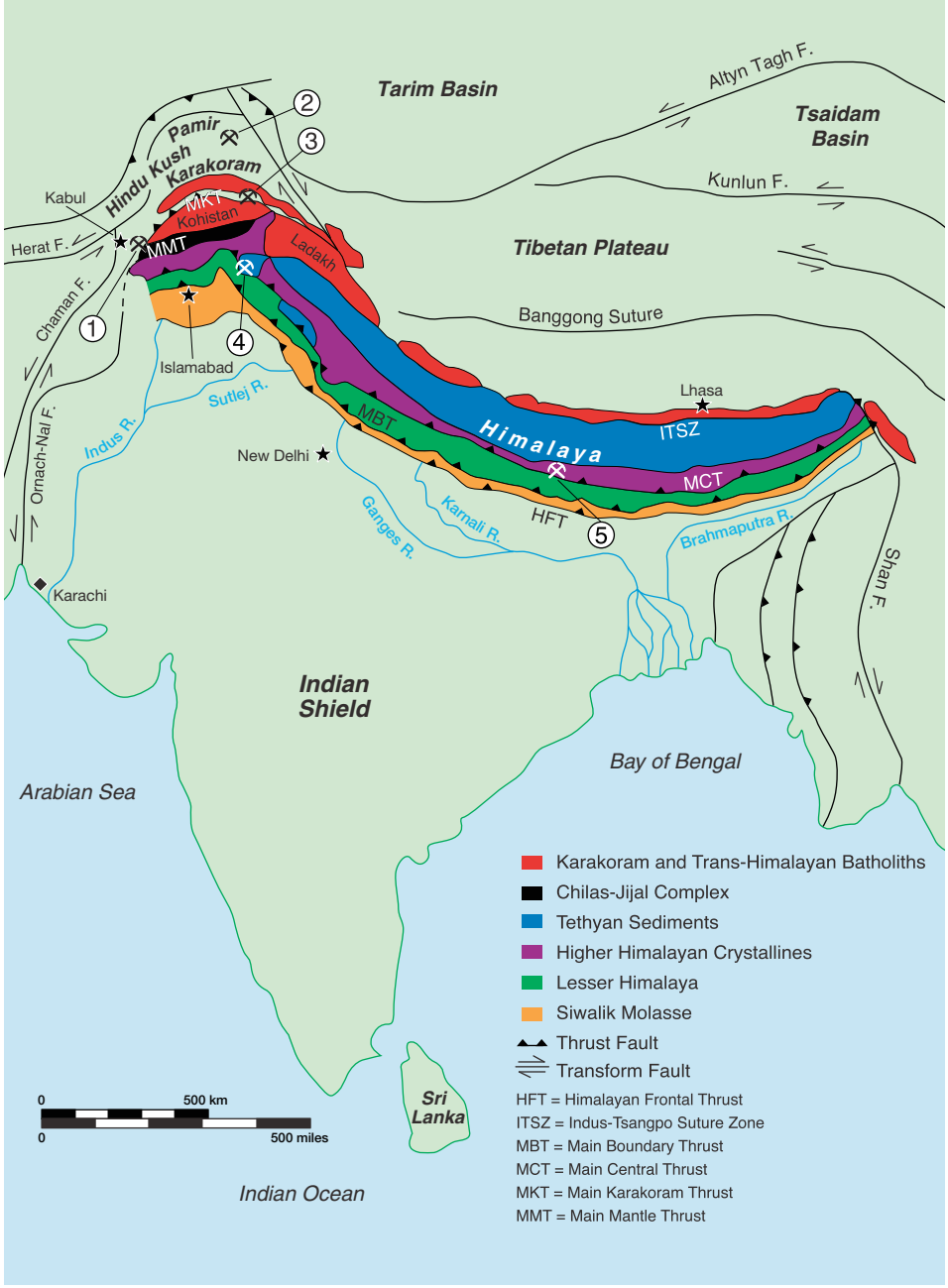

Figure 3. In South Asia, several marble-hosted ruby deposits are found within the continental collision zone between the Asian and Indian plates, including (1) Jegdalek; (2) Tajikistan; (3) Hunza, Pakistan; (4) Azad Kashmir; and (5) Nepal. Geology after Sorkhabi and Stump (1993); HFT = Himalayan Frontal Thrust, ITSZ = Indus-Tsangpo Suture Zone, MBT = Main Boundary Thrust, MCT = Main Central Thrust, MKT = Main Karakoram Thrust, and MMT = Main Mantle Thrust.

Indian plates (figure 3), in a regional geologic setting similar to that of other ruby deposits in South Asia (i.e., Tajikistan [Smith, 1998]; Hunza, Pakistan [Gübelin, 1982]; Azad Kashmir [Kane, 1997]; and Nepal [Smith et al., 1997]). These deposits are hosted by metamorphosed limestones (marbles) that were originally deposited along the margins of one or both of the two plates. Although the age of ruby formation at these deposits is unknown, their spatial association suggests that they are related to the regional metamorphism—and in some cases, the granitic magmatism—that accompanied the continental collision. The major collision between South Asia and the Indian subcontinent is estimated to have taken place 55–66 million years [m.y.] ago, although it may have begun as recently as 40 m.y. ago (Powell and Conaghan, 1973). Still ongoing today, the collision resulted in the formation of the Himalaya, Karakoram, Hindu Kush, and Pamir mountain ranges (again, see figure 3).

As stated by Kazmi (1989), three distinct geotectonic domains or terranes are recognized in Pakistan and the adjacent regions of Iran and Afghanistan. From south to north, they are (1) southern or Gondwanic, (2) central or Tethyan, and (3) northern or Eurasian. The Jegdalek deposits lie within the central (Tethyan) terrane, which is a complex assemblage of ophiolitic rocks, geosynclinal sediments, island arcs, and micro-continents that probably collided with the southern edge of Eurasia in the early Jurassic.

LOCAL GEOLOGY AND OCCURRENCE OF RUBY AND SAPPHIRE

The geology of the Jegdalek area has been described by Griesbach (1886, 1892), Barlow (1915), Orlov et al. (1974), and Rossovsky (1980). The rocks at the Jegdalek deposit are composed of interstratified Proterozoic gneisses and marbles (Nuristan series) that strike east-west. According to Rossovsky (1980), the marble is approximately 1,550–1,970 m.y. old.

The marble horizons range from 0.5 m up to 200–300 m (1.5 to 650–990 feet) thick and from several hundred meters to 7–8 km (4–5 miles) long (see, e.g., figure 4). The marbles are essentially pure calcite, with small amounts of magnesium impurities (0.68–4.78 wt.% MgO). The associated gneisses are composed of kyanite–amphibole–pyroxene, pyroxene–biotite, biotite–amphibole, and other assemblages. The gneisses and marbles are intruded by numerous dikes of granite and desilicated pegmatites of the Oligocene-age Laghman complex (about 30 m.y. old; Debon et al., 1987).

The Jegdalek deposit probably formed by regional metamorphism of the marble and gneiss, with local contact metasomatic effects from the intruded granitic rocks. The aluminum, magnesium, and chromium necessary for the development of ruby and associated minerals were likely present within the host marbles as impurities (e.g., clay minerals) that were concentrated as a result of chemical weathering before the marbles were metamorphosed (see, e.g., Okrusch et al., 1976).

Ruby and sapphire are mined from two separate zones of mineralized marble—north and south—which are separated from each other by a maximum of 600–800 m, and joined in the west. The vertical extent of the corundum mineralization is more than 400 m. Characteristic of the ruby-bearing marble is its coarse grain size. Ruby occurs in irregularly shaped lenses, rarely more than 2–3 cm wide, that are oriented lengthwise within individual horizons and beds of marble (Orlov et al., 1974).

MINING METHODS

In 1886, Griesbach wrote that there were about 300 men extracting rubies with hammer and chisel in the Jegdalek region. The senior author witnessed a similar mining situation in 1992, 1996, and 1998. Small-scale mining methods are used throughout the region. The gem-bearing marble is broken up with hammers, picks, prybars (figure 5), and, in a few cases, pneumatic drills (figure 6) and dynamite. The broken rock is lifted from the mine pits (see figure 7) by a simple pulley system. Some of this material is stacked nearby to form rudimentary shelters (figure 8). Within these shelters, the gem-quality ruby and sapphire crystals are separated from the marble for cutting.

About 20 mines at Jegdalek have been named, and there are many small unnamed diggings. Today, approximately 400 miners are active. Most work in

Figure 4. The senior author and miners are shown near the Jegdalek mining area. Several mine workings are visible along the mineralized marble belt that stretches eastward in the distance. Photo by Khudai Nazar Akbari.

Figure 5. Workers remove marble with prybars to uncover the gem corundum at Jegdalek. Most of the mining techniques used today are the same as those reported by Griesbach in 1892. Photo by Gary Bowersox.

Figure 6. Mining at Jegdalek is small scale. The only mechanized equipment consists of a few pneumatic hand drills. Photo by Gary Bowersox.

Figure 7. In 1996, the miners started new trenches on the western end of the Jegdalek deposit. These trenches follow the veins in an east-to-west direction. Photo by Gary Bowersox.

groups of five to six; groups of 15–20 miners operate the larger mines. This accounts for full employment of available workers, as most of the villagers have left the area because of tribal warfare. All miners share profits equally among the members of their group, after providing local military commanders with a commission of approximately 5%.

PRODUCTION AND DISTRIBUTION

Approximately 75% of the production is pink sapphire, 15% is ruby, 5% is mixed blue and red-to-pink corundum, and 5% is blue sapphire. Because it is commonly semitransparent, most of the material is fashioned into cabochons. Only about 3% of the corundum is facetable, but some very fine stones have been cut. The best-quality rubies are comparable in face-up appearance to the best found elsewhere. The largest crystal seen by the senior author weighed 174 ct (see figure 37 in Bowersox and Chamberlin, 1995); semitransparent rough typically ranges up to 1.5 to 3.0 cm. Good-quality rubies have been faceted up to 32 ct, but top-quality material rarely exceeds 5 ct. Well-crystallized material is often left in matrix and sold as mineral specimens (figure 9).

Most of the gem material is sold in Peshawar, Pakistan, and from there is sent to Karachi and New Delhi. Approximately 5% of the lower-grade goods are taken directly to India via Kabul and Dubai. This route is expected to increase in importance as more material is available. The finest-quality material typically goes directly to Europe from Afghan suppliers.

The miners have numerous independent distribution channels, so it is difficult to determine the quantity produced. The senior author estimates that about US$500,000 worth of gem corundum is mined annually from the Jegdalek deposit. While in Peshawar in 1999, the senior author viewed over 100,000 carats of rough rubies and sapphires, reportedly from Jegdalek, with an estimated wholesale value of nearly $1 million. The length of time over which this material was mined is unknown.

MATERIALS AND METHODS

All of the samples studied were collected by the senior author in Afghanistan, directly from the miners at the deposit, and therefore have not been heat treated. (This was confirmed by detailed

microscopic examination.) The polished samples (11 faceted stones and 26 cabochons, ranging from 0.51 to 16.50 ct) were cut from this material under the senior author's supervision. Also included in this study were numerous rough crystals, some of which were embedded in the marble host rock. This collection represented the full range of colors (tone and saturation, as well as hue) that the senior author has observed in ruby and sapphire from Jegdalek. On the basis of color, we defined three general groups: fancy-color sapphire (9), blue sapphire (1), and ruby (27).

We used standard gemological instruments to record the refractive indices, birefringence, optic character, pleochroism, optical absorption spectra (desk-model spectroscope), and reaction to long- and short-wave ultraviolet radiation (365 nm and 254 nm, respectively) on the 37 fashioned samples; specific gravity was determined hydrostatically. The internal features of all samples were studied with a binocular microscope and fiber-optic and other lighting techniques.

We used a Perkin Elmer Lambda 19 spectrophotometer, with a beam condenser and polarizing filters, for polarized spectroscopy in the UV-visible through near-infrared region (between 280 and 880 nm) on 11 samples. Infrared spectra were collected on 10 of the higher-quality fashioned samples with a Pye-Unicam Fourier-transform (FTIR) 9624 spectrometer in the region between 400 and 6000 cm^{-1}; a diffuse reflectance unit was used for sample measurement. Energy-dispersive X-ray fluorescence (EDXRF) chemical analyses were performed on all 37 fashioned samples using a Spectrace TN5000 system, with a proprietary program specially developed for the Gübelin Gem Lab by Prof. W. B. Stern for the semi-quantitative analysis of corundum. This software uses chemically pure element standards and three sets of operating conditions that focus on light, medium, and heavy elements, so that the measurements of trace elements can be interpreted to three decimal places; a beam condenser was used to measure small areas or zones of a stone. More extensive trace-element data were obtained for a medium-red ruby by means of inductively coupled plasma-atomic emission spectrometry (ICP–AES) at the U.S. Geological Survey in Denver, Colorado. The analysis was done by P. H. Briggs using a Thermo Jarrell Ash Model 1160 instrument, with an argon plasma generated at 1,250 W; 200 mg of sample was dissolved by the hydrogen peroxide sinter method.

Figure 8. Marble from the trenches is used to build shelters for the miners, where the corundum is sorted. Working conditions are better than in other mines in Afghanistan, as the ruby and sapphire mines are lower in altitude and accessible all year. Photo by Gary Bowersox.

To analyze the internal growth structures of all the semitransparent to transparent polished stones, one of the authors (CS) used a horizontal microscope, a specially designed stone holder, and a

Figure 9. Fine mineral specimens, such as this ruby in marble matrix, are occasionally produced from the Jegdalek mines. The larger crystal shown here is approximately 1 cm high. Courtesy of William Larson; photo by Jeff Scovil.

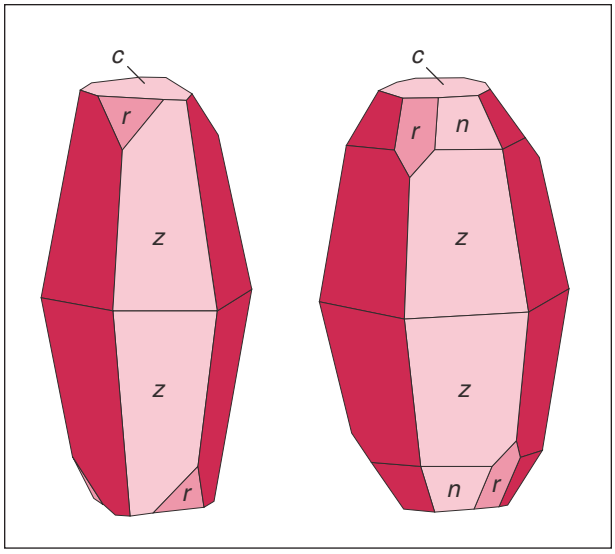

Figure 10. Two crystal habits are most typical in the rubies and sapphires from Jegdalek. The primary crystal form is dominated by dipyramidal z *(22$\bar{4}$1) faces, with subordinate basal pinacoid* c *(0001) and positive rhombohedral* r *(10$\bar{1}$1) faces. This crystal form was also modified by subordinate to intermediate dipyramidal* n *(22$\bar{4}$3) faces.*

Figure 11. These three ruby specimens show the appearance of corundum crystals from Jegdalek. The two smaller crystals are typical, whereas the longer crystal in the middle has relatively large pyramidal faces. Two sets of twinning lines parallel to r *{10$\bar{1}$1} are also visible in the largest crystal, which measures 2.0 cm long. Photo by Maha DeMaggio.*

mini-goniometer attached to one of the oculars on the microscope, employing the methods described by Schmetzer (1986a and b), Kiefert and Schmetzer (1991), and Smith (1996). For the identification of most mineral inclusions, we used a Renishaw 2000 laser Raman microspectrometer, with an argon laser source (514.5 nm), in the spectral range between 100 and 2000 cm^{-1}; other mineral inclusions were identified by X-ray diffraction analysis.

RESULTS

Crystal Morphology. Corundum from Jegdalek is typically subhedral, although some attractive euhedral crystals are found (figure 9; see also the cover of the Summer 1998 issue of *Gems & Gemology*). The smaller crystals (<2 ct) tend to be better formed, with

Figure 12. Cabochons of ruby and pink to pinkish violet sapphire from Jegdalek are cut in a range of colors, including some bicolored stones. These samples (3.38–6.28 ct) formed a portion of those examined for this study. The cabochons in the inset (3.12–15.51 ct) show the typical "pure" red color of Jegdalek rubies. Photos by Maha DeMaggio.

Figure 13. These faceted rubies and pink sapphires from Jegdalek weigh 0.68–1.25 ct. Photo by Jeff Scovil.

distinct crystal faces and sharp edges, whereas the external crystal forms of the larger crystals tend to be more heavily modified. Typically, there is little or no evidence of natural etching on the crystal faces. Two primary forms dominate the morphology of the Jegdalek corundum (figure 10; see also figure 11). Both consist of dipyramidal crystal habits composed of larger, dominant hexagonal dipyramidal *z* $(22\bar{4}1)$ faces and smaller, subordinate basal pinacoid *c* (0001) and positive rhombohedral *r* $(10\bar{1}1)$ faces. In the second primary form, the basic crystal habit *c*, *r*, *z* is modified by hexagonal dipyramidal n $(22\bar{4}3)$ faces. Much less frequently, we encountered crystal forms with dominant hexagonal dipyramidal ω $(14\ 14\ \bar{2}8\ 3)$ faces and subordinate *c*, *r,* and occasionally *n* faces.

Gemological Characteristics. *Visual Appearance.* The fancy-color sapphire samples commonly showed both blue and red/pink color zones, so the overall appearance ranged from bluish violet, through violet and purple, to reddish purple (see, e.g., figure 12). We examined only one sample of a "pure" blue sapphire (mounted in the ring shown in figure 1), which is consistent with the very small amount of cuttable blue sapphire seen at the mines. The rubies ranged from "pure" red to purplish red (see, e.g., figures 12 [inset] and 13); some also had blue zones (see Growth Characteristics below). Most of the fancy-color sapphires and rubies were medium to dark in tone, with variable weak to strong saturation. For the most part, the faceted stones were semitransparent to transparent, and the cabochons were semitransparent to translucent. Several of the samples also had translucent whitish areas, which microscopic examination indicated were remnants of the marble host rock (figure 14).

Physical Properties. The standard gemological properties (table 1) were consistent with corundum in general (see, e.g., Liddicoat, 1989; Webster, 1994) and with the rubies and fancy-color sapphires from Jegdalek described previously (e.g., Hughes, 1994).

Reaction to Ultraviolet Radiation. A range of fluorescence responses was noted according to the different colors. The fancy-color sapphires typically revealed a faint to medium red or orange-red fluorescence to long-wave UV. The distribution of the fluorescence was homogeneous in some samples and uneven in others. In addition, a few samples revealed zones of orange fluorescence. A chalky blue fluorescence also was noted in areas of those samples that still had some of the marble matrix. Similar but weaker reactions were observed with short-wave UV; a few of the stones were inert. The blue sapphire sample was inert to both long- and short-wave UV.

The rubies typically fluoresced an evenly distributed medium to strong red to long-wave UV, and faint to medium red to short-wave UV. The few

Figure 14. Translucent white masses were frequently encountered at the surface of the polished corundums in this study. These remnants of the marble host rock were typically composed of calcite, sometimes with apatite and/or margarite. Photomicrograph by Christopher P. Smith; magnified 25×.

TABLE 1. Gemological characteristics of the rubies and sapphires from Jegdalek, Afghanistan.

Property	Rubies (9)[a]	Fancy-color sapphires (27)	Blue sapphire (1)
Color	Red to purplish red	Ranges from bluish violet, through violet and purple, to reddish purple	Blue
Clarity (all groups)	Very clean to heavily included; most are moderately to heavily included		
Refractive index (all groups)	n_ε = 1.760–1.762 n_ω = 1.76–1.770 n = 1.76–1.77 (spot)		
Birefringence (all groups)	0.008 – 0.009		
Specific gravity (all groups)	3.97 – 3.99: typical range 3.73 – 3.96: contained carbonate impurities		
Pleochroism			
Parallel to the c axis	Reddish orange to orangy red	Mostly greenish blue, or bluish violet to purple	Greenish blue to blue
Perpendicular to the c-axis	Red-purple to purplish red	Mostly violet to purple, or purple-red to orangy red	Violet
UV fluorescence[b]			
Long-wave	Medium to strong red (blue zones are inert)	Faint to medium red or orange-red (+orange zones)	Inert
Short-wave	Faint to medium red (blue zones are inert)	Inert to very faint red (+orange zones)	Inert
Inclusions and internal growth features (all groups)	Numerous partially healed and nonhealed fracture planes with a frosted texture, lamellar twinning, color zoning, a variety of flake-like and stringer inclusion patterns, brush-stroke or nebulous inclusion patterns, very fine grained bluish white clouds, weak to moderate growth structures, negative crystals with tiny graphite platelets, clouds of short rutile needles, and crystalline inclusions of: mica, apatite, calcite, zircon, rutile, graphite, boehmite, pyrite, marcasite, and pyrrhotite.		
Visible absorption spectrum	General absorption up to approximately 450 nm 468 nm (sharp, narrow) 475 nm (sharp, weak to moderate) 476 nm (sharp, narrow) 525-585 nm (broad band, width dependent on Cr content) 659 nm (faint, narrow) 668 nm (faint, narrow) 675 nm (very faint, narrow when present) 692 nm (sharp, narrow) 694 nm (sharp, narrow)		Spectrum not taken

[a] *Number of samples shown in parentheses.*
[b] *Several stones additionally revealed a distinct chalky blue fluorescence to both long- and short-wave UV, due to the presence of marble matrix at the surface.*

samples with distinct blue color zones showed no fluorescence in those zones. Again, a chalky blue fluorescence was noted with both long- and short-wave UV in those samples that contained remnants of the marble matrix.

Specific Gravity. In general, the specific gravity of "pure" corundum is relatively constant, between 3.98 and 4.01. Twenty-eight of the fashioned samples had S.G. values near this range, between 3.97 and 3.99. The remaining nine samples had lower S.G. values, which were due to the presence of carbonate, either as mineral inclusions or as large areas of marble matrix that were not fully removed during cutting. Seven of these samples had S.G.'s between 3.91 and 3.96, whereas the two samples with the largest masses of marble matrix had S.G.'s of 3.86 and 3.73.

Growth Characteristics. *Twinning.* Most of the fancy-color sapphire and ruby samples revealed numerous lamellar twin planes parallel to two or three directions of the positive rhombohedron *r* $(10\bar{1}1)$; these are partially responsible for the low transparency. The better-quality samples typically had only one dominant system of twin planes parallel to *r*, whereas others also had a minor secondary system. The blue sapphire was not twinned.

Internal Growth Structures. Because of the high degree of twinning—and, in many cases, large number of inclusions—we could not observe internal growth structures in any of the translucent and most of the semitransparent samples studied. In a few of the semitransparent samples, and all the transparent stones, we did note weak to moderate growth structures: straight and angular sequences of the dipyramidal crystal faces *z* $(22\bar{4}1)$ or *n* $(22\bar{4}3)$ and the positive rhombohedron *r* $(10\bar{1}1)$, as illustrated in figure 15.

Color Zoning. We saw weak to distinct color zoning in many of our samples. The fancy-color sapphires typically had both blue and red/pink color zones. In this group, the two colors tended to blend, producing a rather even face-up coloration. In two of these samples, however, we noted narrow dark blue bands parallel to the positive rhombohedron *r* (figure 16). The blue sapphire was homogeneous in color.

Most of the rubies were homogeneous in color. However, a few stones revealed adjacent red and pink zones, which followed the internal growth structures. Several of the samples in this group also displayed

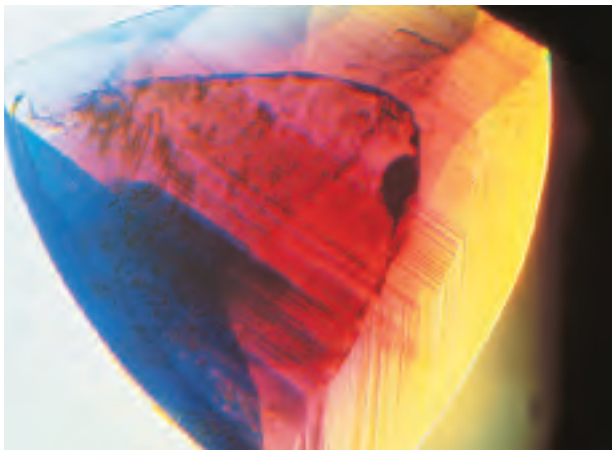

Figure 15. Weak to moderate planar and angular sequences of internal growth structures were noted in a few of the rubies from Jegdalek. These typically consisted of combinations of the dipyramids z *or* n*, as well as the positive rhombohedron* r*. In this sample, we see a combination of* z *growth planes. Photomicrograph by Christopher P. Smith; immersion, magnified 15×.*

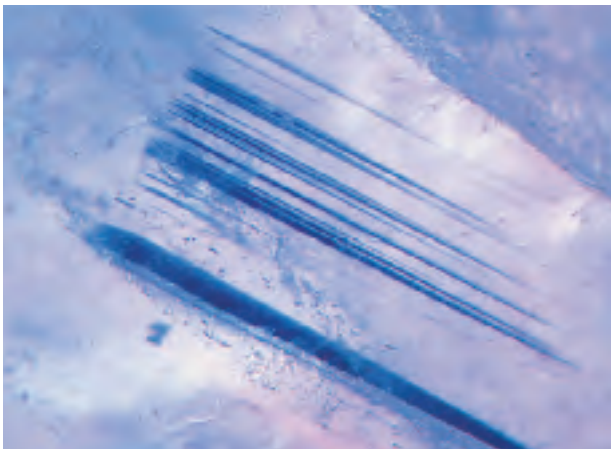

Figure 16. Sharply defined blue lamellar color zoning was seen in some of the corundum samples. Photomicrograph by John I. Koivula; magnified 15×.

zones of dark to medium blue, which stood in stark contrast to the surrounding ruby (figure 17). For the most part, these distinct blue zones tended to occur parallel to the positive rhombohedron *r*, although they were also noted following the growth banding parallel to the dipyramidal planes *n* and *z* (figure 18).

In general, these blue color zones tended to form narrow bands, although they also were observed as larger areas. Occasionally we noted distinct geometric formations, which resulted from the blue coloration following a sequence of dipyramidal and rhombohedral growth planes.

Inclusions. Dense concentrations of partially healed and nonhealed fracture planes, in addition to numerous twin planes, were responsible for the reduced transparency of many of the samples in this study. Many of the partially healed fracture planes revealed a distinctly "frosted" texture (figure 19), and a few had an orange-to-brown epigenetic staining.

A variety of mineral inclusions were noted;

Figure 17. Strong blue color zones were observed in many of the Jegdalek rubies. Also note the flake-like inclusions associated with the blue zones in this 1.19 ct sample. Photomicrograph by Christopher P. Smith; magnified 25×.

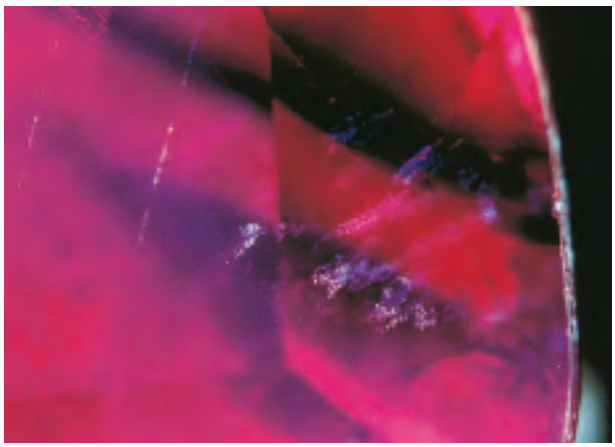

Figure 18. Typically the blue color zones corresponded to growth in certain crystallographic orientations—that is, along the r, n, *and* z *faces. The large blue color zone in this sample follows two positive rhombohedral and two dipyramidal growth planes. Photomicrograph by Christopher P. Smith; immersion, magnified 20×.*

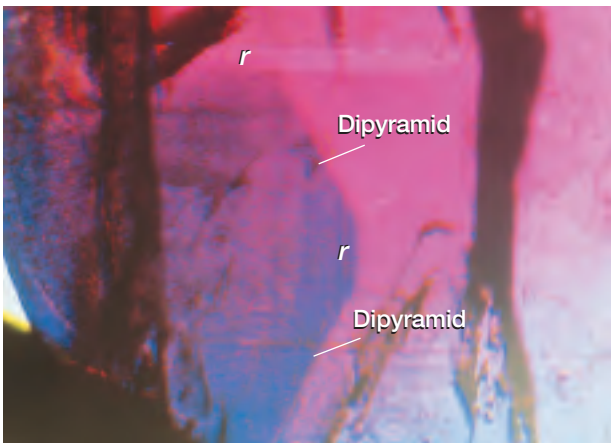

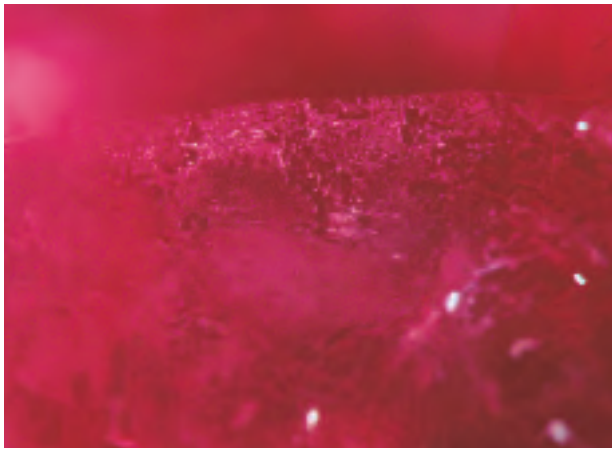

Figure 19. Most of the rubies and fancy-color sapphires in this study had a high concentration of partially healed fracture planes. One consistent feature of these planes was the distinctly "frosted" texture. Photomicrograph by Christopher P. Smith; magnified 50×.

transparent colorless to translucent white crystals of calcite were the most common (figure 20). Also present in some stones were transparent to translucent colorless crystals of apatite; most of these were rounded (figure 21), although some had a more prismatic habit. Some small transparent colorless rounded crystals proved to be zircon. Transparent colorless and translucent white masses at the surface of several polished samples were identified as calcite, apatite, margarite, or a combination of these three (again, see figure 14). Analytical testing was required to make these distinctions.

Iron sulfide minerals, such as pyrite, marcasite, and pyrrhotite, were present along fracture and twin planes (figure 22), although they were also seen rarely as isolated grains or masses (figure 23). Graphite frequently was observed as solitary geometric platelets, as well as clustered in groups. In addition, tiny graphite scales were noted in many of the multi-phase negative crystals that composed the healed fracture planes (figure 24). Transparent brown platelets of mica were occasionally noted in close association with calcite crystals. Very dark orange to black crystals of rutile could be seen isolated or in close proximity to apatite crystals (again, see figure 21). Rarely, very fine iridescent needles of rutile were concentrated in patches (figure 25). One intriguing inclusion was a colorless prismatic crystal, which could not be conclusively identified.

Among the more interesting internal features seen in some of the samples were a variety of flake-like inclusions and stringers that were very fine in some instances and rather coarse in others (figure 26). Similar types of inclusions had a more "brush-stroke" or "nebulous" patterning (figure 27). Observed in only a small number of samples was a very fine-grained bluish white zonal cloud that followed the development of the internal growth structures (figure 28).

Irregular "veins" of AlO(OH) (typically boehmite—see "Infrared Spectroscopy" below) were

Figure 20. Common to most marble-type deposits of corundum, transparent colorless rounded forms of calcite were identified in a number of the rubies and fancy-color sapphires from Jegdalek. In this ruby, the calcite formed a cluster of inclusions in a nearly parallel formation. Photomicrograph by Christopher P. Smith; magnified 60×.

Figure 21. Colorless, rounded, high-relief crystals of apatite and stubby, dark orange to black crystals of rutile were common inclusions in the Jegdalek corundum. Photomicrograph by John I. Koivula; magnified 20×.

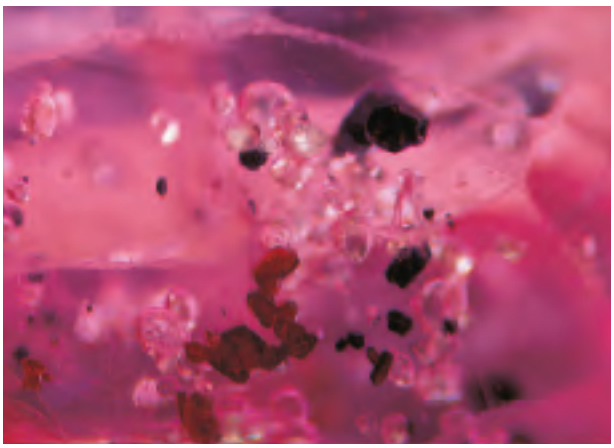

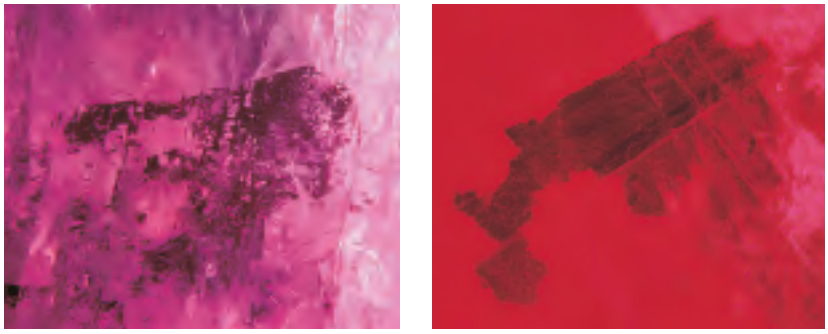

Figure 22. One distinctive inclusion feature in the rubies and fancy-color sapphires from Jegdalek consists of iron sulfide minerals such as pyrite, marcasite, and pyrrhotite that were present along healed fracture planes (left; magnified 20×) and parting planes (right; magnified 15×). Photomicrographs by Christopher P. Smith.

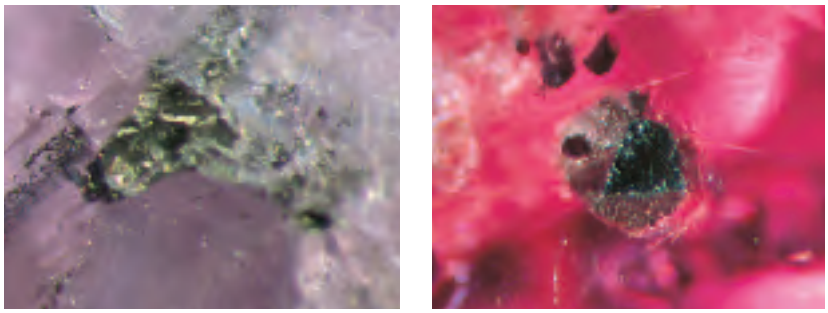

Figure 23. Pyrite formed irregular brassy masses in one of the sapphire samples (left); a surface-reaching grain of iron sulfide was also present in a ruby sample (right). Photomicrographs by John I. Koivula; both magnified 15×.

also noted traversing several of the polished gems. In reflected light, the reduced luster of these veins, as compared to the higher luster of the host corundum (figure 29), could be mistaken for the glass-like fillings observed in heat-treated rubies. Such inclusions are the result of an alteration process, where a retrograde metamorphic reaction alters the corundum, in the presence of water, to an aluminum hydroxide (Haas, 1972). These alteration products also formed needle-like inclusions that coated the surface of "intersection tubules" created at the junction of two twin planes and were seen lining the twin planes.

Figure 24. Tiny graphite platelets were commonly found within isomorphic negative crystals. Photomicrograph by Christopher P. Smith; magnified 80×.

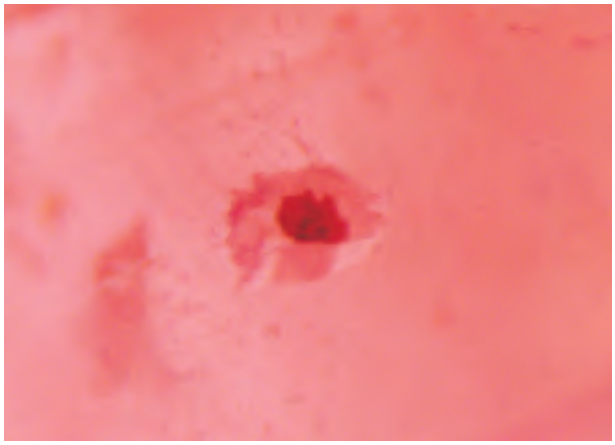

UV-Vis-NIR Spectroscopy. With a desk-model or handheld spectroscope, the following features were noted in the visible region for the fancy-color sapphires and rubies: general absorption up to approximately 450 nm, a broad band at 525–585 nm, and sharp lines at 468, 475, 476, 692, and 694 nm; faint lines were sometimes seen at 659, 668, and 675 nm (table 1). The UV–Vis–NIR polarized absorption

Figure 25. Rutile needles are not typical in rubies from Jegdalek, although very fine, short rutile needles were observed in two samples. Their appearance was markedly different from the long, iridescent rutile needles typically found in rubies from marble-type deposits, such as at Mogok, Myanmar. Photomicrograph by Christopher P. Smith; magnified 30×.

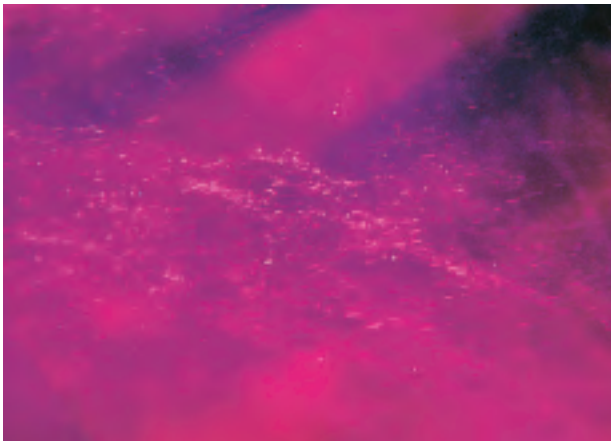

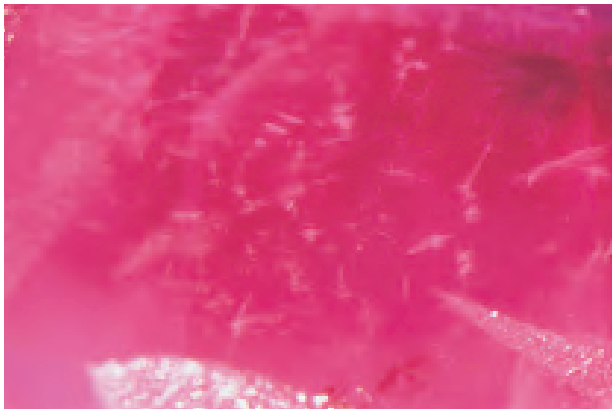

Figure 26. One of the more characteristic features of rubies from Jegdalek consists of flake-like inclusion patterns and stringers that were finely textured in some samples and coarser in others. Similar inclusion features may be found in rubies from Vietnam and Mong Hsu (Myanmar). Photomicrograph by Christopher P. Smith; magnified 35×.

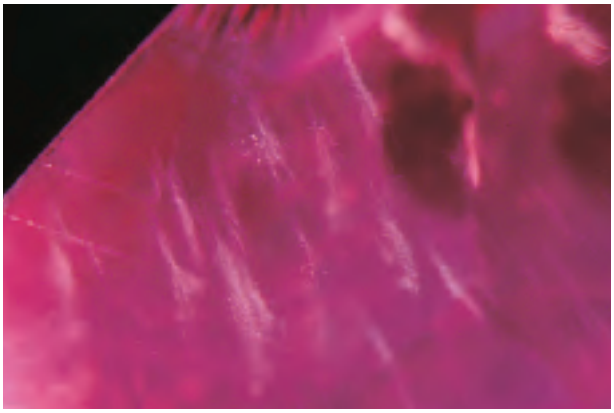

Figure 27. Other distinctive inclusion patterns showed a brush-stroke or more nebulous appearance. Photomicrograph by Christopher P. Smith; magnified 30×.

spectra were dominated by Cr^{3+} absorption features that were weaker in those stones that were more purple to violet, and more intense in those that were purer red. A secondary absorption influence was seen as a result of the $Fe^{2+} \leftrightarrow Ti^{4+}$ intervalence charge transfer responsible for the blue color component in the violet stones. These features are characteristic of all natural and synthetic ruby and pink sapphire, regardless of origin.

Infrared Spectroscopy. In addition to the dominant absorption characteristics of corundum between approximately 400 and 1000 cm^{-1} (peak positions at about 760, 642, 602, and 450 cm^{-1}; Wefers and Bell, 1972), the rubies and fancy-color sapphires in this study (none of which were heat treated) revealed a series of absorption bands in the 1900–4000 cm^{-1} region. The two most dominant bands were located at approximately 3320 cm^{-1} and 3085 cm^{-1}, with an additional pair of weaker bands at approximately 2100 and

Figure 28. Bluish white clouds followed the zonal growth structures in a small number of the Jegdalek samples. Such clouds may impart a kind of "sheen" to the stone, and have also been observed in rubies from Vietnam and Tajikistan. Photomicrograph by Christopher P. Smith; magnified 25×.

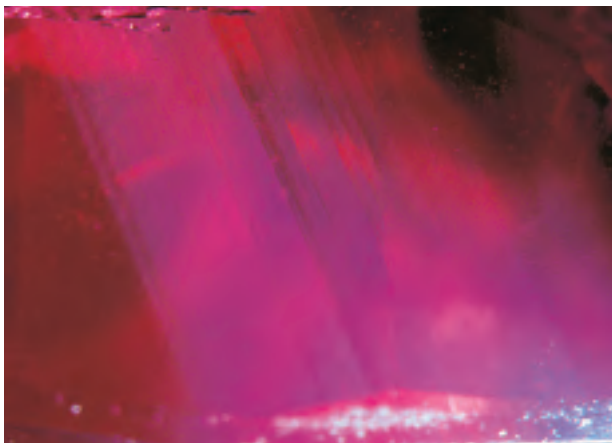

Figure 29. The reduced luster of a seam or vein of aluminum hydroxide (such as boehmite) visible on the surface of a ruby or sapphire from Jegdalek may at first resemble the glass-like residues present in many heat-treated rubies. With closer inspection, however, the inclusion features should clearly reveal the nonheated condition of such a stone. Photomicrograph by Christopher P. Smith; reflected light, magnified 25×.

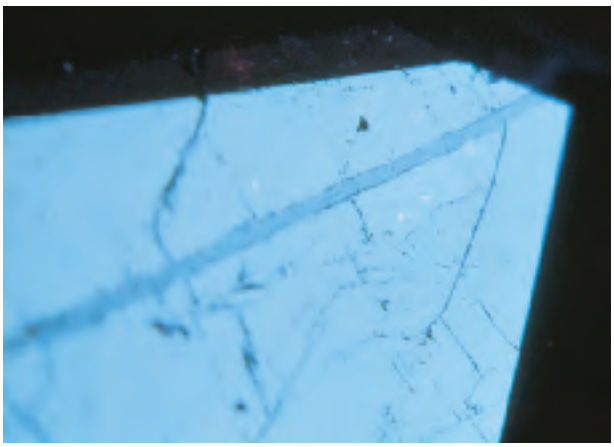

1980 cm^{-1} (figure 30). These absorption bands are related to OH-stretching frequencies and indicate the presence of the mineral boehmite (Farmer, 1974; Wefers and Misra, 1987). Several of the samples displayed such strong AlO(OH) absorption features that it was not possible to determine which aluminum hydroxide was present (i.e., boehmite or diaspore). However, not all samples had the AlO(OH)-related bands. Absorption bands associated with mica and calcite were also recorded occasionally.

Chemical Composition. The most significant trace-element variations recorded were in chromium concentration (table 2); in both the fancy-color sapphires and rubies, Cr concentration correlated directly to depth of red to pink color in the area measured. The other color-causing transition metals, titanium and iron, were the next most significant trace elements recorded, followed by measurable amounts of vanadium and gallium. The presence of additional trace elements (i.e., calcium, zirconium, potassium, manganese, and zinc) was related to inclusions at or just below the surface of the area analyzed.

Chemical fluctuations between consecutive periods of crystal growth, as well as a preferential crystallographic orientation of the color-causing mechanisms of Cr^{3+} (ruby) or $Fe^{2+} \leftrightarrow Ti^{4+}$ (blue sapphire), are responsible for the color zoning observed in the samples.

Figure 30. Many of the rubies and fancy-color sapphires from Jegdalek revealed infrared absorption bands at 3320 and 3085 cm^{-1} and weaker peaks at 2100 and 1980 cm^{-1}. These indicate the presence of boehmite, which was seen in veins or lining parting planes. Such absorption characteristics are helpful not only in identifying foreign mineral phases that may be present, but also for indicating that the gem has not been heat treated.

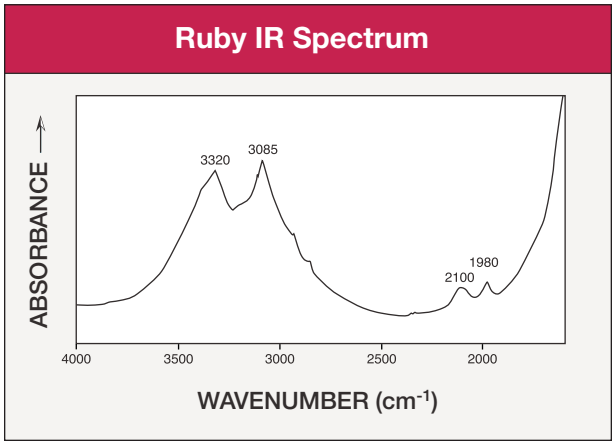

TABLE 2. Semi-quantitative chemical analyses by EDXRF for rubies and fancy-color sapphires from Jegdalek, Afghanistan.

Oxide (wt.%)	Rubies (16)[a]	Fancy-color sapphires (20)	Blue sapphire (1)
Al_2O_3	92.9 - 99.6[b]	99.1 - 99.7[b]	99.3
Cr_2O_3	0.250 - 1.971	0.037 - 0.445	0.009
TiO_2	0.002 - 0.078	0.008 - 0.145	0.046
Fe_2O_3	0.016 - 0.174	0.068 - 0.431	0.068
V_2O_5	0.013 - 0.062	0.005 - 0.035	0.012
Ga_2O_3	0.003 - 0.031	0.009 - 0.061	nd[c]

[a] *Number of samples are shown in parentheses. Trace-element analyses by ICP-AES were also obtained for one medium red ruby: 0.31 wt.% CaO, 0.006 wt.% V_2O_5, 0.35 wt.% Cr_2O_3, 0.36 wt.% FeO, 0.17 wt.% MgO, 0.20 wt.% K_2O, <30 ppm Mn, 50 ppm Cu, 370 ppm Zn, 36 ppm Sr, 45 ppm Nb, 8 ppm Ba, 32 ppm Pb; Be and Ga were below the detection limits of 8 ppm and 30 ppm, respectively. See also EDXRF analyses of Jegdalek rubies reported by Muhlmeister et al. (1998).*

[b] *The Al_2O_3 concentration of some samples was reduced by the presence of other minor and trace elements from mineral inclusions located at or just below the surface of the area measured.*

[c] *Not detected.*

DISCUSSION

A few previous studies have documented some of the gemological characteristics of corundum (primarily rubies) from this deposit (Bowersox, 1985, 1995; Hughes, 1994, 1997). In general, our results are consistent with those of other studies, although certain mineral inclusions described by Hughes (1994, 1997) were not encountered during this study. These include macro-size crystals of garnet, chondrodite, spinel, hornblende, and dolomite.

Since this study included only one blue sapphire and the majority of the fancy-color sapphire samples were lower quality, it will not be possible to do a competent comparison to similar-colored sapphires from other marble-type sources. Therefore, the bulk of this discussion will compare Jegdalek *rubies* with those from other deposits.

If one uses the combination of inclusion patterns (e.g., clouds, "flakes" [actually, groups of pinpoints], and stringers, specific mineral inclusions, internal growth structures, and chemical composition, it should not be a problem to separate Afghan rubies from those of basaltic deposits (e.g., Thailand, Laos, Cambodia, and Australia), or metasomatic deposits (e.g., Madagascar, Tanzania, and Kenya). In general, Afghan rubies and fancy-color sapphires are similar to those from other marble-type sources (e.g., Southeast Asia and Africa, as well as Pakistan and

Tajikistan). However, the specific inclusion features and internal growth structures of the Afghan rubies closely resemble those found at only a few of these deposits: Nepal, Mong Hsu (Myanmar), northern Vietnam, and, to a lesser degree, Tajikistan. Therefore, we shall limit the discussion of source distinction to comparison with ruby deposits in Nepal, Mong Hsu, and northern Vietnam. Note that the internal features that separate Jegdalek rubies from those of other localities will also clearly separate them from most synthetic corundum.

Nepal. There are several similarities between Afghan rubies and those from Nepal (see Harding and Scarratt, 1986; Kiefert and Schmetzer, 1986, 1987; Bank et al., 1988; Smith et al., 1997), and their separation may not be possible in all cases. For example, rubies from both localities may contain large rutile crystals and zones of short, very fine rutile needles (see figure 25); transparent colorless crystals of calcite and margarite; and AlO(OH) [both diaspore and boehmite]. However, there are some noteworthy distinctions. On the one hand, the euhedral, hexagonal, and rod-shaped crystals of apatite identified in rubies from Nepal were not encountered in the rubies from Jegdalek. On the other, the rounded colorless crystals of zircon in the Jegdalek samples have not been reported in Nepalese ruby. Similarly, while rubies from both localities contain partially healed fracture planes, only in the Afghan stones was a "frosted" texture noted on these planes.

The iron-sulfide inclusions and bluish white zonal clouds seen in some Afghan rubies (see figures 23 and 28, respectively) were not present in the Nepal samples. In contrast, uvite tourmaline, anorthite feldspar, and a black mineral grain surrounded by minute rutile needles documented in Nepal samples were not seen in the Afghan samples. Geometric platelets of graphite were noted in many of the Jegdalek samples, as were graphite scales in negative crystals (see figure 24). In the Nepal rubies, graphite was present only as coarse grains, often within larger mineral inclusions. The various flake-like and other inclusion patterns of the Jegdalek rubies were not observed in the Nepal rubies, whereas the antennae-like inclusion patterns so prevalent in Nepal rubies were not seen in the Jegdalek stones.

Although the internal growth structures and color zoning of corundum from both sources are almost identical, the wedge-shaped or wispy blue color zones in the Nepal stones are unique.

Mong Hsu. Rubies from Mong Hsu (Smith and Surdez, 1994; Smith, 1995; Peretti et al., 1995) and Jegdalek may seem similar at first, but a thorough investigation should reveal distinct differences. First, to remove the dark violetish blue color zone in the core of Mong Hsu rubies, the vast majority are heat treated. Therefore, an unheated ruby probably is not from Mong Hsu.

Macro-size mineral inclusions, although relatively common in the Jegdalek samples, are encountered infrequently in Mong Hsu rubies. Minerals identified as inclusions in Mong Hsu rubies to date include crystals of dolomite, apatite, diaspore, rutile, fluorite, and spinel.

"Cross-hatch," flake-like, and stringer formations are characteristic of rubies from Mong Hsu. Although the flake-like and stringer formations in rubies from Jegdalek (see, e.g., figure 26) may appear similar, closer scrutiny will reveal the unique texture, concentration, and crystallographic association of these inclusions in the Mong Hsu rubies.

The differences in internal growth structures are also conclusive. In Mong Hsu rubies, the prominent *c*, *r*, *n*, ω growth sequence, combined with the *c*, *n* core zone formation, contrasts sharply with the mostly subtle *z*, *n*, and *r* structures present in the Jegdalek samples.

Northern Vietnam. There are several similarities between rubies from northern Vietnam (Kane et al., 1991; Smith, 1996) and Afghanistan, and their separation may prove impossible in some cases. Rubies from both sources are known to contain macro-sized crystals of rutile, as well as zones of short, very fine rutile needles. However, long, iridescent rutile needles have not been recorded in Jegdalek rubies. Transparent colorless crystals of calcite, apatite, and zircon, as well as the general presence of AlO(OH) [both diaspore and boehmite], in addition to the very fine-grained bluish white clouds, also do not offer much insight into the probable source. However, the rod-shaped crystals of calcite identified in rubies from northern Vietnam were not encountered in the Jegdalek rubies. Conversely, neither the "frosted" texture noted in the healed fracture planes of the Afghan stones (see figure 19), nor the iron-sulfide inclusions that line fracture or parting planes (see figure 22), have been seen in Vietnamese rubies.

Pyrrhotite occurs as black rods in Vietnamese rubies, and the epigenetic inclusion nordstrandite may be present. However, Vietnamese rubies have not been seen to contain the geometric platelets of

Figure 31. The Jegdalek deposits should continue to produce attractive ruby and pink sapphires. The 10.88 ct ruby in this 18K pendant/brooch has been carved in the Glyptic Illusion style. The piece was designed by Beverly Bevington and manufactured by Gary Mills. Photo by Jeffrey Scovil.

graphite noted in many of the Jegdalek samples, nor the graphite scales present in the negative crystals.

Although there are many similarities in the flake-like and other inclusion patterns of the rubies from both sources, the flake-like inclusions in many Jegdalek samples have a coarser texture. The internal growth structures and color zoning also may be similar, although rubies from northern Vietnam frequently show prominent growth structure sequences, which we have not observed in the Afghan samples. In addition, Vietnamese rubies reveal a much wider range of dipyramidal crystal habits, including additional crystal faces of the dipyramids *v* and *ω* and the negative rhombohedron *d*.

Trace Elements. The concentrations of V, Ti, Fe, and Ga may provide some evidence for locality determination, although the specific distinctions are very subtle and beyond the scope of this article.

Infrared Spectra. Certain trends were evident when absorption features related to AlO(OH) inclusions were present. Boehmite-related features were seen more frequently in rubies from Jegdalek, Nepal, and Vietnam, whereas rubies from Mong Hsu more typically revealed absorption bands related to diaspore. However, when dominant IR absorption bands between approximately 2600 and 3800 cm^{-1} are quite strong, a clear distinction between diaspore and boehmite is not always possible. The presence of AlO(OH) in the spectrum also may provide welcome proof that a ruby is not heat treated, as well as a very good indication of whether it is natural or synthetic.

CONCLUSION

Over the past century, the Jegdalek deposit in east-central Afghanistan has supplied large quantities of cabochon-grade ruby (figure 31), and pink sapphire to the gem trade. Some very fine stones from this locality have also been cut. The semitransparent to translucent nature of the material is due to dense concentrations of fractures, as well as to the high degree of twinning in some samples. The most commonly observed internal features are partially healed and nonhealed fracture planes, lamellar twin planes parallel to *r*, color zoning (i.e., red/pink and blue areas), and mineral inclusions of calcite, apatite, zircon, mica, iron sulfides, graphite, rutile, and aluminum hydroxide. Rubies from Jegdalek usually can be separated from those of other localities by evaluating a combination of the inclusion patterns, mineral inclusions, and internal growth structures.

Although the Jegdalek deposit has the potential for year-round production of rubies and fancy-color sapphires that are suitable for fine jewelry, exploration and mining have been hindered by the political environment in Afghanistan. Although local tribal leaders are interested in using modern technology and equipment to increase production, they must wait until a stable and favorable government is formed in Kabul.

Acknowledgments: The authors acknowledge the assistance of the following individuals: Commanders Ahmed Shah Massoud, Mahmud, Anwar Khan, and Alhaj Moulawi Ahmadjan (Minister of Mines and Industry) for providing the senior author with permission, transportation, and security for visiting the mining area; and Commander Sher Mohammed, Jamal Khan, Engineer Abdul Hakim, Khudai Nazar Akbari, Mir Waees Khan, Commander Mohammed Omar Tahdar, and Abdul Rafi for their field work with the exploration team. Nancy Dupree (Peshawar, Pakistan) and Abdul Aurab (ex-Minister of Mineral

Promotion, Kabul, Afghanistan) furnished information on the tribal people and the history of ruby mining in the Jegdalek area. Sam Muhlmeister and Dino DeGhionno (both of the GIA Gem Trade Laboratory, Carlsbad) assisted with some of the Raman analyses and gemological studies. John Koivula is thanked for Raman analyses and photomicrography. Larry Snee (U.S. Geological Survey, Denver, Colorado) provided helpful comments on the manuscript.

REFERENCES

Bank H., Gübelin E., Harding H.H., Henn U., Scarratt K., Schmetzer K. (1988) An unusual ruby from Nepal. *Journal of Gemmology*, Vol. 21, No. 4, pp. 222–226.

Barlow A.E. (1915) *Corundum: Its Occurrence, Distribution, Exploitation, and Uses*. Department of Mines, Government Printing Bureau, Ottawa, Canada.

Bowersox G.W. (1985) A status report on gemstones from Afghanistan. *Gems & Gemology*, Vol. 21, No. 4, pp. 192–204.

Bowersox G.W., Chamberlin B.E. (1995) *Gemstones of Afghanistan*. Geoscience Press, Tucson, 221 pp.

Bretschneider E. (1887) *Medieval Researchers from Eastern Asiatic Sources*. Kegan Paul, Trench, Trubner & Co., London, 334 pp.

Debon F., Afzali H., Le Fort P., Sonet J. (1987) Major intrusive stages in Afghanistan: typology, age and geodynamic setting. *Geologische Rundschau*, Vol. 76, No. 1, pp. 245–264.

Farmer V.C. (1974) The infrared spectra of minerals. *Mineralogical Society Monograph 4*, Mineralogical Society, London.

Griesbach C.L. (1886) Afghan and Persian field notes. *Records of the Geological Survey of India*, Vol. 19, Pt. 1, pp. 48–65.

Griesbach C.L. (1892) The geology of the Safed Koh. *Records of the Geological Survey of India*, Vol. 25, Pt. 2.

Gübelin E.J. (1982) Gemstones of Pakistan: Emerald, ruby, and spinel. *Gems & Gemology*, Vol. 18, No. 3, pp. 123–139.

Haas H. (1972) Diaspore-corundum equilibrium determined by epitaxis of diaspore on corundum. *American Mineralogist*, Vol. 57, pp. 1375–1385.

Harding R.R., Scarratt K. (1986) A description of ruby from Nepal. *Journal of Gemmology*, Vol. 20, No. 1, pp. 3–10.

Hughes R.W. (1994) The rubies and spinels of Afghanistan: A brief history. *Journal of Gemmology*, Vol. 24, No. 4, pp. 256–267.

Hughes R.W. (1997) *Ruby & Sapphire*. RWH Publishing, Boulder, 512 pp.

Kane R.E. (1997) Kashmir ruby—a preliminary report on the deposit at Nangimali, Azad Kashmir, Pakistan. *Proceedings of the 26th International Gemological Congress*, Sept. 27 to Oct. 3, Idar-Oberstein, Germany, pp. 28–30.

Kane R.E., McClure S.F., Kammerling R.C., Khoa N.D., Mora C., Repetto S., Khai N.D., Koivula J.I. (1991) Rubies and fancy sapphires from Vietnam. *Gems & Gemology*, Vol. 27, No. 3, pp. 136–155.

Kazmi A.H. (1989) A brief overview of the geology and metallogenic provinces of Pakistan. In A.H. Kazmi and L.W. Snee, Eds., *Emeralds of Pakistan: Geology, Gemology, and Genesis*. Van Nostrand Reinhold, New York, pp. 1–11.

Kiefert L., Schmetzer K. (1986) Rosafarbene und violette Sapphire aus Nepal. *Zeitschrift der Deutschen Gemmologischen Gesellschaft*, Vol. 35, pp. 113–125.

Kiefert L., Schmetzer K. (1987) Pink and violet sapphires from Nepal. *Australian Gemmologist*, Vol. 16, No. 6, pp. 225–230.

Kiefert L., Schmetzer K. (1991) The microscopic determination of structural properties for the characterization of optical uniaxial natural and synthetic gemstones, part I: General considerations and description of the methods. *Journal of Gemmology*, Vol. 22, No. 6, pp. 344–354.

Liddicoat R.T. Jr. (1989) *Handbook of Gem Identification*, 12th rev. ed. Gemological Institute of America, Santa Monica, CA.

Muhlmeister S., Fritsch E., Shigley J.E., Devouard B., Laurs B.M. (1998) Separating natural and synthetic rubies on the basis of trace-element chemistry. *Gems & Gemology*, Vol. 34, No. 2, pp. 80–101.

Okrusch M., Bunch T.E., Bank H. (1976) Paragenesis and petrogenesis of a corundum-bearing marble at Hunza (Kashmir). *Mineralium Deposita*, Vol. 11, pp. 278–297.

Orlov G.A., Tsabolov G.S., Eriomenko G.K., Zhdan A.V., Matveev P.S., Ghawari S.A. (1974) *Report by the Jegdalek Crew on the Work in 1973–74*. Department of Geological and Mineral Survey, Kabul.

Peretti A., Schmetzer K., Bernhardt H.-J., Mouawad F. (1995) Rubies from Mong Hsu. *Gems & Gemology*, Vol. 31, No. 1, pp. 2–26.

Powell C.A., Conaghan P.J. (1973) Plate tectonics and the Himalayas. *Earth and Planetary Science Letters*, Vol. 20, pp. 1–20.

Rossovsky L.N. (1980) Mestorozhdeniya dragotsennykh kamney Afghanistana [Gemstone deposits of Afghanistan]. *Geologiya Rudnykh Mestorozhdenii* [Geology of Ore Deposits], Vol. 22, No. 3, pp. 74–88.

Schmetzer K. (1986a) An improved sample holder and its use in the distinction of natural and synthetic ruby as well as natural and synthetic amethyst. *Journal of Gemmology*, Vol. 20, No. 1, pp. 20–33.

Schmetzer K. (1986b) *Natürliche und synthetische Rubine—Eigenschaften und Bestimmung*. Schweizerbart, Stuttgart, Germany.

Shareq A., Chmyriov V.M., Stazhilo-Alekseev K.F., Doronov V.I., Gannon P.J., Lubemov B.K., Kafarskiy A.Kh., Malyarov E.P., Rossovsky L.N. (1977) *Mineral Resources of Afghanistan, 2nd ed.* United Nations Development Program, AFG/74/012, 419 pp.

Smith C.P. (1995) Contribution to the nature of the infrared spectrum for Mong Hsu rubies. *Journal of Gemmology*, Vol. 24, No. 5, pp. 321–335.

Smith C.P. (1996) Introduction to analyzing internal growth structures: Identification of the negative *d* plane in natural ruby. *Gems & Gemology*, Vol. 32, No. 3, pp. 170–184.

Smith C.P. (1998) Rubies and pink sapphires from the Pamir Mountain Range in Tajikistan, former USSR. *Journal of Gemmology*, Vol. 26, No. 2, pp. 103–109.

Smith C.P., Surdez N. (1994) The Mong Hsu ruby: A new type of Burmese ruby. *JewelSiam*, Vol. 4, No. 6, pp. 82–98.

Smith C.P., Gübelin E.J., Bassett A.M., Manandhar M.N. (1997) Rubies and fancy-color sapphires from Nepal. *Gems & Gemology*, Vol. 33, No. 1, pp. 24–41.

Sorkhabi R.B., Stump E. (1993) Rise of the Himalaya: A geochronologic approach. *GSA Today*, Vol. 3, No. 4, pp. 85, 88–92.

Webster R. (1994) *Gems: Their Sources, Descriptions, and Identification*, 5th ed. P. G. Read, Ed., Butterworth-Heinemann, London.

Wefers K., Bell G.M. (1972) *Oxides and Hydroxides of Alumina, Alcoa Research Laboratories Technical Paper No. 19*, Alcoa Research Laboratories, St. Louis, MO.

Wefers K., Misra C. (1987) *Oxides and Hydroxides of Alumina, Alcoa Research Laboratories Technical Paper No. 19, Revised*. Alcoa Research Laboratories, St. Louis, MO.

Wood J. (1841) *A Journey to the Source of the River Oxus*. London, John Murray, 2nd ed., 1872, reprinted 1976, Oxford University Press, 280 pp.

Wyart J., Bariand P., Filippi J. (1981) Lapis-lazuli from Sar-e-Sang, Badakhshan, Afghanistan. *Gems & Gemology*, Vol. 17, No. 4, pp. 184–190.

IDENTIFICATION OF HPHT-TREATED YELLOW TO GREEN DIAMONDS

By Ilene M. Reinitz, Peter R. Buerki, James E. Shigley, Shane F. McClure, and Thomas M. Moses

Examination of recently introduced greenish yellow to yellowish green HPHT-treated diamonds from three companies revealed several identifying characteristics. Gemological properties include a highly saturated body color, well-defined brown to yellow octahedral graining, moderate to strong green "transmission" luminescence to visible light (associated with the graining), and visual evidence of heating. Most of the treated diamonds, including some from each of the three sources, exhibit chalky greenish yellow to yellow-green fluorescence to UV radiation (long- and short-wave). Distinctive features seen with a hand-held spectroscope include a 415 nm line, a strong band from about 480 to 500 nm, a strong line at 503 nm, and emission lines at 505 and 515 nm. IR spectra reveal that they are type Ia diamonds. Near-IR spectra show a peak at 985 nm, an indicator of high-temperature exposure. A small number of these HPHT-treated diamonds are yellow to brownish yellow; they do not show any green transmission, but other properties identify them as treated.

ABOUT THE AUTHORS

Dr. Reinitz is manager of Research and Development, and Mr. Moses is vice president of Research and Identification, at the GIA Gem Trade Laboratory, New York. Dr. Buerki is a research scientist, and Dr. Shigley is director, at GIA Research, Carlsbad. Mr. McClure is director of Identification Services at the GIA Gem Trade Laboratory, Carlsbad.

Please see acknowledgments at the end of the article.

Gems & Gemology, Vol. 36, No. 2, pp. 128–137

Several companies are now treating brown diamonds with high pressure and high temperature (HPHT) to transform their color to greenish yellow, yellowish green, yellow, or brownish yellow (figure 1). These include the General Electric (GE) Company, Novatek, and unidentified organizations in both Russia and Sweden. Both GE and Novatek are concentrating their efforts on producing colors with an obvious green component (Templeman, 2000; Federman, 2000; Anthony et al., 2000). In contrast, the Swedish manufacturer apparently is trying to produce colors similar to those of natural yellow diamonds (J. Menzies, pers. comm., 2000). Moses and Reinitz (1999) briefly described some of the treated diamonds from these various manufacturers. The present article reports the gemological and spectroscopic properties of a large number of diamonds treated in this fashion, and discusses how the gemological properties compare to those of the rarest and most desirable of the stones that they resemble: natural-color greenish yellow to yellow-green diamonds.

BACKGROUND

An article by Shigley et al. (1993) on gem-quality synthetic yellow diamonds from Novosibirsk, Russia, described three greenish yellow to yellow synthetic diamonds that had been heat treated at high pressure to alter their color. This treatment was done in the same apparatus in which the diamonds were synthesized. Although the gemological and spectral properties of those synthetics are rather different from the treated-color natural diamonds reported on here, we believe that article was the first report in the gemological literature on HPHT treatment to alter diamond color.

From fall 1996 through winter 1997, approximately 50 natural diamonds of unusual greenish yellow to yellow-green color were submitted to the GIA Gem Trade Laboratory for identification reports (Reinitz and Moses,

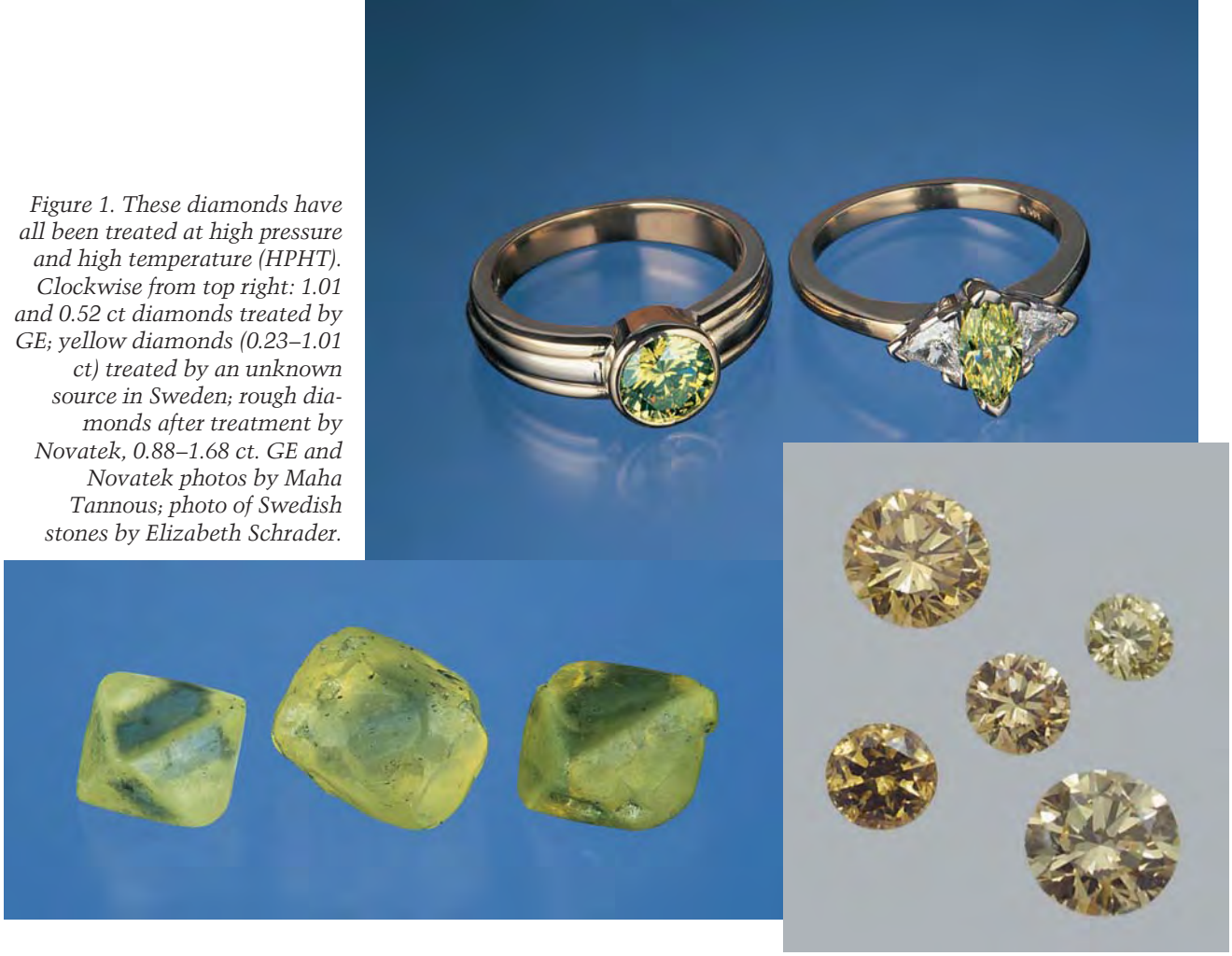

Figure 1. These diamonds have all been treated at high pressure and high temperature (HPHT). Clockwise from top right: 1.01 and 0.52 ct diamonds treated by GE; yellow diamonds (0.23–1.01 ct) treated by an unknown source in Sweden; rough diamonds after treatment by Novatek, 0.88–1.68 ct. GE and Novatek photos by Maha Tannous; photo of Swedish stones by Elizabeth Schrader.

1997). These diamonds displayed gemological and spectroscopic properties—saturated color, strong graining, burn marks and other visual evidence suggestive of heating, and certain bands in the absorption spectra—that, in light of the current study, suggest that some of them may have been treated using HPHT technology very similar to the current technique. We do not know where those diamonds were treated. However, Van Bockstael (1998) described diamonds with similar colors and gemological characteristics, and stated that they had undergone HPHT treatment in Russia. Henn and Milisenda (1999) reported on similar material, as did De Weerdt and Van Royen (2000). Buerki et al. (1999) wrote a technical report on the spectra and features of both natural and treated type Ia yellow diamonds with green luminescence, and hypothesized as to what kinds of treatment might yield the features observed. Recently, Collins et al. (2000) reported the infrared- and visible-range spectroscopic features of HPHT-treated diamonds, and discussed how the treatment conditions affect the color centers in type Ia diamond.

Both GE and Novatek have been open to discussing details of how they perform these treatments (T. Anthony and D. Hall, pers. comms., 2000). Using the same types of apparatus as are used to synthesize single-crystal diamonds, they place natural diamonds under a high confining pressure of about 6 Gigapascals (GPa, equal to 60 kilobars). While the stones are at high pressure, they expose them to high temperatures, up to 2100°C, for short periods (i.e., less than 30 minutes, in some cases much less). These conditions are similar to those used by GE to decolorize diamonds (Anthony and Casey, 1999), but the starting materials are nitrogen-bearing type Ia brown diamonds, rather than nominally nitrogen-free type IIa diamonds. As with the GE POL decolorization process, however, polished diamonds must be repolished to remove surface damage after HPHT exposure. Although the treated diamonds produced from these two sources are generally similar in appearance and gemological properties, this does not mean that these companies are using identical HPHT equipment and treatment conditions. However, it is not our intention to compare in detail the specific products of the various manufacturers. Rather, this article will focus on those gemological characteristics that will facilitate identification of this kind of treated diamond in general.

Figure 2. Brown to yellow planar graining was found in most of the treated diamonds examined in this study. Photomicrograph by James E. Shigley; magnified 10×.

MATERIALS AND METHODS

For this study, we examined 63 diamonds that were known to have been HPHT treated: 41 faceted (round brilliants and fancy shapes) and 22 rough. Thirty-one of the samples were from GE, 25 were from Novatek (including all 22 rough stones), and seven were from the Swedish manufacturer. Seven of the rough diamonds were examined before and after they were treated by Novatek. We polished small "windows" on 11 of the rough samples (including two of the before-and-after samples) to facilitate examination of their internal features and recording of spectra. All samples were examined with a binocular gemological microscope and various illumination techniques, a long-wave (366 nm) and short-wave (254 nm) Ultraviolet Products UV lamp unit, and both a Beck prism and a Discan digital-scanning diffraction-grating spectroscope. Two Hitachi U-4000 series spectrophotometers were used to record absorption spectra at liquid-nitrogen temperature over the range of 250–1000 nm. Infrared spectra were recorded with a Nicolet 760 Fourier-transform infrared (FTIR) spectrometer over the range 400–25,000 cm^{-1}, or a Nicolet 550 FTIR spectrometer over the range 400-11,000 cm^{-1}. Photomicrographs were taken with a Nikon SMZ-U Photomicroscope.

RESULTS

Description of the Treated Samples. In our overall observations, the diamonds from all three treaters showed comparable properties. On the basis of

TABLE 1. Properties of HPHT-treated diamonds from GE, Novatek, and an undisclosed source in Sweden.

Property	Major group (57)[a]	Minor group (6)
Color	Greenish yellow to yellow-green (36); yellow-green to yellowish green (21)	Yellow to brownish yellow (6)
Color zoning (seen in diffused light)	Brown to yellow graining (41); none (16)	Brown graining (4); none (2)
Microscopic features	Etched naturals or feathers, or tension fractures, often containing graphite (32); naturals without a frosted appearance (2); no naturals or fractures (23)	Etched naturals or feathers (5); no naturals or fractures (1)
UV fluorescence		
Long-wave	Greenish yellow to yellowish green, strong in most cases, with a chalky appearance (39); blue, plus yellow or greenish yellow, with a chalky appearance (17); none (1)	Green to greenish yellow (3); blue plus yellow (1); chalky appearance (4); none (2)
Short-wave	Greenish yellow to yellowish green (53); yellow (4); chalky appearance (40—includes the 4 that showed yellow)	Green to greenish yellow (3); yellowish green + blue (3); chalky appearance (4)
Luminescence excited by visible light ("transmission")	Moderate to strong green (56); moderate green plus weak blue(1)	None (4); weak blue plus green (2)
Spectroscope spectrum	Strong 503 nm line (57); dark band from 480–500 nm (41)—of these 21 show a 415 nm line and 20 show emission lines at 505 and 515 nm	415 nm line (1); no lines (5)
UV-Vis-NIR absorption spectra	Weak peak at 415 nm, strong to very strong peak at 503 nm, and weak to strong peak at 985 nm (45); weak broad band centered at 550 nm (29); weak peak at 535 nm (21); weak peak at 637 nm (14); or weak peaks at 415 and 503 nm, weak to moderate peak at 985 nm, and rising absorption toward shorter wavelengths (9)	Sharp rise in absorption toward shorter wavelengths with no sharp peaks (4); or, sharp rise in absorption toward shorter wavelengths with weak peak at 985 nm (1); weak peaks at 415 and 503 nm, weak to moderate peak at 985 nm, and rising absorption toward shorter wavelengths (1)
Mid-infrared spectrum (diamond type)	IaB >A (26) IaA >B (14) IaA ~ B (14) IaA (3)	IaA >B (2) IaB >A (2) IaA ~ B (2)
Other mid-infrared features	3144 cm^{-1} (2)	None

[a] *Number of samples in parentheses.*

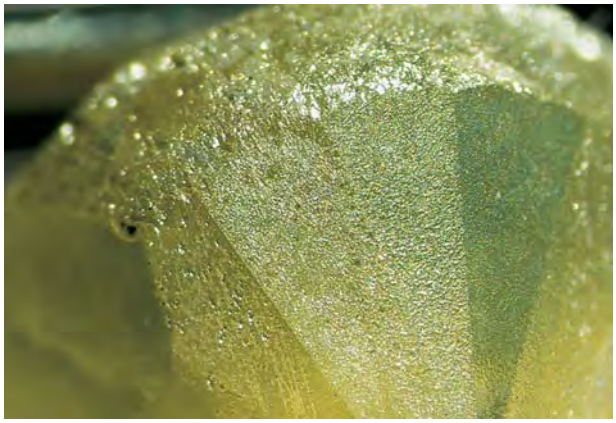

Figure 3. After HPHT treatment, etching and pitting of the surface of this 0.53 ct Novatek diamond obscured the internal features. Fashioned stones always require repolishing after treatment. Photomicrograph by Shane Elen; magnified 10×.

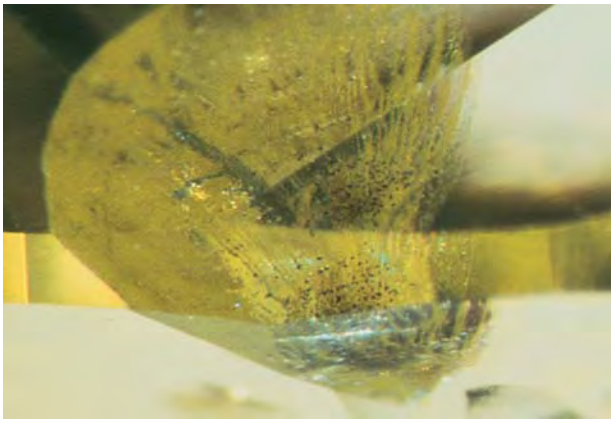

Figure 4. The conditions used for HPHT treatment lead to etching of surfaces that can be observed even after repolishing. Note the translucent, frosted appearance of this fracture. Photomicrograph by Shane Elen; magnified 10×.

these properties, we found that the 63 samples divided naturally into two groups: those that did or did not show significant green luminescence to visible light (table 1). Because there are many more samples that showed green luminescence (57) than did not (6), we refer to these two groups as "major" and "minor" in table 1.

Color. The colors of all the treated samples were highly saturated (see again figure 1), and many of them were dark in tone. Most were greenish yellow to yellow-green, but six were yellow to brownish yellow. The greenish yellow to yellowish green hues shifted noticeably with different light sources. In particular, direct sunlight excited green luminescence in these diamonds, enhancing the green component considerably. The overall color, including this green luminescence, also was enhanced temporarily (became more saturated) just after the diamonds were exposed to temperatures typical of those used for jewelry repair (up to 1,000°C), but the color reverted to its original appearance as it cooled (T. Anthony, pers. comm., 2000; TMM also observed this color difference in the course of setting one of the jewelry pieces in figure 1).

Features Seen with Magnification. The most common feature seen with magnification (observed in 45 samples) was brown-to-yellow planar graining that was oriented along one or more octahedral directions, forming banded or intersecting patterns of color zoning, as shown in figure 2. This colored graining varied in intensity from weak to very strong. The treated rough samples and one fashioned sample (not yet repolished) from Novatek showed etching and pitting of their surfaces (figure 3), which obscured internal features. Eighteen polished diamonds showed microscopic evidence of heating, such as etched and/or pitted naturals, etched or graphitized fractures (figures 4 and 5), or crystalline inclusions with tension fractures around them. Two polished diamonds with small naturals did not show any etching or graphitization.

Figure 5. In some of the diamonds, graphite formed along fracture surfaces during HPHT treatment. Photomicrograph by James E. Shigley; magnified 10×.

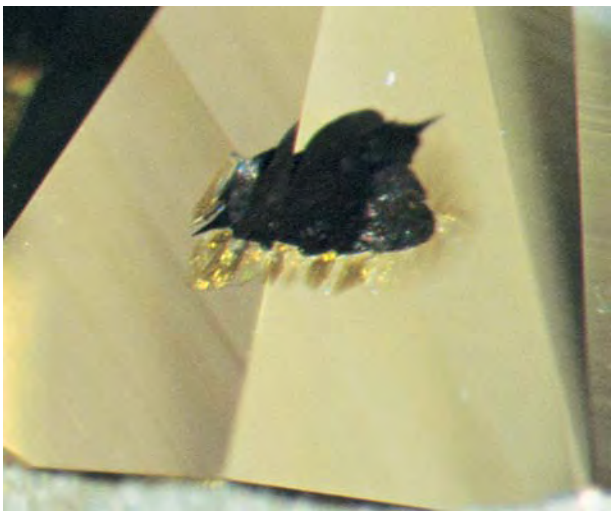

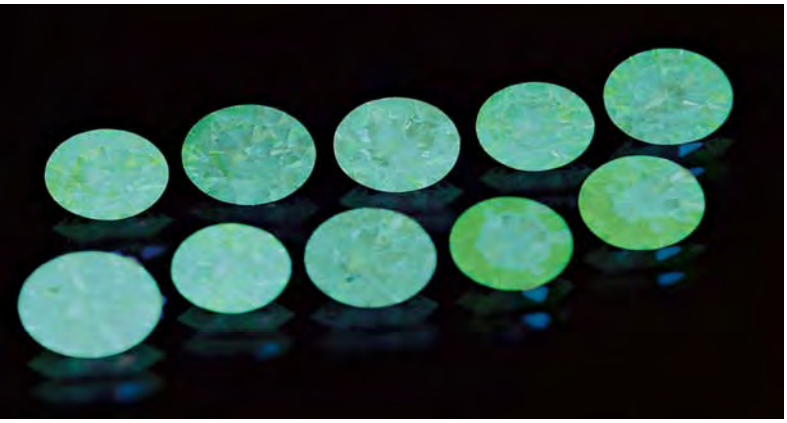

Figure 6. The typical reaction of these treated diamonds (0.45–0.70 ct) to long-wave UV is chalky greenish yellow to yellowish green. Photo by Maha Tannous.

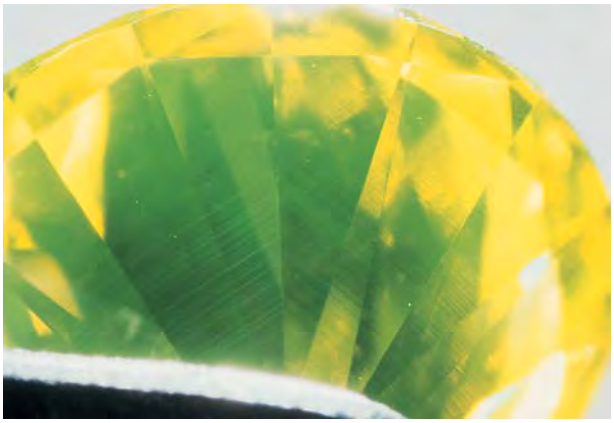

Figure 7. The strong green "transmission" (luminescence to visible light) displayed by these typical HPHT-treated yellow diamonds emanates from graining planes. Photomicrograph by James E. Shigley; magnified 10×.

Luminescence. We observed moderate to strong, greenish yellow to yellowish green fluorescence to long-wave UV radiation in 68% of the greenish yellow to yellowish green samples; the remaining 32% showed a mixture of blue with yellow or greenish yellow. In 56 of the 63 diamonds, regardless of the fluorescence color, the reaction appeared chalky or hazy (figure 6); in some faceted samples, this chalkiness appeared particularly strong at the culet. The yellow to brownish yellow diamonds showed weaker fluorescence to long-wave UV, in colors similar to those of the other diamonds. When exposed to short-wave UV, 93% of the greenish yellow to yellowish green samples showed moderate to strong greenish yellow to yellowish green fluorescence, and the remainder fluoresced yellow; 40 of these reactions appeared chalky. The yellow to brownish yellow samples again showed weaker fluorescence in similar colors. In general, the fluorescence was more intense to long-wave than to short-wave UV, although a few samples exhibited the same intensity to both wavelengths and three that fluoresced weakly to short-wave UV showed no reaction to long-wave UV.

When illuminated by a strong visible light source, such as a fiber-optic lamp, all but the six yellow to brownish yellow samples exhibited moderate to strong green luminescence (green "transmission"). When these diamonds were examined with fiber-optic lighting at 10× magnification, this luminescence was clearly seen to originate from the brown to yellow planar internal graining in 35 of the 41 samples with graining (figure 7); in some samples, the etched surface prevented observation of the distribution of the green transmission.

Spectra. With a handheld or desk-model spectroscope and transmitted light, we usually saw a strong

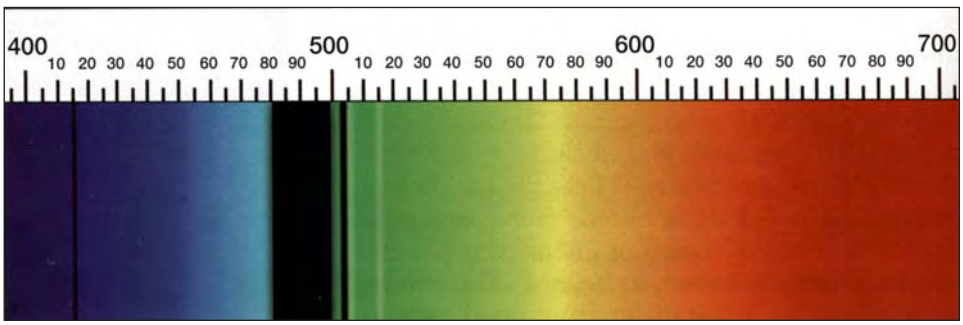

Figure 8. The hand or desk-model spectroscope shows a spectrum that is characteristic for most HPHT diamonds: a strong band at about 480–500 nm, a strong line at 503 nm, and sometimes a weak line at 415 nm and/or emission lines at 505 and 515 nm.

absorption line at 503 nm and a dark band from about 480–500 nm in the greenish yellow to yellowish green treated diamonds. A weak to moderate 415 nm line also was observed in 22 of the samples, including one brownish yellow diamond, and green emission lines at 505 and 515 nm were seen in 20 samples (not all of which had the 415 nm line). All of these features are shown in figure 8. With reflected light, many samples showed a distinct line at 494 nm and a narrower dark band at a slightly lower wavelength. Five of the yellow samples showed no features in the hand spectroscope.

The UV–Vis–NIR spectra fell into three categories, as shown in figure 9. The most common spectrum (seen in 45 greenish yellow to yellowish green samples; figure 9A) revealed the presence of a weak N3 band (primary line at 415 nm), a strong to very strong H3 band (primary line at 503 nm), and a weak to strong H2 band (primary line at 985 nm); the first two lines correspond to those seen in the hand spectroscope. The emission lines observed with the hand spectroscope were not recorded by the spectrophotometer. (See Clark et al. [1992] for a thorough discussion of color centers in diamond, their associated absorption features, and their transformations during annealing.) One or more of three additional features were seen in about half of these samples: a weak to moderate broad peak centered around 550 nm; a weak, sharp peak at 535 nm; and/or a weak, sharp peak at 637 nm (associated with the NV center). Ten samples (nine greenish yellow to yellowish green and one brownish yellow) showed features similar to those in the first category, but with different relative intensities, overlaid on a steep overall rise in absorbance from about 500 nm toward the shorter wavelengths (figure 9B). In the third category, five of the six yellow to brownish yellow samples showed a sharp rise toward shorter wavelengths but no N3 or H3 features (figure 9C); only one of these five samples showed an H2 absorption.

FTIR spectra in the near-infrared range, taken at room temperature, also showed the 985 nm peak. Although one of our FTIR instruments (the Nicolet 550) detected this feature less well than the low-temperature visible-NIR spectrometer, the other FTIR instrument detected it with distinctly higher sensitivity. The mid-infrared spectra of all samples showed features typical of type Ia diamonds. The aggregation states of nitrogen varied: Three samples showed A aggregates alone; the remainder showed absorption peaks for both A and B aggregates, with about half showing stronger B-aggregate absorption and half showing stronger A-aggregate features (Evans, 1992). In several cases, two infrared spectra of the same sample showed slight differences in the relative heights of the A and B aggregate peaks—an indication of the inherently inhomogeneous distribution of nitrogen in diamond. Two samples showed weak absorption peaks at 1344 cm^{-1}, a feature associated with single substitutional nitrogen.

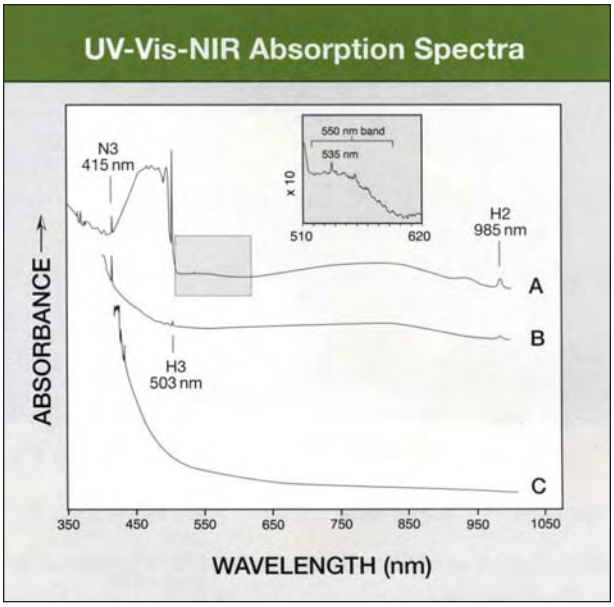

Figure 9. The low-temperature UV–Vis–NIR absorption spectra of these HPHT treated diamonds show some distinctive features. (A) The samples most commonly exhibit weak absorption at the N3 band (415 nm), strong absorption at the H3 band (503 nm), moderate absorption at the H2 center (985 nm), and in some cases, a weak to moderate broad peak centered at 550 nm, a weak sharp peak at 535 nm, and a weak peak at 637 nm. A vertical expansion of 10× is used to emphasize the subtle features between 510 and 620 nm (see inset). (B) A smaller number of the HPHT-treated diamonds show rising absorption from about 500 nm toward shorter wavelengths, as well as the N3, H3, and H2 bands. (C) The spectra of the yellow to brownish yellow diamonds showed simply a smooth rise in absorption toward the shorter wavelengths.

Comparison of Samples Before and After Treatment. The "after" observations of six crystals examined both before and after HPHT treatment and one crystal before and after partial processing (J. Fox, Novatek, pers. comm., 2000) by Novatek

TABLE 2. Properties of seven diamond crystals, in three color categories, before and after HPHT treatment by Novatek.[a]

Property	Before	After
Color	A. Pale yellow (1) B. Dark brown (1) C. Brown (5)	A. Brownish yellow (1) B. Brownish yellow (1) C. Greenish yellow (5)
Microscopic features	Worn, translucent surface (7)	Etched, pitted surface (7); graphitized fractures (7)
UV fluorescence		
Long-wave	A. Moderate blue B. Weak yellow C. Weak to moderate greenish yellow	A. Moderate blue + green B. Weak green C. Strong to very strong greenish yellow to green-yellow, very chalky
Short-wave	A. Weak yellow B. None C. None (2); weak yellow (3)	A. Very weak yellowish green B. Very weak, chalky green-yellow C. Moderate, chalky green-yellow (5)
Green luminescence excited by visible light	A. None B. Very weak C. Weak to moderate, some patchy	A. None B. Very weak, along graining C. Strong
Spectroscope spectrum	A. 415 nm line B. 415 nm line, weak 503 nm line C. 415 nm line, weak 503 nm line	A. 415 nm line B. 415 nm line, moderate 494 and 503 nm lines C. 415 nm line, band at about 480–500 nm, strong 503 nm line, emission lines at 505 and 515 nm
UV-Vis-NIR absorption spectra	A. N3 and very weak 535 nm peak B. Rising absorption toward shorter wavelengths, N3 band with principal line at 415 nm, weak H3 band with principal line at 503 nm, weak broad band at 550 nm C. Rising absorption toward shorter wavelengths, N3, weak H3, 550 nm broad band	A. N3 and weak H3 B. Rising absorption toward shorter wavelengths, N3, moderate H3, weak NV band at 637 nm, and H2 band with principal line at 985 nm C. N3, strong H3, weak NV and H2 bands (5); four still show 550 nm broad band
Infrared absorption spectra	Mixed IaA and IaB nitrogen aggregation (7) Amber center at 4166 cm^{-1} (6; not in pale yellow sample)	Mixed IaA and IaB nitrogen aggregation (7) No amber centers

[a] *Where appropriate, results have been categorized (A,B, and C) according to diamond color. The number of samples is given in parentheses. "A" is the partially processed sample.*

are included in the results described above. In this section, we will examine how the properties of these samples changed with treatment (see table 2). Both the pale yellow crystal (that underwent partial processing) and a dark brown one were brownish yellow after treatment; the other five changed from brown to greenish yellow (figure 10). Before treatment, all seven had worn, translucent surfaces that obscured the view of the interior; brown graining was observed in the single dark brown sample, one of the two on which a window had been polished. After treatment, all seven crystals had etched, pitted surfaces, and graphitized fractures.

With treatment, the fluorescence to long-wave UV became greener in all seven samples, and it became stronger in both intensity and chalkiness in the five diamonds that turned greenish yellow. The fluorescence to short-wave UV developed or became greener in all seven samples, and increased in both intensity and chalkiness in six samples. Green luminescence to visible light was observed in the six brown crystals before treatment, ranging from very weak to moderate. Green transmission did not develop in the partially processed pale yellow crystal, and it remained weak in the dark brown one. The other five samples showed a substantially stronger green transmission luminescence after treatment. The etched, pitted surfaces prevented us from determining whether this green transmission was zoned along colored graining.

The pale yellow crystal showed no change in a desk-model spectroscope after partial processing. The dark brown crystal showed a stronger line at 503 nm after treatment, and an additional line at 494 nm. The remaining five samples developed the characteristic spectrum observed in many of the diamonds examined for this study (see again figure 8 and table 2).

The spectra in figure 11 show the effects of treatment in both the UV-Vis-NIR and infrared regions. All seven samples showed production or substantial growth of the peak at 503 nm related to the H3 center; all but the partially processed sample showed development of smaller peaks at 985 nm (associated with the H2 center) and 637 nm (associated with the NV center; see figure 11A). The mid-infrared spectra showed no significant change in the state of nitrogen aggregation (1333 to 800 cm^{-1}), but before treatment the six brown samples showed a structure around 4166 cm^{-1} (known as the amber center; Du Preez, 1965) that was entirely absent after treatment. A marked reduction of the platelet peak near

Figure 10. These five diamond crystals (1.90 to 4.45 ct) changed from brown to greenish yellow due to HPHT treatment by Novatek. Photos by Elizabeth Schrader

1360 cm^{-1} was also observed, possibly due to the destruction of a substantial number of platelets (and the associated formation of dislocation loops), as described by Woods (1986).

DISCUSSION

According to the standard phase diagram for carbon (e.g., Levin et al., 1964), temperatures above 1850°C at a pressure of 6 GPa are in the graphite stability zone, where diamond begins to transform into graphite. This transformation does not happen instantly, in bulk, at these conditions. Rather, crystal surfaces and fracture surfaces are affected first, resulting in the etching and pitting, as well as graphitization, that we saw in these samples. Collins et al. (2000) suggested that growth of diamond may also occur on the surfaces of crystals during HPHT treatment, if the diamonds are processed in graphite capsules; however, we did not observe any growth features in these samples. In addition, the expansion or contraction of included minerals during HPHT treatment could lead to the formation of tension cracks.

Although the etched surface can be polished

Figure 11. These spectra, taken before and after HPHT treatment by Novatek, provide additional insight into how this treatment transforms the color of brown type Ia diamonds. (A) The UV–Vis–NIR spectra show the development of strong absorptions by the H3 and H2 centers (503 and 985 nm), and a weak 637 nm line (related to the NV center). (B) The mid-infrared spectra show an insignificant change in the ratio of A to B aggregates (1333 to 800 cm^{-1}), the disappearance of a peak around 4166 cm^{-1} (the amber center) and a substantial reduction of the platelet peak (near 1360 cm^{-1}) after the HPHT treatment. A vertical expansion of 30× is used to highlight the peak associated with the amber center (see inset).

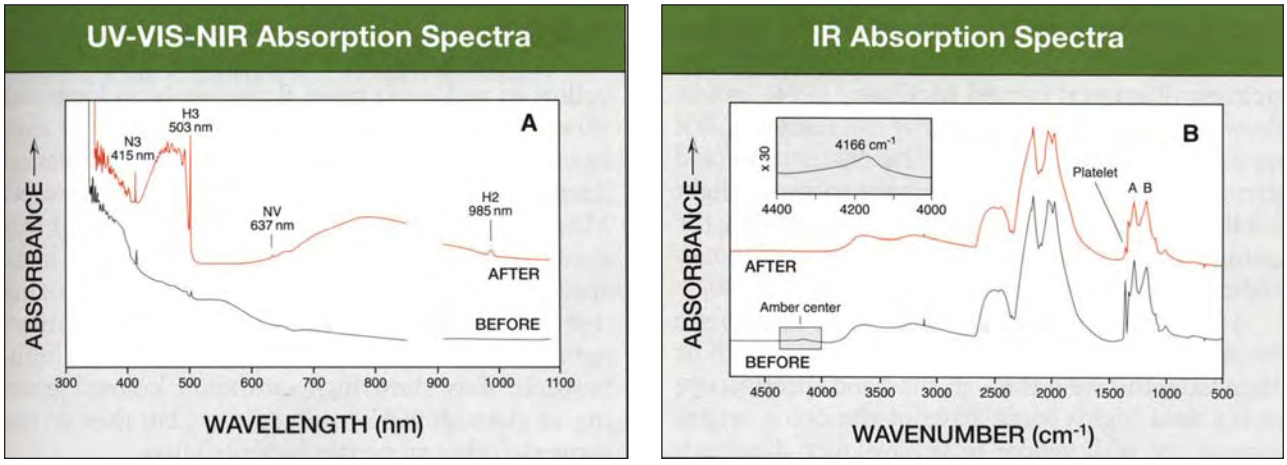

away, remnants sometimes remain at facet junctions and on naturals, and the outer portions of feathers sometimes are etched or graphitized (again, see figures 4 and 5). Experience is necessary to distinguish burned features from the many textures that natural etching produces on diamond. (See Koivula [2000] for photomicrographs of etched textures in natural, treated, and synthetic diamonds.) The presence of etched features or tension cracks is indicative of HPHT processes, but the fact that two samples had naturals that did not appear etched suggests that the lack of such features does not guarantee that a diamond is of natural color.

Brown to yellow graining is presumed to be intrinsic to most of these diamonds, before treatment as well as after. Unlike the type IIa GE POL diamonds that are HPHT treated to eliminate the brown color associated with their graining, most of these type Ia treated diamonds show yellow to brown graining. By comparison, many natural-color yellow, brown, or greenish yellow diamonds exhibit brown graining, but relatively few have yellow graining (Scarratt, 1982).

In our experience, only a fraction of diamonds with a brown to yellow body color exhibit any green luminescence to visible light, and in only some cases is this luminescence strong enough to affect the face-up color. Very high saturation of this combination of yellow and luminescent-green colors is quite rare in natural-color diamonds, although a few such diamonds are known (Moses, 1997).

The moderate-to-strong, chalky, greenish yellow to yellowish green luminescence to both long- and short-wave UV radiation shown by most of these samples provides a simple way to test for the possibility of HPHT treatment, especially for parcels of colored diamonds. In contrast, many natural-color yellow to brown diamonds with green transmission show a combination of blue and yellow fluorescence, often with the yellow emanating from brown graining (Kammerling and McClure, 1994); others show yellow or greenish yellow fluorescence, but typically with no chalkiness. The distribution (and strength) of the green luminescence to visible light is a less reliable indicator, since it is found along the graining both in these treated diamonds and in natural-color yellow to brown diamonds (Kane, 1980).

Although a spectrophotometer is needed to see the spectral details in sufficient completeness to be diagnostic, the view through the hand spectroscope yields data highly suggestive of the color origin. Natural greenish yellow to yellow-green diamonds show a distinct pair of lines at 494 and 503 nm (due to the H3 center), and typically show a weak to moderate absorption line at 415 nm (due to the N3 color center) as well (Maddison and Kammerling, 1993; Moses, 1997). If the diamond is cooled with freon or another apparatus (see, e.g., Hofer and Manson, 1981), a weak line at 595 nm sometimes can be observed (Scarratt, 1982). This spectrum stands in stark contrast to the dark 480–500 nm band, strong 503 nm line, and emission bands at 505 and 515 nm and/or weak 415 nm line displayed in the hand spectroscope by HPHT-treated diamonds in this color range.

Our spectral observations, especially those from before and after HPHT treatment (again, see figure 11), generally agree with those of Collins et al. (2000). However, only two of our samples showed the 1344 cm^{-1} absorption line reported by those authors. The destruction of the amber center by HPHT treatment is quite interesting, and unexplained at this time.

CONCLUSION

In March 1999, the diamond industry was startled by the news that General Electric Company had developed a process to remove color from brown type IIa diamonds. Similar HPHT technology is being used by several companies on brown type Ia diamonds to produce colors that range from greenish yellow to yellowish green and yellow to brownish yellow. Conclusive identification of these treated-color diamonds requires both infrared and low-temperature visible spectroscopy, but a number of gemological properties provide some indication of HPHT treatment.

These gemological properties typically include very high saturation and often darker tones of the color; internal yellow to brown graining; etched naturals or fractures, often containing graphite; tension cracks around crystalline inclusions; chalky greenish yellow to yellowish green fluorescence to long- and short-wave UV; and a strong line at 503 nm, a dark band from about 480 to 500 nm, and green emission lines at 505 and 515 nm visible in the spectroscope. Most of the treated diamonds we examined for this study showed several of these properties; a hand spectroscope is particularly useful for recognizing these colored HPHT treated diamonds. In contrast, natural diamonds with green "transmission" luminescence may show high saturation, colored graining, or greenish yellow fluorescence, but they do not show the other properties presented here.

Acknowledgments: The authors thank the following persons for loaning treated diamonds for this study: Dr. Tom Anthony of the General Electric Company, Schenectady, New York; David Hall of Novatek, Provo, Utah; and Joseph Menzies of Joseph M. Menzies Inc., New York. We also thank Matt Hall and Kim Rockwell of the GIA Gem Trade Laboratory for gathering some of the spectroscopic data. This research was supported in part by funds provided by DeBeers, Argyle Diamond Mines Pty. Ltd., and Jewelers' Circular Keystone *magazine.*

REFERENCES

Anthony T., Casey J. (1999) Research on diamonds at the General Electric Company. In T.M. Moses, J.E. Shigley, S.F. McClure, M. Van Daele, Observations on GE-processed diamonds: A photographic record, *Gems & Gemology*, Vol. 35, No. 3, p. 15.

Anthony T., Casey J., Vagarali S., Shigley J., Moses T., Hall M.S. (2000) GE/POL yellowish green diamonds enter the marketplace. *Professional Jeweler*, Vol. 3, No. 5, pp. 36, 38, 40-42.

Buerki P.R., Reinitz I.M., Muhlmeister S., Elen S. (1999) Observation of the H2 defect in gem-quality type Ia diamonds. *Diamond and Related Materials*, Vol. 8, pp. 1061–1066.

Clark C.D., Collins A.T., Woods G.S. (1992) Absorption and luminescence spectroscopy. In J.E. Field, Ed., *The Properties of Natural and Synthetic Diamond*, Academic Press, London, pp. 35–80.

Collins A.T., Kanda H., Kitawaki H. (2000) Colour changes produced in natural brown diamonds by high-pressure, high-temperature treatment. *Diamond and Related Materials*, Vol. 9, pp. 113–122.

De Weerdt F., Van Royen J. (2000) HPHT treated diamonds. *Antwerp Facets*, No. 34, pp. 36–37.

Du Preez L. (1965) Electron paramagnetic resonance and optical investigations of defect centres in diamond. Ph.D. thesis, University of the Witwatersrand, Johannesburg.

Evans T. (1992) Aggregation of nitrogen in diamond. In J.E. Field, Ed., *The Properties of Natural and Synthetic Diamond*, Academic Press, London, pp. 259–290.

Federman D. (2000) The three-minute rainbow. *Modern Jeweler*, Vol. 99, No. 3, pp. 34–38, 120–121.

Henn U., Milisenda C.C. (1999) Gemmologische Kurzinformationen: Ein neuer Typ farbbehandelter Diamanten. *Gemmologie—Zeitschrift der Deutschen Gemmologischen Gesellschaft*, Vol. 48, No. 1, pp. 43–45.

Hofer S.C., Manson D.V. (1981) Cryogenics, an aid to gemstone testing. *Gems & Gemology*, Vol. 17, No. 3, pp. 143–149.

Kammerling R.C., McClure S.F. (1994) Gem Trade Lab notes: Diamond with unusual color zoning. *Gems & Gemology*, Vol. 30, No. 2, p. 116.

Kane R.E. (1980) The elusive nature of graining in gem quality diamonds. *Gems & Gemology*, Vol. 16, No. 2, pp. 294–314.

Koivula J.I. (2000) *The Microworld of Diamonds: A Visual Reference Guide.* Gemworld International, Northbrook, IL, 157 pp.

Levin E.M., Robbins C.R., McMurdie H.F. (1964) *Phase Diagrams for Ceramists, Volume I (Figures 1–2066)*. American Ceramic Society, Columbus, OH, p. 47.

Maddison P., Kammerling R.C. (1993) Gem Trade Lab notes: Brown-pink diamond with "green graining." *Gems & Gemology*, Vol. 29, No. 3, pp. 198–199.

Moses T. (1997) Gem Trade Lab notes: Two noteworthy stones from the Americas. *Gems & Gemology*, Vol. 33, No. 1, pp. 54–55.

Moses T., Reinitz I. (1999) Gem Trade Lab notes: Yellow to yellow-green diamonds treated by HPHT, from GE and others. *Gems & Gemology*, Vol. 35, No. 4, pp. 203–204.

Reinitz I., Moses T. (1997) Gem Trade Lab notes: Treated-color yellow diamonds with green graining. *Gems & Gemology*, Vol. 33, No. 2, p. 136.

Scarratt K.V.G. (1982) The identification of artificial coloration in diamond. *Gems & Gemology*, Vol. 18, No. 2, pp. 72–78.

Shigley J.E., Fritsch E., Koivula J.I., Sobolev N.V., Malinovsky I.Y., Pal'yanov Y.N. (1993) The gemological properties of Russian gem-quality synthetic yellow diamonds. *Gems & Gemology*, Vol. 29, No. 4, pp. 228–248.

Templeman T. (2000) NovaDiamond introduces new enhancement. *Rapaport Diamond Report*, Vol. 23, No. 1, pp. 1, 29–30.

Van Bockstael M. (1998) Enhancing low quality coloured diamonds. *Jewellery News Asia*, No. 169, pp. 320, 322.

Woods G.S. (1986) Platelets and the infrared absorption of type Ia diamonds. *Proceedings of the Royal Society of London A*, Vol. 407, pp. 219–238.

A NEW LASERING TECHNIQUE FOR DIAMOND

Shane F. McClure, John M. King, John I. Koivula, and Thomas M. Moses

A new laser treatment for diamonds, which typically does not have a surface-reaching drill hole, recently entered the trade. For a better understanding of this new technique, observations were made on several round-brilliant-cut diamonds before and after treatment. Diamonds with dark inclusions near the surface are favored for this new method, which causes small cleavages to develop or expand around an inclusion. Once the cleavage reaches the surface, it serves as a conduit for the solution that is used to bleach the dark inclusion. Irregular, wormhole-like channels are used to widen the cleavage to facilitate entry of the bleaching solution.

In February 2000, researchers at the GIA Gem Trade Laboratory first encountered what appeared to be a new laser treatment for diamonds. We had heard rumors of a lasering technique developed in Israel that did not show the typical surface-reaching drill hole, but we had not yet seen examples. Our first encounter was a diamond submitted to the laboratory for a grading report. While examining the stone, one of the graders noted a cleavage (or "feather"—for the purposes of this article, we will use these terms interchangeably) with some unusual dark lines in the center. Careful microscopic examination revealed oddly formed channels within the feather that were clearly not of natural origin (see, e.g., figure 1). Their appearance suggested that a laser had been used to expand or widen the feather. These unusual channels were observed in several other diamonds submitted to the laboratory shortly thereafter, and we were convinced that these stones had been treated by the new lasering process. We published two brief reports on our initial observations (GIA News, 2000; McClure et al., 2000).

While we were investigating the origin of this treatment, *Gems & Gemology* editors received correspondence on the subject from Yoichi Horikawa of the Central Gem Laboratory in Tokyo. He reported the introduction of a new type of diamond treatment that broadened cleavages with a laser beam and was specifically adapted to remove "carbon" from within them. He also reported that the process was called the "KM treatment," with the initials referring to *Kiduah Meyuhad*, which means "special drill" in Hebrew. Another new laser drilling technique, which forms a channel of parallel drill holes, has recently been reported (see GIA News, 2000; Guptill et al., 2000), but will not be addressed in this article.

With traditional laser drilling, a hole is drilled into a diamond until it reaches the dark inclusion (figure 2; Crowningshield, 1970). The resulting

ABOUT THE AUTHORS

Mr. McClure (smcclure@gia.edu) is director of West Coast Identification Services, and Mr. Koivula is chief research gemologist, at the GIA Gem Trade Laboratory, Carlsbad, California. Mr. King is laboratory projects officer, and Mr. Moses is vice president of Research and Identification, at the GIA Gem Trade Laboratory, New York.

Acknowledgments: GIA thanks De Beers for financial support of this research project.

Gems & Gemology, *Vol. 36, No. 2, pp. 138–146.*

channel serves as a conduit for a strong acid (e.g., sulfuric or hydrochloric) to "bleach" the material or remove it altogether. The clarity grade may or may not be affected, but the resulting "white" appearance is generally considered more acceptable in the diamond trade than a dark spot that does not return any light (Pagel-Theisen, 1976). Since the early 1970s, laser drilling has been an accepted trade practice as long as it is disclosed.

In almost all of the approximately 40 to 50 diamonds we examined that appeared to be treated by this new process, we did not observe the surface-reaching drill hole that is normally associated with laser drilling. From our examination of these stones, we surmised that diamonds with shallow black or dark-appearing inclusions (such as various sulfides or graphite; see Koivula, 2000) with some type of associated tension fracture or cleavage were the most likely candidates for this procedure. One or more pulsed lasers focused on such an inclusion would produce sufficient heat to cause the inclusion to expand (and possibly even melt), and thus create enough stress to extend the cleavage to the surface. This now surface-reaching cleavage would provide an opening for the acids to enter the diamond and bleach or dissolve the inclusions. Note that it is not necessary to have a hole at the surface of a diamond to use a laser. The primary purpose of the hole is to allow entry of the bleaching solution, although it also allows the escape of gases created during the vaporization of the diamond. With this new treatment, the feather created by the laser permits entry of the solutions and allows any gases to vent.

To further investigate this theory, and the procedure itself, we submitted a carefully selected group of nine diamonds for treatment by this new technique, and documented their appearance before and after lasering (table 1). We also examined and photographed approximately 25–30 diamonds seen in the laboratory that had been treated by this method.

Figure 1. The appearance within feathers of unnatural, irregular, wormhole-like channels provided the first clue that a new laser treatment had entered the market. Photomicrograph by Vincent Cracco; magnified 63×.

Figure 2. Traditional laser drilling usually leaves a straight, tube-like channel that extends from the surface of the stone to a dark inclusion. Photomicrograph by John I. Koivula; magnified 20×.

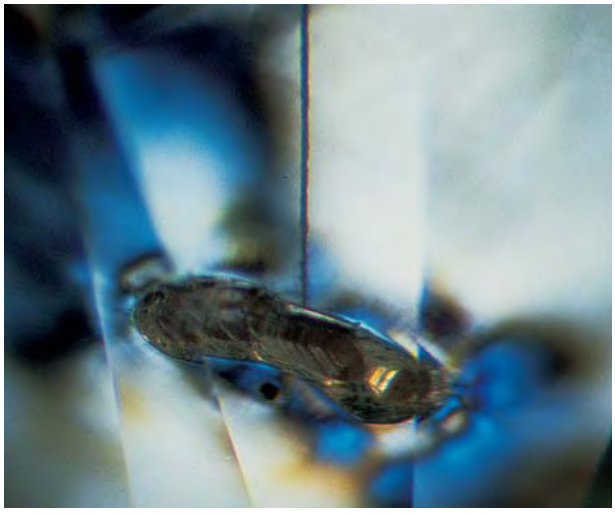

TABLE 1. Color and clarity of the nine round-brilliant-cut diamonds before and after treatment.

Sample number	Weight (ct)	Color grade[a]	Clarity before treatment	Clarity after treatment
1	0.30	F	I_1	I_1
2	0.31	F	SI_2	I_1
3	0.33	F	SI_2	Not treated[b]
4	0.50	I	SI_1	SI_2
5	0.58	J	SI_2	SI_2
6	0.51	K	SI_2	I_1
7	0.36	N	I_1	Not treated[b]
8	0.39	N	I_1	Not treated[b]
9	0.31	O	SI_1	SI_1

[a]*No change in color grade was noted following treatment.*
[b]*These three diamonds showed no evidence of treatment when they were returned.*

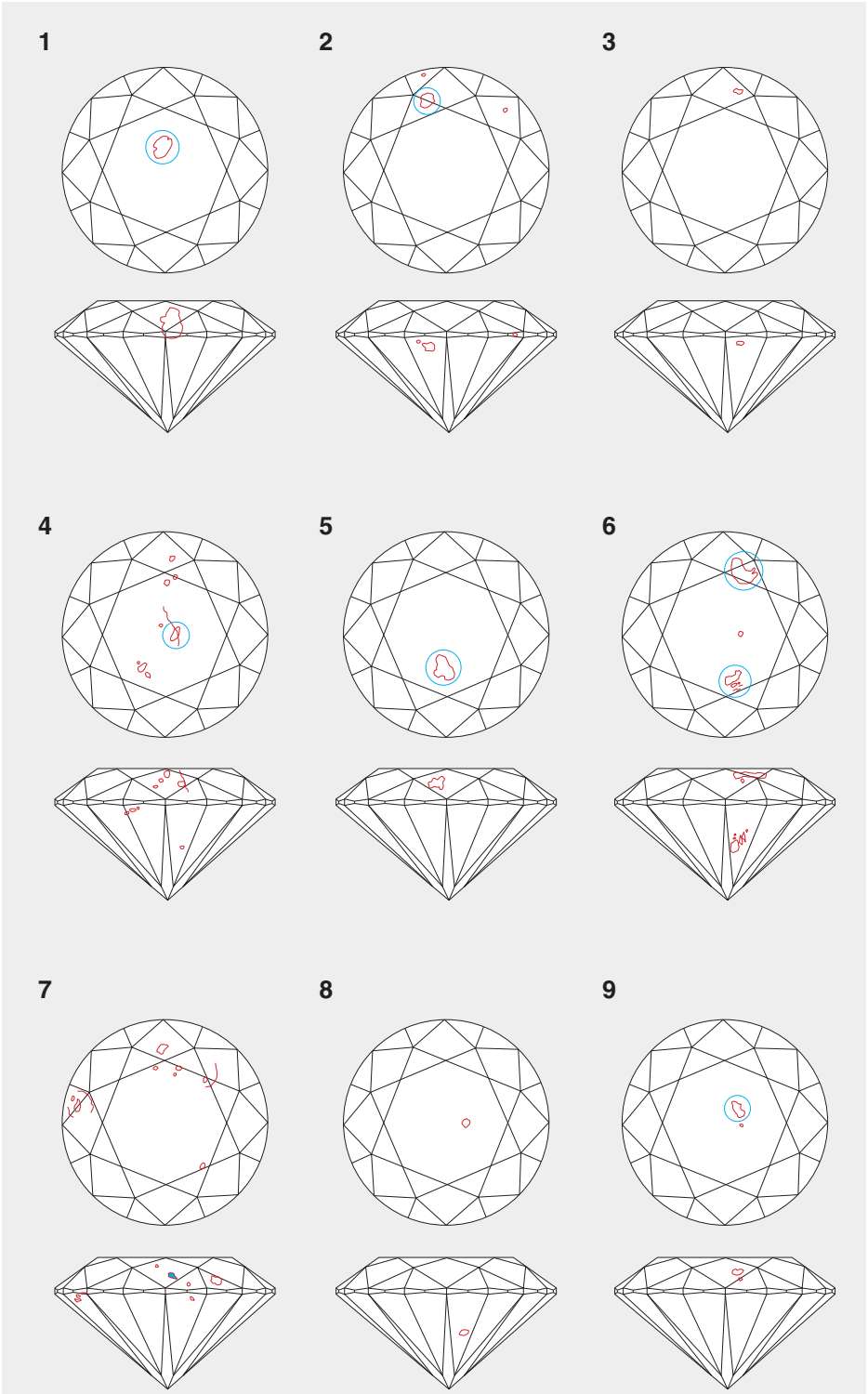

Figure 3. These plots were made on all nine diamonds in the test sample before laser treatment. Profile views are provided to illustrate the relative depth of inclusions within each stone. Note that when an included crystal is surrounded by a feather, it is plotted as one larger crystal. Following is a description of the key inclusions in each diamond and the treatment result. Those crystals that were affected by the treatment are circled in blue on the face-up view. (1) crystal with black feather—treatment created feather to surface of table; (2) crystal with black feather—treatment created feather to surface of pavilion; (3) black crystal with no feather—not treated; (4) crystal just under surface of table surrounded by black—treatment created small feather to surface of table, but several black crystals with no feathers were not treated; (5) two adjacent small crystals with black feathers—treatment created feathers to surface of table, but only one crystal was treated; (6) two large crystals with black feathers under crown and near pavilion—treatment created feathers to surface of crown and pavilion; (7) two small crystals with black feathers under bezel and edge of table, plus other crystals either not black or without feathers—not treated; (8) black crystal with no feather—not treated; (9) crystal with black feather—treatment created feather to surface of table. Plots by Joshua Cohn.

MATERIALS AND METHODS

All nine test diamonds were round brilliant cuts; they ranged from 0.30 to 0.58 ct. To test our hypothesis on the relevance of location in this process, we chose diamonds that had dark inclusions near the surface *and* deep within the stone (figure 3). Readily visible tension cracks were associated with some, but not all, of the dark inclusions. All of

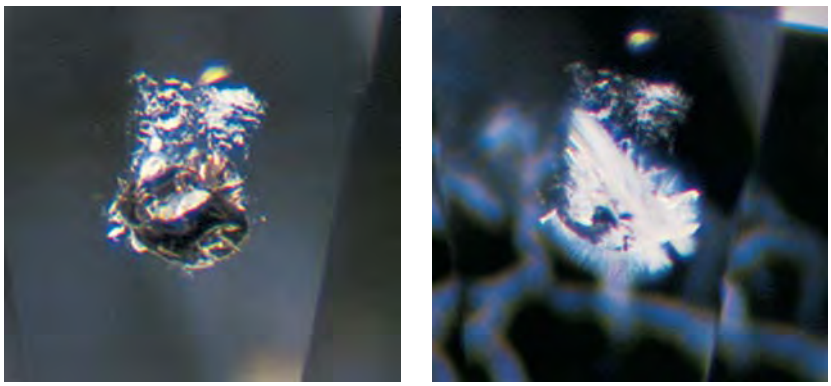

Figure 4. The first thing we noticed in those diamonds that did show evidence of treatment was the presence of new feathers leading from the inclusions to the surface of the stone. On the left we see a crystal surrounded by black feathers as it appeared before lasering in sample no. 2. After lasering (right), the inclusion is no longer black, but there is a bright new feather extending from the crystal to the surface. Photomicrographs by Shane F. McClure; magnified 40×.

these features were documented with photomicrographs, and the diamonds graded for color and clarity, before they were given to a third party to send out for treatment. On their return, the diamonds were once again photographed and graded. Our study of these samples mainly involved examination with a binocular microscope, under diverse lighting conditions, and photography with Nikon SMZ-10 photomicroscopes.

RESULTS

After the diamonds were returned, we examined them carefully, both face-up and in the table-to-culet position, using darkfield, brightfield, and fiber-optic illumination. We saw no evidence of treatment in three of the nine diamonds (nos. 3, 7, and 8 in figure 3 and table 1). Two of these three samples (nos. 3 and 8) contained a black crystal with no tension fractures that was located relatively deep within the stone. The third diamond (no. 7) contained two dark crystals with small tension fractures that were located near the surface of the crown. Five of the remaining stones had one treated inclusion, and the sixth (no. 6) had two, for a total of seven treated inclusions. One of these stones (no. 4) had several solid black inclusions—with no tension cracks—that were not treated. The black was completely removed from three of the treated inclusions (nos. 1, 4, and 5), and it was mostly removed from the remaining four.

One of the first features we noticed following treatment was the presence of new feathers (or extensions of preexisting feathers) at the treated inclusions (figure 4). In all six stones that showed evidence of treatment, mirror-like or transparent feathers were present where none had been before, connecting the original inclusion to the surface of the stone. These new feathers usually extended in directions unrelated to any preexisting feathers (figure 5). In two cases, several new feathers in different cleavage directions created a step-like progression to the surface of the diamond (figure 6).

All of the new feathers had irregular, unnatural-appearing channels similar to those we had noted

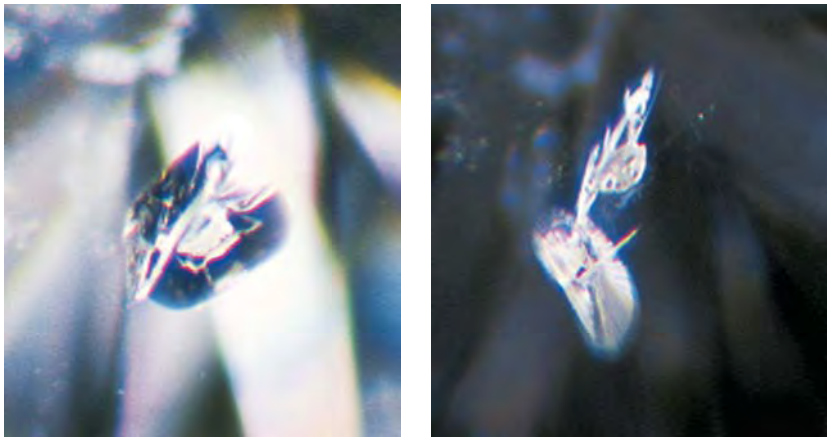

Figure 5. The most significant discovery in the treated diamonds is that some of the feathers created were new and not just extensions of preexisting feathers. The image on the left shows a black inclusion in sample no. 1 before treatment. After treatment (right), the black has been removed, but there is now a bright new feather extending from the tension crack around the crystal to the surface of the stone that is not an extension of the ones present before. Photomicrographs by Shane F. McClure; magnified 40×.

Figure 6. This treatment may be used to produce tiny cleavages that form a step-like progression from the inclusion to the surface of the diamond. In this way, the treater can take the shortest route to the surface, even if that route does not correspond to a cleavage direction. (Note that the single feature is duplicated here in a facet reflection.) Photomicrograph by Shane F. McClure; magnified 40×.

in the treated stones that had been submitted to the laboratory. These channels were usually present along the center of the feathers (figure 7). They ranged from fairly straight single lines to very convoluted multiple channels that resembled wormholes (see figures 1 and 8). They tended to be much narrower than the channels left by the traditional drilling procedure and appeared dark when viewed in transmitted light (figure 9). This typically black appearance in transmitted light often made them easier to find, since the reflective nature of the feathers sometimes made the channels difficult to see in darkfield (compare figure 9 to figure 6).

Figure 7. The treated samples (here, no. 5) always had channels—some straight and some irregular—down the middle of the new feathers; in some areas, these channels appeared black. Photomicrograph by Shane F. McClure; magnified 40×.

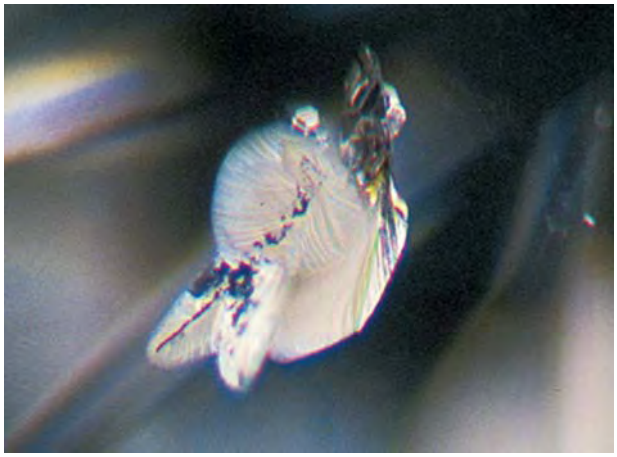

Four of the seven treated inclusions in the test diamonds had holes at the surface that were related to the treatment. These holes were located in the center of the induced feathers where they broke the surface of the stone. They were smaller and more irregular in shape than traditional laser drill holes, and appeared to be caused by the channels reaching the surface.

The appearance of most of the inclusions changed dramatically with the laser treatment, in that they no longer were dark or black (figure 10), although four inclusions were not completely bleached out and still had some minor black areas. One stone (no. 5) had two black inclusions (small

Figure 8. The wormhole-like channels took on a variety of appearances in these treated diamonds. These channels lead from the feather on the surface to a group of crystals and accompanying feathers. Note that the large crystal on the upper right has not been treated. Photomicrograph by Vincent Cracco; magnified 63×.

Figure 9. Most of the laser channels appeared dark in transmitted light. In some cases, such as with the step-like series of cleavages in figure 6, this was the best way to see them. Photomicrograph by Shane F. McClure; magnified 40×.

crystals with tension feathers) adjacent to each other under the table. After treatment, it appeared that the induced feather had reached only one of the inclusions, so that one was now colorless and the inclusion next to it was still black (figure 11).

One stone (no. 4) had a rectangular cavity in the center of the table—not present before treatment—where a piece of diamond had come out (figure 12). The lasering extended from the inclusion to the bottom of this cavity.

DISCUSSION

We believe that the three diamonds that did not show any evidence of enhancement (nos. 3, 7, and 8) were deemed unsuitable for this process because of the absence of tension cracks or because the dark inclusion was too deep within the host (again, see figure 3). It is possible that the one stone (no. 7) that had two small dark crystals with small tension cracks was not treated because these inclusions had minimal effect on the overall clarity of the stone. This would support our theory that the treatment works best on dark inclusions near the surface, as

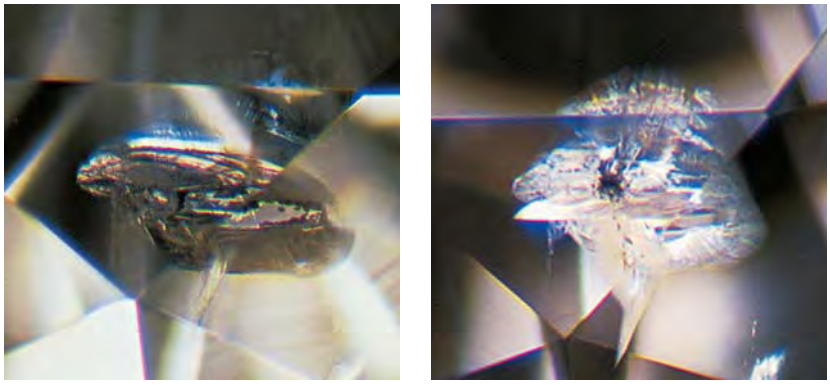

Figure 10. The new laser technique dramatically improved the appearance of most of the treated inclusions by removing the black coloration as seen here in sample no. 6. The view before treatment is on the left. Photomicrographs by Shane F. McClure; magnified 40×.

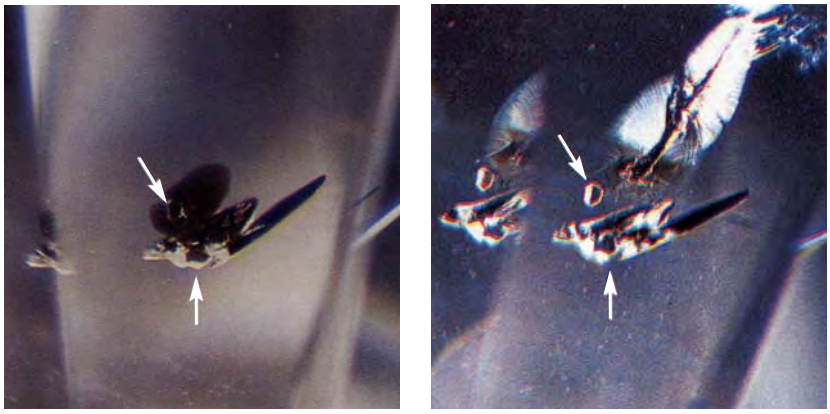

Figure 11. Before treatment (left), this diamond (sample no. 5) had two included crystals, both surrounded by dark feathers, that were adjacent to each other. After treatment (right), the feather at the top is no longer dark and the crystal is now clearly visible. However, the treatment did not reach the second inclusion, so it remains unchanged. Note the large, bright feather leading to the surface that was created by the treatment. Photomicrographs by Shane F. McClure; magnified 40×.

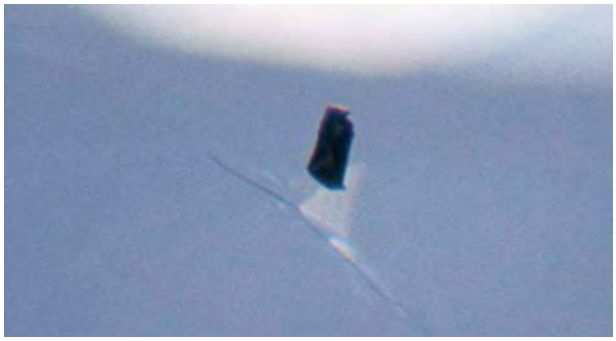

Figure 12. This cavity, which appears black in reflected light, was not present before the diamond (sample no. 4) was treated, which suggests that there is some risk involved in using this new technique. Photomicrograph by Shane F. McClure; magnified 40×.

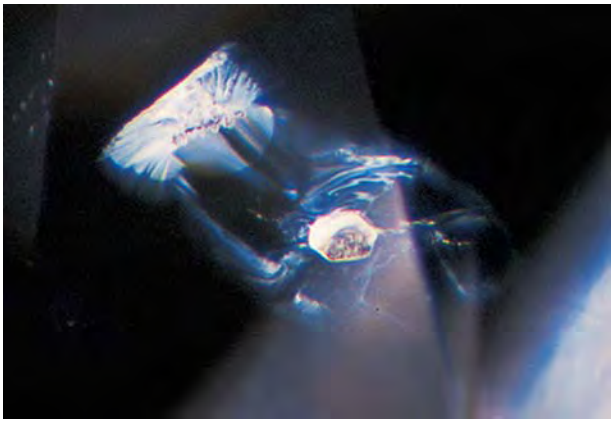

Figure 13. The new laser treatment has extended the feather surrounding the crystal in this stone to reach the surface. The preexisting feather is very transparent in this photo, while the new portion is much more reflective. Photomicrograph by Shane F. McClure; magnified 40×.

was the case with the remaining six diamonds. Inducing a surface-reaching feather from a deep inclusion would probably result in a clarity feature that was more noticeable than the original inclusion. One of the inclusions treated in our test sample (no. 6) was located deep in the diamond, but a feather was induced to the surface of the pavilion, allowing the inclusion to be bleached.

The most significant discovery from our sample diamonds was that the new treatment process not only extends existing feathers (figure 13), but it also creates entirely new ones. The presence of a step-like pattern in some of the treated feathers suggests that the treatment process is very controllable. By inducing small cleavages in this step-like pattern, the treaters seem to be able to join the inclusion to the surface by the most direct path, even if that path does not correspond to a cleavage direction of the diamond.

It appears that the wormhole-like channels were

Figure 14. It appears that the channels, shown here in the center of the bright area, serve to widen the feathers, thus allowing penetration of the acids used to bleach the inclusions. This is evidenced by the higher visibility of the areas immediately surrounding the channels. Photomicrograph by Vincent Cracco; magnified 63×.

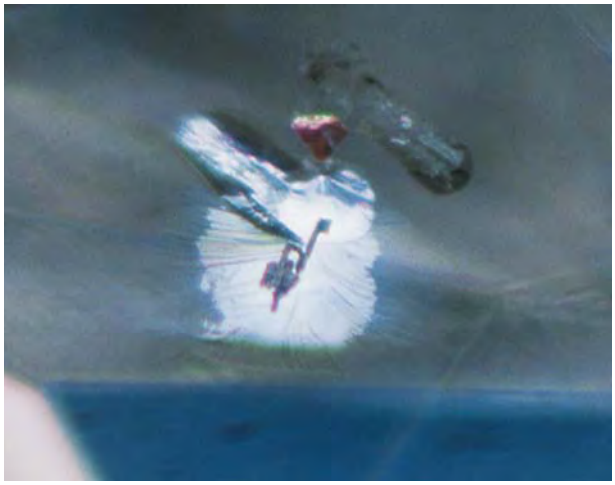

Figure 15. Several large feathers were present around an included crystal in this diamond when it was subjected to bleaching. Remnants of black material are still present in several of the feathers. Photomicrograph by Shane F. McClure; magnified 40×.

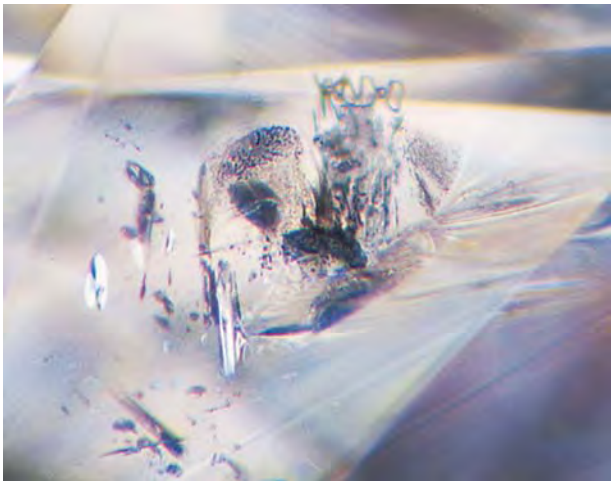

being used to widen parts of the induced feathers; this is evident in the microscope as areas of higher visibility within the feathers that immediately surround the channels (figure 14). This is undoubtedly being done to allow easier penetration of the acids used to bleach the inclusions. Nevertheless, the treatment was not always successful at removing all of the black material (figure 15). This may have been because the lasering was inadequate, or because the materials being removed respond differently to the bleaching process. For example, sulfides are easily attacked by acids, while graphite is not. The size of the inclusion does not appear to be a problem, however, as we have seen diamonds in which large crystals were dissolved with this technique (figure 16).

When we examined the new laser-treated diamonds that were submitted directly to the laboratory, we felt that one advantage to this treatment might be the lack of a hole at the surface to accept contaminants such as dirt or grease. Yet four of the treated inclusions in the test stones had holes that reached the surface. This inconsistency could be because the stones in our test sample were relatively small. Most of the diamonds treated in this fashion that have come through the laboratory have weighed between 1 and 2 ct.

Clearly the cavity in sample 4 was caused by the treatment, which indicates that there is some risk involved in this new technique. It is reasonable to assume that a treatment that involves controlled cracking of a stone could result in such undesired breakage. In fact, as table 1 shows, three of the six samples dropped one clarity grade after treatment because of the new clarity characteristics (e.g., feathers, cavity) created by the treatment.

Figure 16. The original large crystal in this diamond was completely dissolved by the treatment. The induced feather created to reach the crystal is seen just above the inclusion. Note that there are several small crystals around the remnant of the larger one that are still black, because no feathers were induced to reach them. Photomicrograph by John I. Koivula; magnified 30×.

Detection. Identification of this treatment, as with traditional laser treatments, is entirely dependent on a thorough microscopic examination. The diamond must be examined both face-up and in the table-to-culet position using a variety of lighting conditions: darkfield, brightfield, and fiber-optic illumination. Look for the presence of one or more of a number of features in making the identification. The treatment may appear as a mirror-like or transparent feather that extends from an inclusion to the surface of the stone, usually at an angle completely different from the direction of the preexisting internal cleavage. Note that these feathers are often transparent and may not be visible in certain

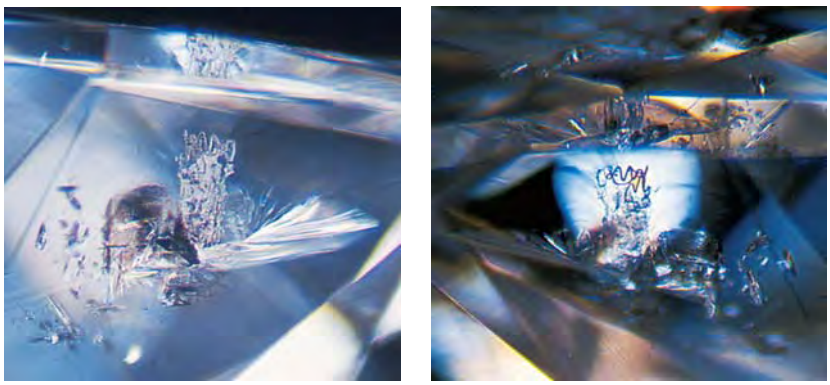

Figure 17. The use of different lighting conditions and various viewing angles is important in detecting this treatment. The wormhole-like channels are clearly seen in the photo on the left, but not the induced feather in which they are contained. By varying the position of the stone, light can be made to reflect off the feather, so that it is easily seen (right). Photomicrographs by Shane F. McClure; magnified 40×.

Figure 18. The internal channels became very difficult to see when light was reflected off the host feather, as is the case with the top half of the feather shown here. Note, though, that the widening of the feather is clearly visible. Photomicrograph by Shane F. McClure; magnified 40×.

lighting conditions (figure 17). The cracks themselves are not unknown in untreated diamonds, but their positioning makes them suspect.

There are usually one or more small channels in the center of the cleavage plane that may be relatively straight or very convoluted and often resemble wormholes. These channels may appear black or white in darkfield illumination, but are usually dark in brightfield. Often they are not visible when light is reflecting off the surface of the host feather, which indicates that they are completely contained within the feather (figure 18). Such channels are not seen in untreated diamonds. In some instances, however, the channels are so convoluted that they may be difficult to recognize (again, see figure 8). The treatment also may appear as a series of small step-like cleavages that are close together and have a very unnatural appearance. Typically, they are connected by numerous wormhole-like channels that are best seen in transmitted light (again, see figure 9).

This treatment was very difficult to detect in some diamonds, both in our study sample and in those that came through the lab. This was usually because the distance between the inclusion and the surface of the stone was short, so the features generated by the laser were small and difficult to discern. Also, if an inclusion is very close to the surface of a faceted diamond, then the number of effective viewing angles is greatly reduced, which further increases the difficulty of detecting the treatment.

Laboratory Reporting on Laser Drilling. GIA has disclosed laser drilling on its diamond grading reports since first documenting the process in 1970 (Crowningshield, 1970). To draw attention to its presence, "laser drill hole" is listed first in the key to symbols on GIA's Diamond Grading and Diamond Dossier reports. In those cases where lasering techniques do not result in surface-reaching drill holes, the GIA Gem Trade Laboratory discloses the treatment in the "Comments" section of its reports with the statement "Internal laser drilling is present."

CONCLUSION

This new lasering technique eliminates the drill channel associated with traditional laser drilling by opening or expanding a cleavage to the surface of the diamond to accommodate entrance of a bleaching solution. The resulting feather has a more "natural" appearance than the traditional laser drill channel. Identification of this new laser treatment requires careful microscopic examination with a variety of lighting techniques. It can be recognized by the presence of transparent, mirror-like feathers that contain unnatural-looking irregular channels and connect internal inclusions to the surface of the stone. Regardless of the technique involved, it is critical to the integrity of the diamond industry that treatments such as this be properly disclosed at every level from treater to final consumer.

REFERENCES

Crowningshield G.R. (1970) Laser beams in gemology. *Gems & Gemology*, Vol. 13, No. 7, pp. 224–225.

GIA News (2000) GIA identified new laser drilling treatment. www.gia.edu/news, posted April 14.

Guptill M., Quinn E.P., Tashey T.E. (2000) Laser-drilling in diamonds: A new technique. *Professional Gemologist*, Vol. 3, No. 1, p. 8.

Koivula J.I. (2000) *The Microworld of Diamonds: A Visual Reference Guide.* Gemworld International, Northbrook, IL, 157 pp.

McClure S.F., Koivula J.I., Moses T.M. (2000) Detecting new laser drilling techniques. *Rapaport Diamond Report*, Vol. 23, No. 16, May 5, pp. 1 et passim.

Pagel-Theisen V. (1976) On lased diamonds. *Börsen Bulletin*, September.

NEW FILLING MATERIAL FOR DIAMONDS FROM OVED DIAMOND COMPANY: A PRELIMINARY STUDY

By James E. Shigley, Shane F. McClure, John I. Koivula, and Thomas M. Moses

Diamonds filled with a new glass formulation (XL-21) are being marketed by the Oved Diamond Company. These diamonds are readily identifiable as treated by the intense flash-effect colors seen with magnification. Durability testing on a small number of these treated diamonds indicates that this filler material is more stable to conditions of normal jewelry repair, such as direct heating with a torch, than the filler material produced by the Goldman Oved Company a decade ago. Nevertheless, some damage to the filler was observed in half the new Oved diamonds that were subjected to a standard prong retipping.

A number of comprehensive reports have been written on the characterization and identification of filled diamonds, most in the late 1980s and early to mid-1990s (see, e.g., Kammerling et al., 1994). Since then there have been few new developments in this area. Earlier this year, however, the Oved Diamond Company announced that they intended to market filled diamonds using a new glass formulation (referred to as "XL-21"; figure 1). Oved represented this material as being an improvement on past filler substances, with respect to having a greater resistance to heat damage during normal jewelry repair procedures; the company also stated that all of the new filled stones they sell will have an "Oved" logo inscribed on the bezel facet ("Oved announces . . . ," 2000; Weldon, 2000). This article will describe the visual characteristics of this new product, as well as report on the results of preliminary durability testing.

ABOUT THE AUTHORS

Dr. Shigley is director at GIA Research, Carlsbad. Mr. McClure is director of Identification Services, and Mr. Koivula is chief research gemologist, at the GIA Gem Trade Laboratory, Carlsbad. Mr. Moses is vice president of Research and Identification at the GIA Gem Trade Laboratory, New York.

Please see acknowledgments at the end of the article.

Gems & Gemology, Vol. 36, No. 2, pp. 147–153.

BACKGROUND

The clarity treatment of diamonds by filling surface-reaching cleavages or breaks with a high–refractive index glass began in the late 1980s (see, e.g., Everhart, 1987, 1989). Within a short time, this treatment became widespread. Concerns about the identification of these treated diamonds, and about their durability during jewelry manufacturing or repair situations, led to a series of articles that described this material (Koivula et al., 1989; Scarratt, 1992; Nelson, 1993, 1994; Kammerling et al., 1994; Nassau, 1994; McClure and Kammerling, 1995).

In recent years, however, both the greater availability of lower-clarity diamonds for treatment and

Figure 1. These four diamonds (0.35 to 0.44 ct) were all treated with a new filler formulation developed by the Oved Diamond Company. Photo by Maha Tannous.

the gradual acceptance of filled diamonds in the marketplace have contributed to ongoing efforts by manufacturers to develop more-durable filler substances. Several companies have been working to improve the physical properties of the glass filler used in this kind of diamond treatment. The Oved Diamond Company is the first of these to announce the commercial production of what they claim to be a significantly more heat-durable filler material. In their advertising (see, e.g., page 26 of the May 16, 2000, issue of *National Jeweler*), they state specifically that this new treatment "allows our clarity enhanced diamonds to withstand a jeweler's torch for all normal work—and come out unchanged. Which means that you can re-size and re-tip our diamonds without damaging the treatment."

MATERIALS AND METHODS

For this study, we examined 18 diamonds treated with the XL-21 filler substance. Fourteen of these were obtained directly from Oved, while the remainder were obtained from Oved through a third party. The diamonds, all round brilliants, ranged from 0.35 to 2.25 ct. For comparison purposes only, we also examined four diamonds (0.49–0.61 ct), obtained from Jonathan Oved, that had been treated earlier by the Goldman Oved Company using an older filler substance of a different composition.

We examined all of these samples with a binocular microscope, and photographed the distinctive visual features with Nikon SMZ-10 and SMZ-U photomicroscopes. We also qualitatively analyzed the chemical composition of five samples (one with the older filler substance from Goldman Oved, and four—obtained directly from Oved—with the new XL-21 glass filler) using a Tracor Spectrace 5000 energy-dispersive X-ray fluorescence (EDXRF) system. The operating conditions selected were appropriate for detecting the heavy-atomic-weight elements anticipated to be present in the high-R.I. glass filler substance.

To get a preliminary idea of the durability of the new filler substance, we subjected some of the new Oved treated diamonds to a typical jewelry repair procedure—retipping of a prong—and direct thermal testing. The diamonds were examined with magnification after each test to check for possible damage to the filler substance. For each of these procedures, a Goldman Oved diamond containing the older filler compound was also tested at the same time and under the same conditions for comparison purposes.

For the retipping procedure, we had each of eight diamonds (five directly from Oved, and three from third parties) mounted in a 14K yellow gold solitaire ring with a white gold four-prong head. For each ring, one prong was filed to form a flattened area to simulate wear, and this prong was retipped by a highly experienced bench jeweler. First, the diamond was given a firecoat of a saturated solution of denatured alcohol and boric acid powder. Next, a minute amount of fluxed solder was flowed onto the flattened area of the prong. A small amount of 14K white gold was melted into a ball, flattened into a bead, and then fluxed and soldered into place on the flattened prong with a standard torch using natural gas and compressed oxygen. After this replacement prong was soldered, the ring was cooled in air to prevent thermal shock, and then placed for one minute in a hot pickling solution (temperature between 49° and 60°C [120° and 140°F]) made of Sparex #2. The ring was then placed in an acid-neutralizing bath and, last, rinsed with water. Although there are many procedural variables that are difficult to keep constant from one sample to the next (such as the length of time the torch is placed near the diamond, the exact temperature of the flame, and the extent and location of filled areas in the different diamonds), efforts were made to standardize these variables as much as possible in the experiments we conducted.

To determine the temperature at which visible damage to the filler material would occur, we placed three filled diamonds (two directly from Oved, and the other from a third party; each held in a refractory crucible) in the hot zone of a Blue M model M10A-

1A Lab Heat muffle furnace. The temperature of the furnace was raised in 50°C increments, beginning at 100°C and extending up to about 750°C; the samples were heated in air at each temperature for approximately 15 minutes, and then cooled and examined for damage. The accuracy of temperature measurements in this furnace was estimated to be within ±20°C of the selected value.

RESULTS AND DISCUSSION

Visual Appearance and Magnification. Of the 18 samples treated with the XL-21 filler, 10 (eight from Oved, and two from third parties) did not exhibit the identifying "Oved" logo inscription on a bezel facet. According to Jonathan Oved (pers. comm., June 2000), the diamonds provided directly to GIA had not yet been sent for laser inscription. This also may have been the case with some of the earlier treated diamonds (these two third-party stones were obtained in April). On the eight diamonds that did have the inscription, it was seen easily with 10× magnification (figure 2).

As was reported for Yehuda filled diamonds as early as 1989, the most characteristic visual feature of diamonds filled with such a glass is the flash effect (see, e.g., Koivula et al., 1989; and the report on Yehuda, Koss, and Goldman Oved treated diamonds in Kammerling et al., 1994). This was also the case with the new Oved diamonds. Flash-effect colors are best seen with magnification (binocular microscope or loupe) and a focused beam of intense light. In our Oved samples, the flash effect was typically violetish blue to bluish green in brightfield and yellow to reddish orange in darkfield illumination (figure 3). These optical effects appeared brighter and more intense than we had observed in the Goldman Oved samples with the older filling material (see Kammerling et al., 1994).

In general, the breaks in the new samples were completely filled, except for small areas at the surface. When examined with magnification, these areas of incomplete filling resembled scratches (figure 4), as was reported for the older material (Kammerling et al., 1994, p. 158). Occasionally, the filled breaks had a slightly hazy or cloudy appearance, and some revealed a noticeable flow structure (figure 5). In several instances, the yellow to greenish yellow color of the filler was evident in large open cavities that were filled with the glass (figure 6). In one diamond, a filled laser drill hole was visible (figure 7).

We also noticed localized areas within several filled breaks where the glass was partially devitrified (i.e., it was beginning to crystallize, as evidenced by the presence of numerous tiny, elongate colorless crystals in intersecting arrangements; see figure 8). Trapped gas bubbles were present in many of the filled areas. While most were minute, a few in one diamond were almost eye visible. It is interesting to note that several of the diamonds showed a relatively even distribution of similar-size gas bubbles (figure 9). In contrast, the gas bubbles in the

Figure 2. Oved announced that the "Oved" logo would be inscribed on a bezel facet of every diamond sold with the new filler. Photomicrograph by John I. Koivula; magnified 40×.

Figure 3. This large filled break displays the various flash-effect colors that were typically seen in the new Oved glass-filled diamonds. Against a bright field, these colors are violetish blue; against a dark field, they are yellow or reddish orange. The colors are seen here against adjacent bright and dark backgrounds due to the orientation of the break relative to the facet arrangement. Photomicrograph by James E. Shigley; magnified 15×.

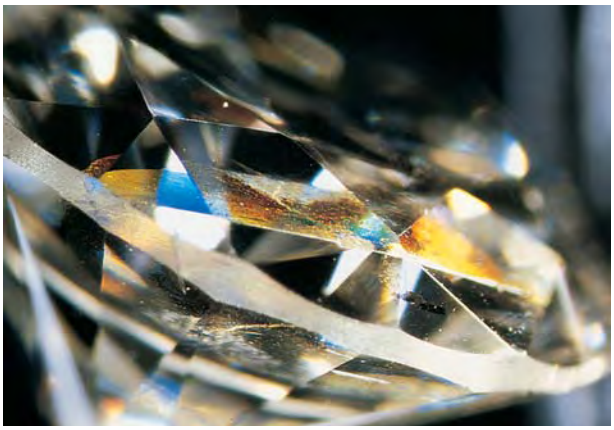

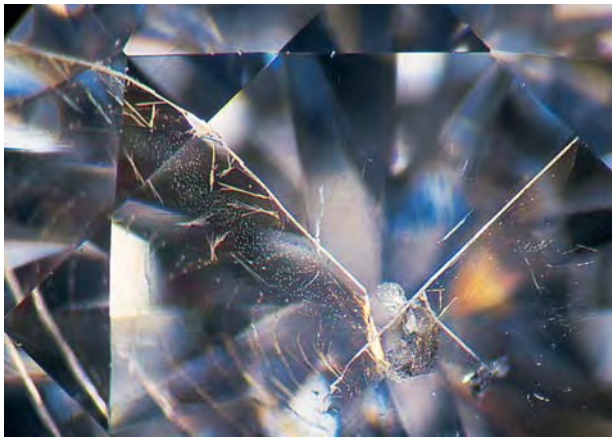

Figure 4. This break in a new Oved filled diamond displays small, unfilled areas at the surface of the stone that resembled scratches. Photomicrograph by Shane F. McClure, magnified 25×.

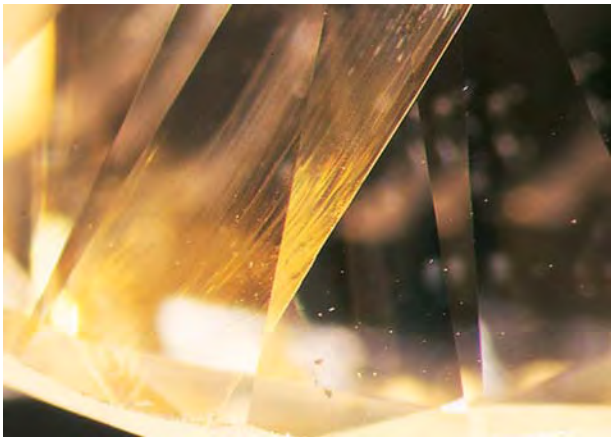

Figure 5. In some of the filled breaks, a distinct flow structure was seen. Photomicrograph by James E. Shigley; magnified 10×.

older Goldman Oved treated diamonds tended to form irregular, fingerprint-like patterns (Kammerling et al., 1994).

The filled areas were much more visible in the new Oved samples than in the old Goldman Oved treated diamonds. They were not difficult to locate, even without supplemental illumination. The easier visibility of the filled areas in the new material could be a result of the stronger flash effect, which makes these areas more apparent. It may also be that the refractive index of the new filler is not as close to that of diamond.

Figure 6. The greenish yellow color of the new filler is readily apparent in this filled cavity on the table facet of an Oved filled diamond. When present in a narrow cleavage, however, the glass appears colorless. Photomicrograph by John I. Koivula; magnified 15×.

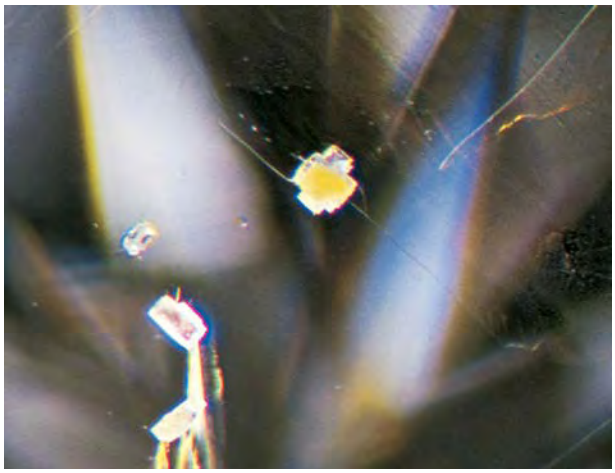

Chemical Composition. Using EDXRF analysis, we detected the presence of lead (Pb) and bromine in a Goldman Oved diamond with the older glass filler (similar to the results in Kammerling et al., 1994, p. 161). In contrast, EDXRF analyses of four Oved diamonds filled with the new XL-21 glass formulation revealed both Pb and bismuth (Bi). (Typically, glasses also contain lighter atomic-weight elements, but such elements were not detected with the analytical conditions we used, or could not be detected at all by this technique.) Pb and Bi were the same two elements found in analyses of Yehuda filled diamonds (Koivula et al., 1989, p. 79; Kammerling et al., 1994, p. 161).

Durability Testing. Of the eight Oved filled diamonds that were subjected to the retipping procedure, four (two from Oved, and two from third parties) displayed minor damage in the form of lost filler material. This created unfilled areas within the fractures that appeared highly reflective (see, e.g., figure 10). The remaining four diamonds (three from Oved and one from a third party) exhibited no visible damage after the retipping procedure. Consistent with our experience in the early 1990s, the filler in the older Goldman Oved stone that was subjected to the same retipping procedure suffered major damage in the process. Consequently, the new Oved filler performed better in the retipping experiments than did the older Goldman Oved filling material.

Note that a number of variables may affect the retipping results. These include the size and width of the glass-filled breaks, their location relative to the area of the jewelry piece being repaired, the size of the diamond (our test samples ranged from 0.37

to 1.34 ct), and the experience (skill) of the bench jeweler. This skill level is critical for the soldering technique used and controlling the torch in the soldering operation. In addition, the nature of the gold solder will have an impact. (We used 14K "easy" white gold solder in our study, with a flow temperature of 754°C [1390°F].) Platinum solders would always have a higher flow temperature. However, some 14K solder as well as higher-karat gold—depending on the manufacturer's formula (alloy)—may have a higher *or lower* flow temperature (S. Kysilka, pers. comm., 2000).

Also, in recent communications with the authors, Jonathan Oved stated that the company uses approximately six glass formulations, each of which contains different mixtures of components, to enhance various kinds of clarity features. We speculate that this reported variation in glass chemistry could result in slight differences in the physical properties of the filler substance. Consequently, we believe that it is still advisable to remove *any* filled diamond from its setting prior to undertaking repair work that involves heating. Also, inasmuch as two of the third-party Oved diamonds did not have the "Oved" laser inscription, and other treaters do not offer such an inscription, all diamonds should be checked for the presence of a filler before they are subjected to any jewelry manufacturing or repair procedure.

Heating of a Goldman Oved diamond (i.e., with the older filler) in a muffle furnace resulted in significant damage to the glass filler at about 400°C. Heating of the three new Oved diamonds also produced major damage, but at a much higher temperature, near 700°C. A significant amount of filler material was lost, some of it depositing on the surface of the stone along the break (see figure 11). At this temperature, the diamonds themselves also showed signs of heat damage.

Figure 7. This laser drill hole was filled by glass during the Oved treatment process. Photomicrograph by Shane F. McClure; magnified 40×.

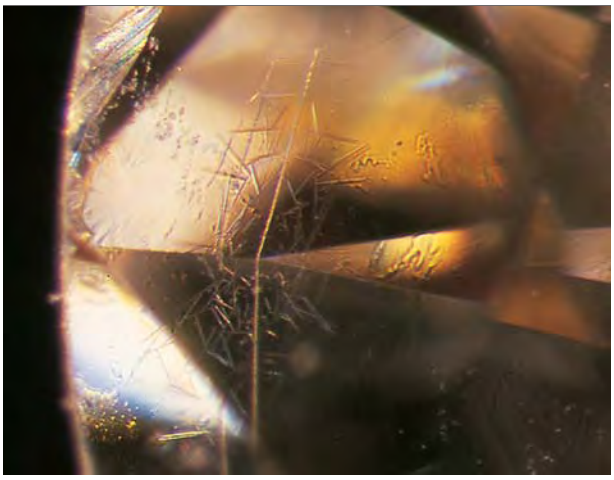

Figure 8. Arrangements of elongate, intersecting colorless crystals were seen in filled breaks in several of the diamonds where the glass was partially devitrified. Photomicrograph by James E. Shigley; magnified 15×.

Yehuda Diamonds. As we were finishing this study, the Yehuda Diamond Company sent us five diamonds that they reportedly had filled with a temperature-resistant substance. Ron Yehuda stated that this formulation had been used on an experimental basis by their company in the mid-1980s,

Figure 9. In addition to a group of intersecting colorless crystals, this break in a new Oved filled diamond shows a pattern of gas bubbles that are relatively evenly dispersed. Photomicrograph by John I. Koivula; magnified 40×.

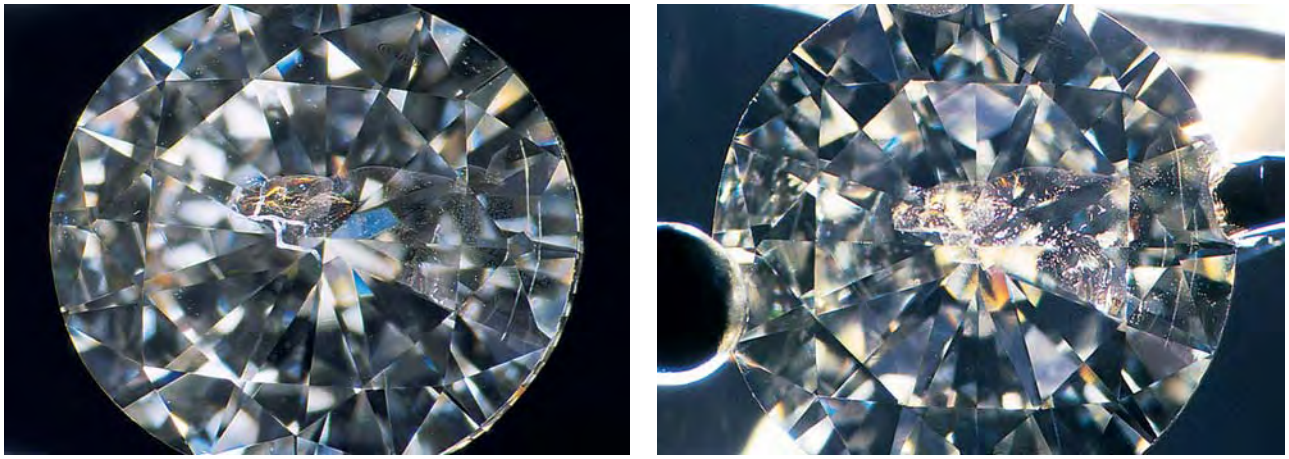

Figure 10. Four of the eight Oved diamonds tested showed minor damage after retipping. The photo on the left shows one of these diamonds (1.03 ct) before retipping. After the procedure (right), the glass-filled fractures showed a loss of filler that appears as reflective areas within the fractures. Photos by John I. Koivula (left) and Shane F. McClure (right).

but was not used commercially (pers. comm., 2000). Due to lack of time, we were not able to subject all of these stones to the durability tests that were performed on the Oved filled diamonds. However, we did test two of them by the retipping procedure, and a third by controlled heating in a muffle furnace, as described above. Of the two stones that were subjected to the retipping procedure, one showed no damage and the other had moderate damage. However, the stone that was subjected to controlled heating in the furnace showed damage at 400°C.

Mr. Yehuda also supplied seven filled diamonds that he had obtained recently from the Oved Diamond Company through a third party (R. Yehuda, pers. comm., 2000). All seven stones were laser inscribed with the Oved logo. We subjected two of these samples to the retipping procedure: One showed major damage, and the other showed minor damage.

CONCLUSION

The new Oved glass-filled diamonds typically exhibit intense flash-effect colors, which make them readily identifiable by members of the jewelry trade. Oved states that they also will inscribe their logo on the bezel facets of all these new filled diamonds, although 10 of the 18 Oved diamonds in our test sample (including two obtained from Oved by a third party in the diamond trade), did not have this logo.

Figure 11. Note the filled break (with a yellow flash effect) along the right edge of this 0.35 ct Oved filled diamond before it was subjected to durability testing (left). After the diamond was heated in a muffle furnace (in air) for 15 minutes at almost 700°C, damage is evident in the filled area (right), as well as in the diamond itself (seen here as small whitish areas on the surface). Photomicrographs by John I. Koivula.

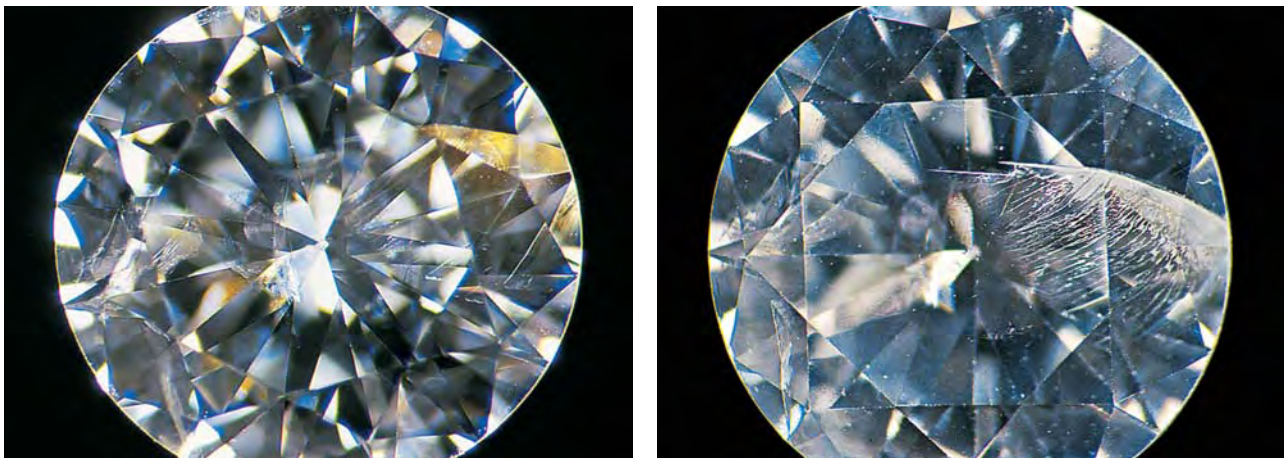

Durability testing of a few of the new Oved filled diamonds indicates that they are more stable to direct heat than the filled diamonds marketed earlier by Goldman Oved. Four of the eight new Oved diamonds were unaltered during the retipping procedure, and the other four sustained only minor damage. Nevertheless, we recommend that care be taken with all filled diamonds and, in particular, that all diamonds identified as containing a filler should be removed from the setting when a repair procedure requires heat.

Acknowledgments: The authors thank Jonathan Oved of Oved Diamond Company, New York, for providing study samples and information. Sherrie Kysilka and Larry Lavitt, of GIA Education's Jewelry Manufacturing Arts Department, Carlsbad, performed the durability testing. Sam Muhlmeister, of the GIA Gem Trade Laboratory, Carlsbad, carried out the EDXRF chemical analyses.

GIA thanks De Beers and Argyle Diamond Mines Pty. Ltd. for their financial support of this research project.

REFERENCES

Everhart J. (1987) Diamond dealers balk at disclosure of new treatment. *National Jeweler*, October 1 Vol. 33 No. 2, pp. 1, 86.

Everhart J. (1989) Diamond treatment that removes flaws hits U.S. market. *National Jeweler*, January 16 Vol. 31 No. 17, pp. 1, 33.

Kammerling R.C., McClure S.F., Johnson M.L., Koivula J.I., Moses T.M., Fritsch E., Shigley J.E. (1994) An update on filled diamonds: Identification and durability. *Gems & Gemology*, Vol. 30, No. 3, pp. 142–177.

Koivula J.I., Kammerling R.C., Fritsch E., Fryer C.W., Hargett D., Kane R.E. (1989) The characteristics and identification of filled diamonds. *Gems & Gemology*, Vol. 25, No. 2, pp. 68–83.

McClure S.F., Kammerling R.C. (1995) A visual guide to the identification of filled diamonds. *Gems & Gemology*, Vol. 31, No. 2, pp. 114–119.

Nassau K. (1994) On diamond-filling glasses and Nelson's speculations. *Journal of Gemmology*, Vol. 24, No. 3, pp. 183–184.

Nelson J.B. (1993) The glass filling of diamonds, part 1: An explanation of the colour flashes. *Journal of Gemmology*, Vol. 23, No. 8, pp. 461–472.

Nelson J.B. (1994) The glass filling of diamonds, part 2: A possible filling process. *Journal of Gemmology*, Vol. 24, No. 2, pp. 94–103.

Oved announces new clarity enhancement process (2000). *Rapaport Diamond Report*, Vol. 23 No. 16, May 5, p. 7.

Scarratt K. (1992) The clarity enhancement of diamonds. *Diamond International*, No. 19, pp. 45–58.

Thank You, Donors

The Treasured Gifts Council, chaired by Richard Greenwood, was established to encourage individual and corporate gifts-in-kind of stones, library materials, and other non-cash assets that can be used directly in GIA's educational and research activities. Gifts-in-kind help GIA serve the gem and jewelry industry worldwide while offering donors significant philanthropic and tax benefits. Treasured Gifts Awards are presented to those who have given gifts valued at $10,000 or more. We extend a sincere thank you to all those who contributed to the Treasured Gifts Council in 1999.

$100,000 or more
William and Jeanne Larson
John and Laura Ramsey
Zvi and Rachel Wertheimer

$10,000 or more
Daniel and Bo Banks
Betty Chachkes
Henry and Gina Haimsohn
Elena Villa Hamann
Stanley J. Marcus, G.G.
P. Lancon, S.A.
D.G. and Helen Parisi
Ramsey Gem Imports, Inc.
Dr. Jules R. Sauer
Robert H. Vanderkay
Zvi and Rachel Wertheimer

$5,000 to $9,999
A.L. David & Company
American Pearl Company
Ben Bridge Jewelers
Ebert & Company
Pala International, Inc.
Michael M. Scott
Sirius Ltd.

$2,500 to $4,999
Penny M. Barreto, G.G.
Rick Canino
Gebrüder Bank Gemstones
Ben Jen Hoo, G.G.
Scott D. Isslieb, G.G.
Harry G. Kazanjian & Sons, Inc.
Nellie R. Lomprey
Betsy Ross Marcinkus
Benjamin Pecherer
The Texas Lone Star Alumni Chapter
Bear R. Williams

$1,500 to $2,499
Charles I. Carmona, G.G., A.S.A.
Contract Services International
Richard T. Liddicoat, Jr., G.G.
Patricia Miller

$1,000 to $1,499
Landstroms' Black Hills Gold
Ronald H. Ringsrud, G.G.
John Sinkankas, Ph.D.

$500 to $999
Victor Arslanyan
Basis
W. Constantin Wild & Co.
William F. Mosher, G.G., C.G.
Nizam Peters
Preusser Jewelers
Fred W. Rowe
Steel Skin
Velma Touraine

$250 to $500
Christopher Amo, G.G., F.G.A.
Carl E. Burris
Deutsche Gemmologische Gesellschaft E.V.
David Frizell
Gems By Ivan
Karen Koven
Herbert Lipman
James Shigley, Ph.D.
SSEF Swiss Gemmological Institute
TSH Hawaiian Jewelry

$100 to $249
K. C. Bell
BHP Diamonds, Inc.
Donald Clary, Gemologist
Helen L. Dahnke
Richard Dietrich
The Durongkapitaya Family
David Fardon
Michael Gray, G.G.
Naryratha Heng, G.G.
Gordon R. Hill
George R. Kaplan
John Koivula, G.G., F.G.A.
Gail Brett Levine, G.G.
Mason-Kay, Inc.
Sofus S. Michelsen, G.G.
Joan Rolls-Gragg
Frank Schaffer
Gerry Stockton

Under $100
Carolyn J. Bomberger, G.G.
Brundage Jewelers
Daniel Campbell, G.G.
Colorado Peridot
Craftstones
Frank J. Cynar, Ph.D.
Eightstar Diamond Company
José Antonio Gómez Gill
Diane C. Goodrich
Sabine Häberli, F.G.A.
Mary L. Johnson, Ph.D.
Brendan M. Laurs, G.G.
Patricia H. Lineberry
Jack Lowell
Laurent Massi
Mountain Minerals International
Renée Newman
Yvonne M. Paquette, G.G.
Maria Pehnec
Hussain Rezayee
Howard Rubin, G.G.
San Diego Historical Society
Anil Sethi
Tomasz Sobczak
Christine M. Tappen
Lila Taylor
David I. Warren Enterprises

In its efforts to serve the gem and jewelry industry, GIA can use a wide variety of gifts. These include natural untreated and treated stones, as well as synthetics and simulants, media resources for the Richard T. Liddicoat Library, and equipment and instruments for ongoing research support. If you are interested in making a donation, and receiving tax deduction information, please call (800) 421-7250, ext. 4139. From outside the U.S. call (760) 603-4139, fax (760) 603-4199. Every effort has been made to avoid errors in this listing. If we have accidentally omitted or misprinted your name, please notify us at one of the above numbers.

GIA GEM TRADE
LAB NOTES

Editors
Thomas Moses, Ilene Reinitz, and Shane F. McClure
GIA Gem Trade Laboratory

Contributing Editors
G. Robert Crowningshield
GIA Gem Trade Laboratory, East Coast
Karin Hurwit, Mary L. Johnson, and Cheryl Y. Wentzell
GIA Gem Trade Laboratory, West Coast

AMBER Assemblage

The 1993 movie *Jurassic Park* sparked a revival in the popularity of amber. Not surprising is the fact that amber containing insects is often more desirable than plain amber. This spring, the East Coast lab received a transparent, 35.65 ct yellow free-form drilled cabochon containing a large, well-preserved insect that resembled a modern-day housefly (figure 1). The client requested both identification of the material and, if possible, a determination of whether the insect was naturally occurring or artificially introduced into the specimen.

Exposure to long-wave ultraviolet radiation revealed a zoned pattern of fluorescence: strong, chalky yellow overall, with a distinctly weaker, less chalky reaction in the area containing the insect (figure 2). A thin line surrounding this area did not fluoresce at all. Another patch of weak fluorescence was seen on the reverse side of the specimen. With short-wave UV radiation, the entire specimen showed weaker fluorescence, less chalkiness, and the zoning was not as distinct. This fluorescence zoning suggested that we were examining an assemblage.

We measured the refractive index by the spot method on several parts of the cabochon, taking multiple readings to improve precision. The area that showed stronger, chalkier fluorescence yielded a reading of 1.54, typical of amber. Each of the two sections that showed weaker fluorescence yielded a reading of 1.56, which is not uncommon for a plastic imitation of amber, and supported the identification of an assembled piece. Thermal reaction testing (TRT) provided additional evidence: The areas with the 1.54 R.I. had a resinous odor, while the areas with the higher R.I. had an acrid odor. We concluded that this cabochon was an assemblage containing plastic and amber, with the insect encased in one of the plastic sections.

Observation with magnification also indicated an assemblage. The interfaces between the sections had a crackled texture, possibly the result of

Figure 1. This 35.65 ct cabochon proved to be an assemblage of amber and plastic that contains a "modern" insect.

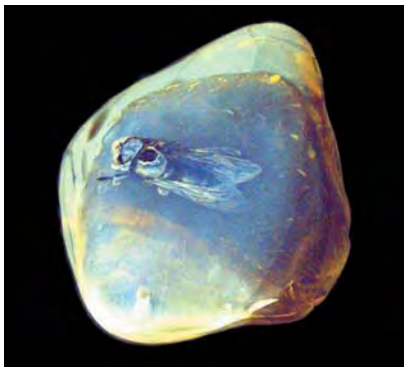

Figure 2. The zoned fluorescence to long-wave UV radiation indicated that the cabochon was an assemblage.

Editor's note: The initials at the end of each item identify the editor(s) or contributing editor(s) who provided that item.

Gems & Gemology, Vol. 36, No. 2, pp. 155–159

Figure 3. The dispersion in these Fancy White diamonds resembles a faint play-of-color. From left to right, the diamonds weigh 1.08, 0.62, and 1.02 ct.

the assembly process, which probably involved "fusing" or melting. The section with the insect also had numerous tiny white gas bubbles that decreased its overall transparency. In contrast, the amber section contained a few colorless gas bubbles, as well as a two-phase inclusion in which the gas bubble was quite movable. Although we do not often see this type of assemblage in the laboratory, it is not unique: We have reported on similar combinations of amber and plastic in two previous Lab Notes (Fall 1983, pp. 171–172; Winter 1987, p. 232).

Wendi Mayerson and KH

DIAMOND

Fancy White

Colorless and near-colorless diamonds are sometimes referred to as "white," in contrast to fancy-color diamonds, but among the fancy colors is a rare appearance described as Fancy White. Such diamonds contain a high concentration of submicroscopic inclusions that scatter light, yielding a translucent "milky" white face-up color. The nature of these inclusions is unknown. These diamonds are sometimes also referred to as "opalescent" because of the flashes of color (caused by dispersion) that are seen in the face-up position. In some instances, the appearance is reminiscent of a white opal with weak play-of-color.

Fancy White diamonds are encountered infrequently in our laboratories, so it was a treat for the East Coast lab to receive three of them this spring for identification (figure 3). The 1.08 ct and 1.02 ct cut-corner rectangular modified brilliants were translucent and showed strong whitish graining. It was particularly unusual to see a matched pair of these stones. The 0.62 ct marquise was translucent, but no distinct inclusions were visible with magnification.

None of the diamonds showed any absorption features with transmitted light through a desk-model spectroscope, although all three exhibited a moderate to strong blue fluorescence to long-wave UV radiation. (Blue fluorescence is typically due to the N3 center, which also gives rise to an absorption line at 415 nm.) The two rectangular modified brilliants showed some yellow fluorescence as well to long-wave UV, in a clover-shaped cloud. The reactions to short-wave UV were similar, but weaker, in each stone. The two larger diamonds showed a weak to medium blue afterglow of more than 10 seconds after the short-wave UV lamp was turned off.

Infrared spectroscopy revealed that these three diamonds were predominantly type IaB, with relatively high concentrations of both nitrogen and hydrogen (as judged by the strength of the absorption peak at 3107 cm^{-1}). Similar white diamonds have been reported in the Gem News column: from Panna, India (Spring 1992, p. 58), and offering an explanation of the opalescent appearance (Spring 1997, p. 60). *TM and IR*

Blue, Zoned

Recently, the East Coast laboratory had the opportunity to examine a strikingly zoned blue 3.43 ct rough diamond (figure 4) and, later, the 1.33 ct round brilliant that was cut from it (figure 5). Strongly color-zoned faceted blue diamonds have been presented in this column in the past (Summer 1985, pp. 108–109). However, in this case we were able to examine the rough diamond and record infrared spectra of both the blue and near-colorless portions.

Trace amounts of boron are the most common natural cause of blue color in diamond; such boron-bearing diamonds have a strong near-infrared absorption band that extends into the visible range, absorbing red light and imparting a gray-to-blue color. Diamonds that contain boron are described as type IIb, and have a characteristic mid-infrared spectrum with peaks at about 1300, 2455, 2800, and 2930 cm^{-1}. (For further information on diamond types, see Box A in E. Fritsch and K. Scarratt, "Natural-color nonconductive gray-to-blue diamonds," *Gems & Gemology*, Spring 1992, pp. 35–42.) Diamonds that are depleted in boron (and nitrogen, i.e., type IIa) do not have these same characteristic peaks in the mid-infrared and exhibit no absorption in the near-infrared or visible range. The IR spectrum of the blue portion of the 3.43 ct rough diamond (figure 6A) displays prominent absorption peaks typical of type IIb diamond, while that of the colorless portion (figure 6B) shows very little absorption at these positions. This demonstrates that the uneven distribution of boron

Figure 4. This irregularly shaped 3.43 ct rough diamond shows strong zoning of the blue color.

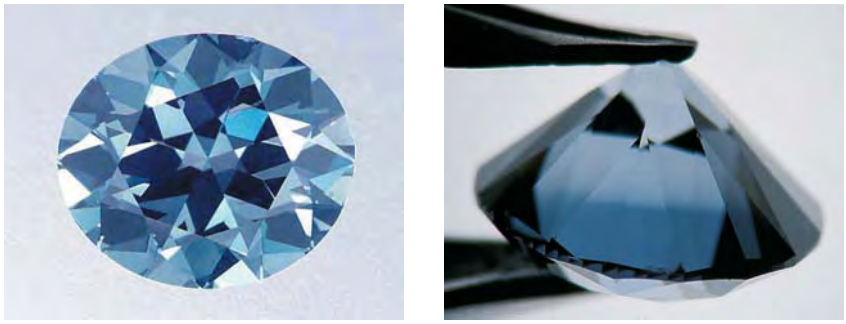

Figure 5. An attractive face-up appearance (left) is shown by the 1.33 ct Fancy Deep Blue round brilliant diamond that was cut from the color-zoned rough shown in figure 4. The view on the right shows how a wedge of the strong blue color was placed at the girdle to take advantage of multiple internal reflections to produce a saturated, well-distributed face-up color.

correlates to the uneven distribution of blue color.

Cutting blue diamonds is often very challenging because of the typically asymmetrical shape of the rough and the irregularity of the color zoning (see also Box B in J. M. King et al., "Characterizing natural-color type IIb blue diamonds," Winter 1998 *Gems & Gemology*, pp. 246–268). The ultimate goal is to achieve a maximum blue saturation with a moderate tone in the face-up position. If the color zone is oriented poorly, low saturation or a dark tone can yield a gray face-up component, which is considered less desirable than a "pure" blue color. Many of the same issues are encountered when cutting blue sapphires; however, the consequences of a mistake with a blue diamond are much more dramatic in terms of both overall face-up appearance and loss of value. This diamond was fashioned so that the strong wedge of blue color penetrated along the girdle plane (figure 5, right). This position takes advantage of internal reflections to produce an attractive, well-distributed face-up color appearance, and the diamond received a grade of Fancy Deep Blue. *Matt Hall and TM*

Unusual Manufactured GLASS

Glass is the oldest manufactured material used as a gem substitute. Whether single-crystal or multi-component, most gem materials familiar to us have been imitated by glass at one time or another. Even though manufactured glass is quite common and its identification is relatively routine, from time to time some unusual glass items submitted to the Gem Trade Laboratory call for extra testing.

Such was the case with the semi-opaque dark red cabochon pictured in figure 7 and represented as "pupurine." The 43.73 ct cabochon measured 29.28 × 19.76 × 7.77 mm and displayed a spotty or patchwork surface reflectivity in incident light that is somewhat reminiscent of the aventurescence or schiller shown by some feldspars.

Examination with a gemological microscope and fiber-optic illumination showed that the cabochon was primarily composed of interlocked nests of dark red needles that were precisely oriented in a sagenitic (gridlike intersecting needles or plates) boxwork pattern within their respective nests. This caused all of the needles within a nest to reflect incident

Figure 6. The mid-infrared spectrum of the blue portion (A) of the 3.43 ct rough diamond displays characteristic boron peaks at about 1300, 2455, 2800, and 2930 cm^{-1}, while the colorless portion (B) mainly shows absorptions typical of type IIa diamond. Spectrum B has been smoothed to remove noise.

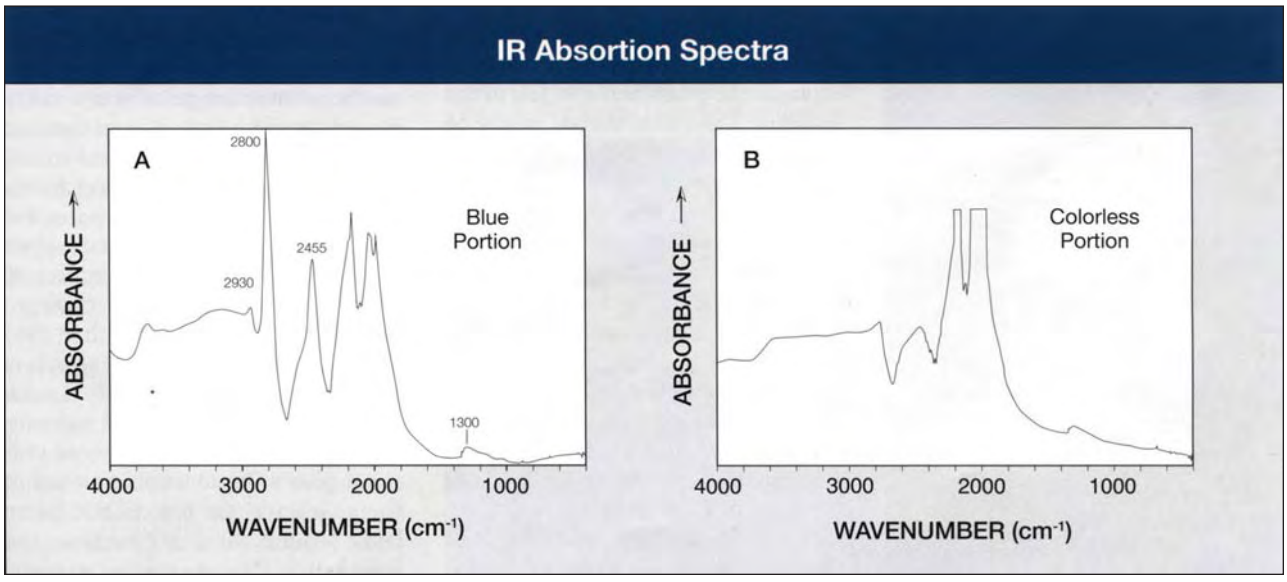

Figure 7. Represented as "pupurine," this 43.73 ct cabochon was identified as a devitrified manufactured glass.

light simultaneously (figure 8), while surrounding nests remained dark. This directional reflective effect, as well as the general microscopic appearance of the nested sagenitic needles, is somewhat similar to the arborescent patterns observed in some devitrified manufactured glasses produced by Iimori Laboratory Ltd. in Tokyo. In reflected light, it was readily apparent that the luster of the acicular inclusions was much higher than that of the surrounding host. Using an analyzer with reflected light, we did not see any pleochroism, which suggests that the cabochon and its inclusions were singly refractive.

Figure 8. Devitrification resulted in the sagenetic boxwork pattern shown by this nest of synthetic cuprite inclusions in the manufactured glass. Magnified 25×.

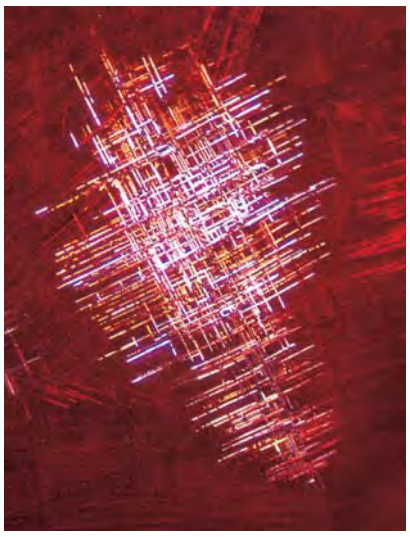

Examination with a Beck prism spectroscope and surface-reflected light showed a weak absorption band positioned between 495 and 500 nm, another weak band between 585 and 594 nm, a band of moderate strength between 608 and 620 nm, and a sharp, fine line at 632 nm. The specific gravity of the cabochon (determined hydrostatically) was 3.68, and the refractive index obtained by the spot method was approximately 1.62. Our ability to obtain an R.I. reading varied considerably from area to area across the cabochon, which suggests that surface-reaching inclusions might interfere with the reading in some areas.

Since many of the needles were exposed on the surface during polishing, and since their higher surface luster made them easy to target, Raman analysis of both the inclusions and the surrounding "matrix" was easily accomplished. The Raman spectra revealed that the dark red needles were cuprite, a bright red copper oxide, while the pattern shown by the surrounding host material was consistent with a glass. Because these crystals are in a manufactured glass, they are also synthetic.

To complete the description of this material, research associate Sam Muhlmeister performed an EDXRF (bulk area) analysis. EDXRF showed the presence of Si together with Sb, Cu, Fe, and Pb, with Cu being the most prominent metallic element. The abundance of cuprite inclusions explains the prominence of Cu in the analysis. The other metals might be contaminants in the synthetic cuprite or present in the host glass.

Inclusions of synthetic cuprite produced by devitrification in manufactured glass have been observed and identified before. For example, a Fall 1984 Gem News item (pp. 176–177) documented synthetic cuprite inclusions that formed brownish red arborescent dendritic "flowers" against a background of opaque brownish green glass manufactured by Iimori, and marketed as Maple Stone.

In the present case, the matrix of the "pupurine" cabochon appears to be essentially the same color as the cuprite inclusions. This was apparent when the cabochon was examined around its edges with a pinpoint fiber-optic light source. The synthetic cuprite inclusions also must contribute significantly to the bodycolor of the cabochon, since they are pervasive throughout the glass matrix. We do not know the manufacturer of this attractive cuprite glass.

John I. Koivula

Baroque CULTURED PEARLS

Figure 9 shows a pair of white baroque pearls that were submitted to the West Coast laboratory for an identification report. They had a particularly high luster and were unusually large and well matched in shape. Each measured approximately 32 × 25 × 21 mm and had been partially drilled at the apex for setting in jewelry.

We immediately noticed that they felt quite heavy for their size. In addition, peculiar blemishes were present on the surface of each: a small dull-looking oval area on the narrow side of one, and a distinct yellowish brown circular area in a more prominent location on the other (visible in figure 9). At 10× magnification with overhead illumination, the dull oval area appeared to be a dense, opaque, white, featureless mass—a nonnacreous material of undetermined identity placed in a natural depression. Magnification showed that the colored area on the companion piece was a circular section of mother-of-pearl that had been carefully attached to the surface.

On the basis of these observations, we suspected that these items had been repaired and/or plugged, so we proceeded with X-radiography to determine the cultured or natural origin of the pearls and whether they had been altered. The X-radiograph of each (see, e.g., figure 10) showed a distinct, partially drilled bead nucleus, which proved that these were cultured pearls. In addition, instead of the characteristic concentric nacre layer around the bead nucleus, the flow pattern of a composite material

Figure 9. These large cultured baroque pearls, each approximately 32 × 25 × 21 mm, showed some unusual blemishes; note the yellowish brown concentration in the center of the pearl on the left.

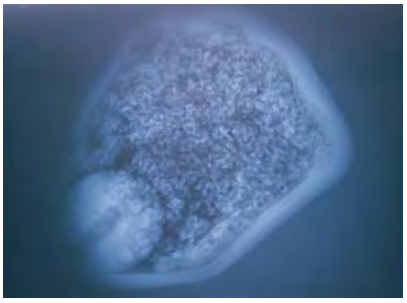

Figure 10. This X-radiograph reveals the filling material around the bead nucleus of one of the baroque cultured pearls shown in figure 9.

was clearly visible. It was readily apparent that these cultured pearls had been filled.

Hollow natural pearls sometimes are filled with a foreign material to provide more stability and add weight. In particular, the increased stability reduces the danger of damage when the pearls are drilled prior to setting (see also Fall 1992 Lab Notes, p. 195). This is the first time we have seen cultured pearls of this size with a substantial filling. We concluded that the eye-visible blemishes covered the areas through which the foreign material had been introduced into these cultured pearls. *KH*

BICOLORED ZOISITE

A Spring 1993 Gem News entry (p. 63) on parti-colored zoisite accurately predicted that additional bicolored zoisites would appear in the trade. Bill Vance recently loaned the West Coast laboratory two fashioned pink-and-yellow bicolored stones (figure 11). He stated that the stones were cut from the same piece of rough zoisite (the largest crystal of a small lot from Tanzania) and that they were not heat treated.

The larger stone, 4.30 ct, showed strong pink color face-up. When viewed through the side, however, it revealed a well-defined color boundary perpendicular to the table; approximately one-third of the stone was purplish pink and the remainder was light yellow. The other stone, 1.62 ct, appeared primarily yellow face up, with a small pink zone in one corner.

The visible spectrum of the larger stone displayed an absorption band at approximately 455 nm and weak general absorption in the green region. The other stone showed no lines in the hand spectroscope. Both stones were biaxial and yielded refractive indices typical for zoisite: 1.690–1.700. Their specific gravity (determined hydrostatically) was 3.37, and each luminesced very weak yellow to long-wave UV and was inert to short-wave UV. Both displayed distinct purplish pink, yellow, and near-colorless trichroism. These gemological properties, as well as their Raman spectra, confirmed that the material was zoisite.

EDXRF analyses by Sam Muhlmeister on the larger stone's pink and yellow zones revealed that in addition to Al, Si, and Ca, both zones contained traces of Ti, V, Mn, Fe, and Sr. The pink zone showed slightly less Sr and slightly more Mn than the yellow zone. It is unclear whether these small variations were related to the difference in color. However, a notably greater amount of Ti was present in the yellow zone, and one could speculate that the yellow zones might change to blue on heating, as commonly occurs with tanzanite. For a more thorough discussion of these elements and their relationships to the color and pleochroism of zoisite, refer to J. Abrecht's "Pink zoisite from the Aar Massif, Switzerland" (*Mineralogical Magazine*, Vol. 44, No. 333, 1981, pp. 45–49) and G. H. Faye and E. H. Nickel's "On the pleochroism of vanadium-bearing zoisite from Tanzania" (*Canadian Mineralogist*, Vol. 10, No. 5, 1971, pp. 812–821). *CYW*

PHOTO CREDITS
Elizabeth Schrader took figures 1ñ3 and 5 (left). Vincent Cracco supplied figures 4 and 5 (right). Maha Tannous took figures 7, 9, and 11. John Koivula provided figure 8.

Figure 11. These bicolored zoisites (1.62 and 4.30 ct) were cut from the same piece of rough. The larger stone appears pink face-up, although well-defined purplish pink and light yellow portions were visible from the side. The smaller stone is mostly yellow with a small pink zone in one corner.

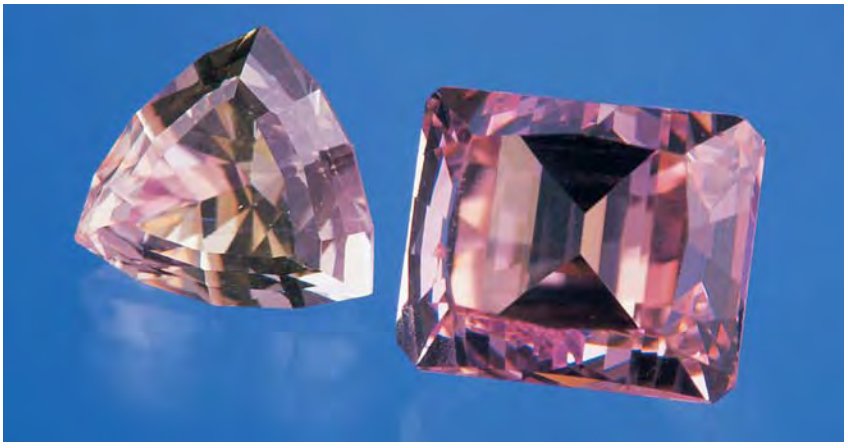

GEM N·E·W·S

Editors • Mary L. Johnson, John I. Koivula, Shane F. McClure, and Dino DeGhionno
GIA Gem Trade Laboratory, Carlsbad, California

Contributing Editors
Emmanuel Fritsch, IMN, University of Nantes, France
Henry A. Hänni, SSEF, Basel, Switzerland
Karl Schmetzer, Petershausen, Germany

DIAMONDS

New diamond cut: "Tycoon cut." At the March 2000 AGS Conclave in Philadelphia, Toros Kejejian of Tycoon, Los Angeles, showed his former instructor (now GIA president) Bill Boyajian a new twist on emerald-cut diamonds. The "Tycoon cut" (figure 1) is a rectangular—or square—mixed cut with step-cut facets on the pavilion and a centered rhombus on the table. The cut (patent pending) is designed to provide more brilliance than a standard emerald cut.

The 6.93 × 5.09 × 3.39 mm F-color diamond shown in figure 1 had the following proportions: table—79%, length-to-width ratio—1.36, total depth—66.6%, and pavilion depth—56.6%. "Tycoon cut|" and a serial number were inscribed on the faceted girdle.

Figure 1. This 1.04 ct colorless diamond has been fashioned as a "Tycoon" cut, a new alternative to emerald or step cuts. Courtesy of Toros Kejejian; photo by Maha Tannous.

Diamond presentations at the PDAC conference. This year's conference of the Prospectors and Developers Association of Canada was held in conjunction with the annual meeting of the Canadian Institute of Mining and Metallurgy on March 5–10 in Toronto. Attendance was very high (12,000), and the mood was optimistic. With so many subjects presented, however, diamonds played a less prominent role than at the 1999 PDAC conference (summarized in the Summer 1999 Gem News, pp. 142–143). Here are highlights of some of the diamond reports.

Matthew Field of De Beers and **Charles Siwawa** of Debswana emphasized the importance of Botswana's Orapa diamond mine: It produces 25.6% of the total rough for De Beers–owned mines (and 6.7% of the world's production). Recent improvements to the recovery process have doubled Orapa's production capability. These developments, combined with the fact that Botswana is politically and economically stable, help ensure that Orapa will be a major and reliable contributor to the world's diamond supply for several decades to come.

Bruce Yago of Lakefield Research Ltd. discussed the important role of modern diamond service laboratories: They enable junior companies to join the hunt for diamonds without having to build their own (expensive) facilities for processing exploration samples. Mr. Yago predicted that the use of organic heavy liquids (such as bromoform, tetrabromoethane, and methylene iodide, all of which give off toxic fumes) for the recovery of diamonds eventually will be proscribed and replaced by mechanical and aqueous methods, such as Wilfley tables, water columns, and miniature dense-media separation plants that use nontoxic ferrosilicon liquids.

Representatives of several diamond exploration and mining companies gave presentations in the **Industry Exchange Forum**. Canada's first diamond mine, Ekati, managed by BHP, is on course at a planned annual production of 3 million carats. The Diavik project (figure 2), managed by Rio Tinto–Kennecott, received a setback last winter when their application for a land-use permit was refused; recent submission of a revised environmen-

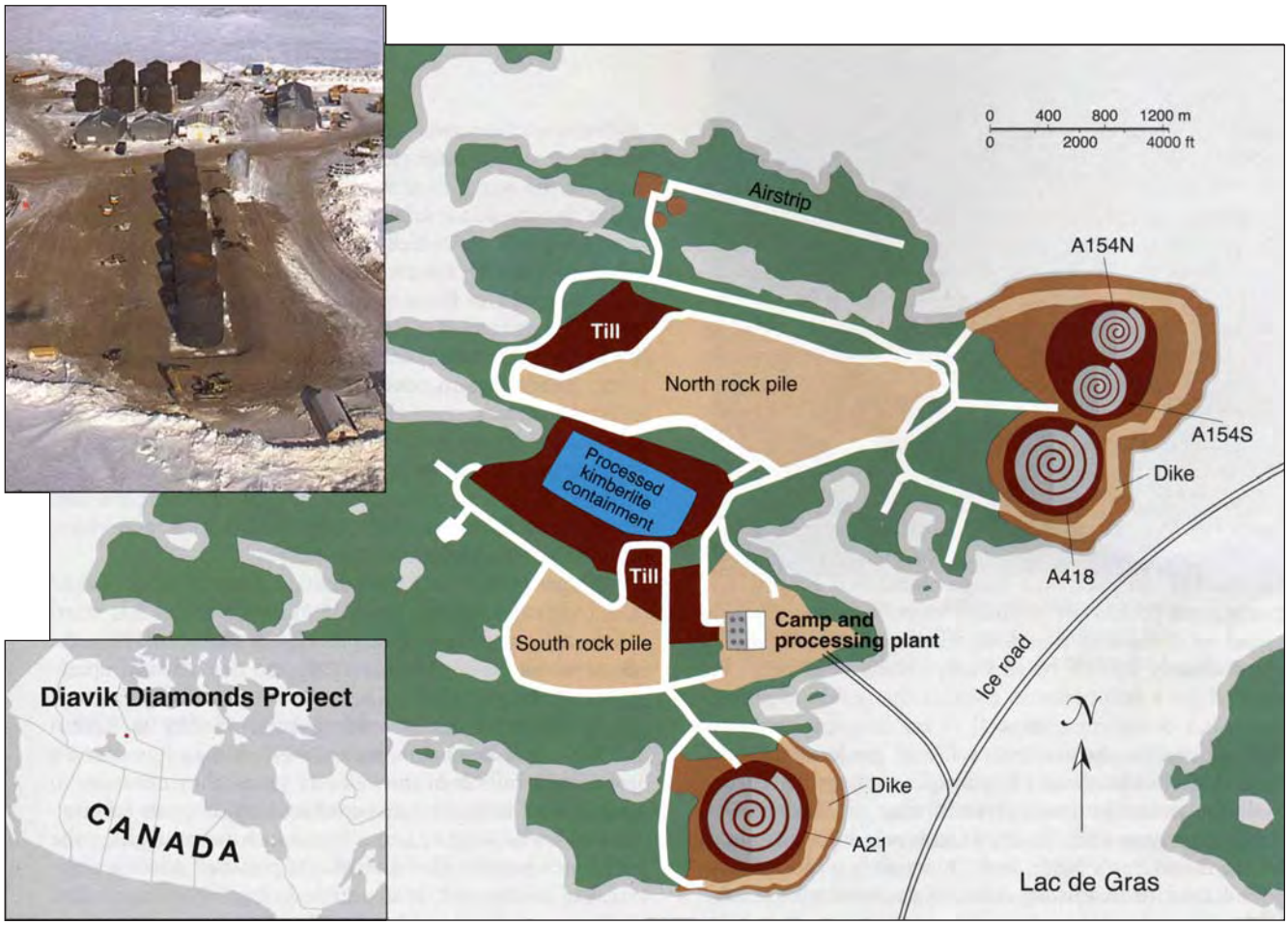

Figure 2. This map shows the projected layout of the Diavik project; the inset photo shows fuel tanks being assembled on-site in April 2000. Map and photo courtesy of Aber Resources.

tal impact statement resulted in the permit being granted just in time for heavy equipment to be rushed to the site while the winter road was still passable. As a result, start-up of the mine is still planned for late 2002 or early 2003. If Diavik has other setbacks, Winspear's Snap Lake property may well become Canada's second diamond mine. Because the Snap Lake operation will leave a much smaller "footprint," the permit process should be easier and faster than at Diavik. Snap Lake involves a small open pit on dry land, which would progress to underground mining of a shallow-dipping kimberlite dike. Operations at two other promising diamond projects—Kennady Lake, managed by Monopros (De Beers), and Jericho, managed by Tahera (previously Lytton)—have not advanced far enough to determine if economic exploitation is feasible.

Diamond exploration is continuing in Alberta, where Ashton has discovered more than two dozen kimberlites in the Buffalo Hills area. Several contain diamonds, but to date none appears to be a promising project. The decision by Monopros to bulk-sample the Victor kimberlite pipe, the largest in a cluster of 15 pipes, has given new impetus to diamond exploration in the James Bay Lowland area of Ontario. Another area of interest is Wawa, along the northeast corner of Lake Superior, where Canabrava, Diabras, and Band Ore are active.

Other ongoing diamond exploration activities worldwide were described in numerous booth displays. There were no formal presentations or booth displays about GE POL diamonds or "conflict diamonds," although both topics were raised in private conversations.

A. J. A. (Bram) Janse
Archon Exploration
Carine, Western Australia

Israel's 2nd International Rough Diamond Conference. An abundance of information was exchanged at this conference, held March 21–23 in Tel Aviv. In attendance were about 240 top people in the diamond industry, plus about 600 local diamantaires. The 13 speakers, whose talks are summarized below, included representatives of major diamond-producing companies, banks, and brokers, as well as various government agencies.

De Beers CEO **Gary Ralfe** discussed the company's "strategic review." Rather than continue to serve as custodian to the diamond industry, De Beers will aim to be a

leader in diamond production and to compete in the rough diamond market. Recognizing these new realities, **Des Kilalea**, diamond analyst for Fleming Martin Securities, said that the comfortable years when the De Beers Central Selling Organisation (CSO) absorbed the world's surplus diamonds are over. For producers, this will mean lower prices, higher cut-off grades, and a search for front-end partners, such as the Aber-Tiffany link. For cutters and manufacturers, it means better links to rough sources, greater cost control, clever technologies, and increased spending on marketing and advertising. For consumers, it means more competitive prices, e-commerce, and branding.

According to **Paul Goris**, managing director of the Antwerp DiamondBank, "We have to reconcile ourselves to the fact that the days of a predictable and stable market, an exclusive single-channeled supply, and guaranteed profits are probably over, and that the diamond business is in transition to a free-market environment already known by so many other industries." He pleaded for a strict ban on conflict diamonds to protect consumer confidence, as well as for frequent consultation among producers, cutters, and bankers to avoid large price fluctuations. He offered a strategy for coping with the future business environment, dubbed "EBT": strong Equity in one's business, a detailed Business plan to submit to one's bank, and Transparency (no secrecy, price fixing, or hidden agendas) in the business process. **Richard Hambro**, chairman of I. Hennig & Co., echoed Paul Goris's theme that the diamond business of the future would be less predictable and more competitive.

Doug Bailey, CEO of Ashton Mining, discussed the risks—and potential rewards—of diamond exploration. For instance, he estimated that although C$1 billion had been spent exploring for diamond properties in Canada, the resulting properties are worth $3.5 billion. Ashton has 40% equity of the Argyle mine, and recently announced the discovery of additional underground reserves of 22 million tonnes valued at US$1 billion, which will extend mine life beyond 2010.

Gordon Gilchrist, managing director of Argyle Diamonds, described the challenges of marketing their product, a high proportion of which are small, brown, heavily included stones. When the mine opened in 1983, it quickly added 25 million carats annually to world diamond production, which had been about 50 million carats a year. Although until mid-1996, most of the production was sold through the CSO, Argyle has continually explored ways to market the brown diamonds on its own. The company helped develop the Indian diamond-cutting industry, which grew 185% in volume and 220% in value from 1983 to 1993. It also launched a promotion of "champagne" and "cognac" diamonds.

James Rothwell, president of BHP Diamonds, explained the three channels through which Ekati mine diamonds are marketed. All the diamonds are sorted and valued by government workers in Yellowknife, Northwest Territories (NWT), so that the Canadian government can extract the exact royalty. Thirty-five percent of the rough is sold under contract to De Beers, and 10% is reserved for sale to diamond-cutting factories that are being set up in Yellowknife. The remaining 55% is sold in Antwerp for the same prices as in Yellowknife. The run-of-the-mine production from the first pipe (Panda) averaged $165/ct, which is very high for a primary deposit. Updating the situation with the Diavik project, **Robert Gannicott**, president of Aber Resources, admitted that at more than $900 million, the capital cost is high. Nevertheless, the project remains economically robust under a wide range of economic variables. **Jake Ootes**, NWT Minister of Education, Culture and Employment, reiterated the importance of diamond mining in the Northwest Territories.

Sergei Oulin, vice president of Almazy Rossi-Sakha Co. (Alrosa), said that since 1996 his company has started mining two new open pits (Jubileynaya in 1996 and Butuobinskaya/Nyurba in 1999) and one alluvial operation (Anabar, in 1997). They also reopened the Zarnitsa pit (1999), and started underground mining at Aikhal (1998) and Internationalaya (1999). Alrosa has spent a total of $2 billion in the last five years; they now aim to sell 70% of their production to domestic buyers and cutters at below world prices. To discourage smuggling, the supply of rough and the output of polished goods will be strictly monitored. It is planned that 97% of polished diamonds will be exported. **Tim Haddon**, president of Archangel Diamond Corp. (ADC), explained Archangel's ongoing struggle to get their Russian partner to carry out the terms of an agreement that would transfer the license for the Verkhotina area to a Russian joint stock company, Almazny Bereg, in which ADC has a 40% equity. He hopes that Vladimir Putin, the new president of Russia, will resolve the matter.

Chris Jennings, of SouthernEra, noted that Angola's Camafuca deposit is the world's largest kimberlite (167 hectares) and is formed by five pipes that lie next to one another beneath the Chicapa River. Rather than divert the river, SouthernEra plans to mine the kimberlite with dredges in paddocks. **Inge Zaamwani**, managing director of Namdeb, discussed the history and development of that company, and noted that more than 50% of the diamonds Namdeb produces now are recovered from offshore deposits.

A. J. A. (Bram) Janse
Archon Exploration Pty. Ltd.
Carine, Western Australia

COLORED STONES AND ORGANIC MATERIALS

Baltic amber with lizard inclusion. Figure 3 illustrates a lizard inclusion in a piece of Baltic amber that was found in June 1997 among Holocene fossil beach sediments in Gdansk-Stogi (Poland). The lizard (preserved length 3.7 cm) is encased in a piece of amber that measures about 3.5 × 2.0 × 1.0 cm. The infrared spectrum led us to identify the amber as succinite (i.e., fossilized tree resin that

contains relatively high amounts of succinic acid). The body structure of the animal suggests that it belongs to the *Lacertidae* family. Although the lizard is incomplete—the front part of the head, dorsal fragment of the trunk, and tip of the tail are missing—it is well preserved; all body elements, which are covered with three types of scales, are perfectly visible. This specimen, from the collection of G. Gierlowska, represents the second almost complete lizard discovered in Baltic amber. It was loaned to the Museum of the Earth, Polish Academy of Sciences, Warsaw, for further investigation; a detailed report was recently published by M. Borsuk-Bialynicka et al. ("A lizard from Baltic amber [Eocene] and the ancestry of the crown group lacertids," *Acta Palaeontologica Polonica*, Vol. 44, No. 4, 1999, pp. 349–382).

G. Gierlowska, W. Gierlowski, and T. Sobczak
Warsaw, Poland

Figure 3. This piece of Baltic amber (succinite), which contains a 3.7-cm-long lizard, was found in Poland in 1997. Photo by G. Gierlowska.

Ametrine with layers of smoky quartz. Ametrine (amethyst-citrine) from Bolivia has been prevalent in the gem trade for many years (see, e.g., Gem News, Fall 1989, pp. 178–179, and Spring 1993, p. 53). At this year's Tucson gem show, H. Marancenbaum of Steinmar Ltd. (Santa Cruz, Bolivia) kindly provided two rough fragments, three slightly polished crystals, and two fantasy-cut specimens of ametrine to the SSEF Swiss Gemmological Institute. Mr. Marancenbaum reported that these samples originated from the Yuruty mine, a new operation that is located in the same geologic unit (Murciélagos limestones) in Bolivia as the well-known Anahí mine (Vasconcelos et al., *Gems & Gemology*, Spring 1994, pp. 4–23).

An investigation of these Yuruty mine samples by the present contributor revealed an interesting new aspect to this bicolored quartz. In addition to the typical amethyst and citrine sectors (along the major and minor rhombohedral forms; again, see Vasconcelos et al., 1994), five of the samples also showed a similar pattern of two distinct layers of smoky quartz. These layers are oriented parallel to the minor rhombohedral form *z* {01$\bar{1}$1}, within the citrine sector (see, e.g., figure 4). In the slightly polished crystals, the smoky layers were observed just below the surface. In this area, the color of both amethyst and citrine is rather pale. The two (broken) fragments that did not show smoky quartz layers were presumably derived from the central portion of a crystal; they did display more intense amethyst/citrine coloration.

Figure 4. Two parallel zones of smoky quartz are evident in these three ametrine specimens (27.3–299.7 ct) from the new Yuruty mine in Bolivia. Photo © SSEF Swiss Gemmological Institute.

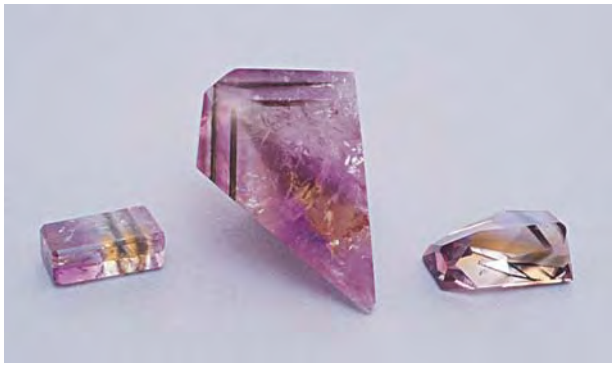

The growth conditions of this unusual ametrine evidently facilitated the enhanced accommodation of aluminum impurities in the *z* sectors. Natural irradiation of these aluminum-rich zones would give rise to the smoky quartz color layers.

Approximately 30 tons of material have been produced at the Yuruty mine since February 1999, according to Mr. Marancenbaum. Large quantities of rough and cut amethyst, citrine, and ametrine from this new mine were available at this year's Tucson show, and he anticipated that about 10,000 carats of cut material monthly could be expected in the near future.

Dr. Michael S. Krzemnicki (gemlab@ssef.ch)
SSEF Swiss Gemmological Institute
Basel, Switzerland

Bicolored cat's-eye beryl from Pakistan. Also at the February 2000 Tucson show, Dudley Blauwet of Dudley Blauwet Gems, Louisville, Colorado, showed this contributor two bicolored beryl cabochons that each displayed an interesting chatoyant band along the color boundary. Mr. Blauwet reports that the rough was mined in 1997–1998 from a pegmatite in the Shigar Valley area, above the village of Haiderabad in Pakistan. The deposit is

situated on the southwest flank of Buspar Peak, at an elevation of about 12,000 feet (3,660 m). Approximately 100 crystals or fragments with the distinctive chatoyant band have been recovered to date, measuring up to 4 × 5 cm. About one dozen cabochons were cut; he loaned the largest one (30.37 ct; figure 5) to GIA for closer examination.

The color boundary, which was sharp and evenly centered, was oriented perpendicular to the c-axis. One half of the stone was greenish blue, and the other was very pale pink. Spot R.I. readings of 1.56 were recorded for both colors. The pink half was transparent to translucent due to abundant "fingerprints" composed of wavy planes of two-phase (liquid-gas) inclusions. The greenish blue half was transparent but contained numerous growth tubes oriented parallel to the c-axis, which caused subtle chatoyancy. With a magnification of 40×, tiny colorless crystals were visible at the ends of these tubes. Scattered dark gray-green prisms (which appear to be tourmaline) also were seen in the greenish blue portion, particularly along the contact with the pink half. The 2.5-mm-wide chatoyant band lay within the greenish blue portion, very near the color boundary. The band appeared colorless due to the scattering of light associated with the chatoyancy; it contained abundant fine structures oriented parallel to the c-axis, as well as the growth tubes described above.

Figure 5. A narrow chatoyant band is present along the color boundary of this 30.37 ct bicolored beryl from Pakistan. Courtesy of Dudley Blauwet; photo by Maha Tannous.

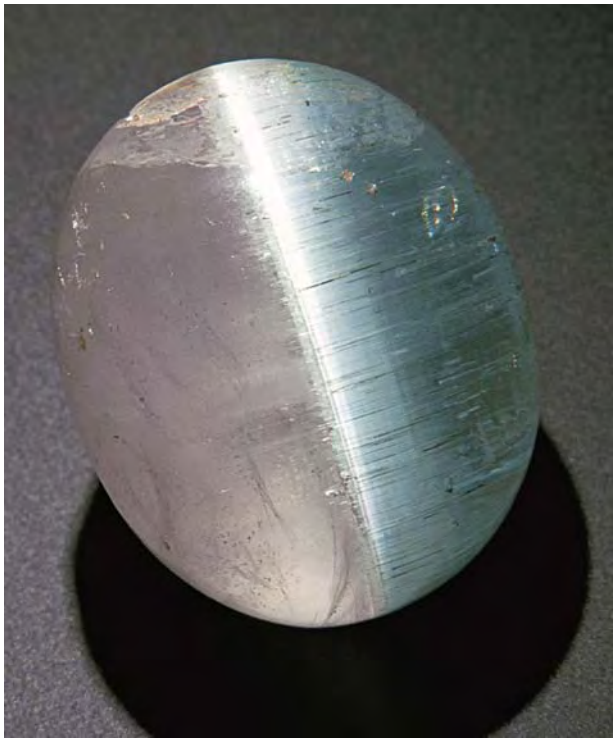

Figure 6. Purchased in Brazil, this 2.36 ct bicolored stone is a natural intergrowth of emerald and colorless quartz. Photo by Jaroslav Hyrsl.

Mr. Blauwet indicated that the pink portion is always present at the crystal terminations, and that the small size of this zone renders most of the rough unusable for cutting bicolored pieces. He also stated that some of the rough failed along the color boundary/chatoyant band during cutting, because of structural weakness in this area. For these reasons, few fashioned stones have been produced.

Brendan M. Laurs
Senior Editor, Gems & Gemology

Natural emerald and quartz intergrowth. A very unusual colorless and green bicolored stone was purchased by this contributor in 1998 in Belo Horizonte, Brazil. The 2.36 ct stone measured 7.96 × 7.53 × 4.84 mm. At first glance, the stone appeared to be an assembled doublet with the join between the two halves oriented perpendicular to the table facet (figure 6), rather than parallel to the table plane as is common with most doublets. However, close examination with a microscope showed that it was actually a natural intergrowth of two separate minerals.

The refractive index of the colorless, semitransparent half was 1.545–1.553, which confirmed it as quartz. The green portion showed an R.I. of 1.583–1.591, was strongly dichroic (bluish green and yellow-green), did not react to a Chelsea filter, and did not show any sign of red transmission; its spectrum with a handheld spectroscope confirmed that it was emerald.

The emerald portion was inert to both long- and short-wave UV radiation, whereas the quartz half fluoresced a strong white (concentrated in fractures) to short-wave UV (with no reaction to long-wave UV). This suggests that this stone was probably "filled" with some type of substance, although none of the known or potential emerald fillers mentioned by Johnson et al. (*Gems & Gemology*,

Figure 7. Subhedral plates of what appear to be mica or chlorite (see arrows) are present in both the emerald and quartz portions, as well as at the contact between them. Photomicrograph by Jaroslav Hyrsl; magnified 10×.

Summer 1999, pp. 82–107) had this type of fluorescence.

Both portions were found to contain natural inclusions. Subhedral brownish green flakes with a distinct basal cleavage, which appear to be mica or chlorite, were present in both halves, as well as in the contact between the two minerals (figure 7). Part of the contact consists of an air-filled crack that appears mirror-like at some angles. The emerald portion is characterized by parallel hollow channels, which rarely contain an anisotropic phase. Some of the channels also contain two-phase inclusions. Very rare, extremely small three-phase inclusions also were observed, but of a type different from those known to occur in emeralds from Colombia. The three-phase inclusions in this stone were either parallelepipeds or asymmetrical; each contained a bubble and a small anisotropic solid phase. On the basis of the inclusions, we believe that this unusual bicolored stone probably comes from the Belmont mine near Itabira in Minas Gerais, Brazil (see H. A. Hänni et al., "The emeralds of the Belmont Mine, Minas Gerais, Brazil," *Journal of Gemmology*, Vol. 20, Nos. 7/8, 1987, pp. 446–456). *Jaroslav Hyrsl (Hyrsl@bbs.infima.cz)*
Kolin, Czech Republic

Update on some Madagascar gem localities. This island nation continues to supply an impressive array of gem varieties, in some cases of high quality and in enormous quantities. To gather first-hand information on the gem production and geology of the deposits, in November-December 1999 this contributor visited three gem-producing areas: the sphene deposits in northern Madagascar; the tourmaline-, beryl-, and spodumene-bearing pegmatites in the central part of the country; and the alluvial gem deposits at Ilakaka in southern Madagascar. The guide for most of the trip was Dr. Federico Pezzotta of the Natural History Museum of Milan, who is involved in several geologic studies throughout Madagascar (in collaboration with the local public institutions) and is a consultant to the Italian-Malagasy joint venture Pyramide Co.

In recent years, Madagascar has become perhaps the world's leading supplier of large facet-grade sphene (or titanite, which is the name currently accepted by the International Mineralogical Association). This attractive green to yellowish brown gemstone shows colorful dispersion (figure 8), but it is rarely faceted in large sizes due to the flat shape of the crystals. However, Madagascar has yielded faceted sphenes over 20 ct (see, e.g., Spring 1998 Gem News, p. 53); Allerton Cushman & Co., of Sun Valley, Idaho, displayed a 35.29 ct Madagascar sphene at the June 2000 JCK Show. The crystals are mined over a large region of northern Madagascar from *in situ* hydrothermal veins (i.e., alpine clefts) that formed during retrograde metamorphism of amphibolite-grade rocks during the late stages of the Pan-African Orogeny, according to Dr. Pezzotta. These veins also contain large quantities of transparent quartz crystals locally associated with albite (pericline), apatite, epidote, rutile, schorl, clinochlore, dolomite, and hematite.

To access the mines, we flew from Antananarivo to Sambava, and then drove three hours on a paved two-lane road to Vohemar on the northeastern coast, and another three hours northwest on a fairly good dirt road to Daraina, a small town where much of the sphene is traded. Production had been sporadic, and we saw very little sphene rough. However, one of the sphene prospects we visited had produced 5 kg of gem rough and

Figure 8. Sphene from northern Madagascar shows a range of color, although "pure" green is most rare. These samples weigh 0.92–2.52 ct. Courtesy of Madagascar Precious Gems (Budsol Co.); photo by Maha Tannous.

Figure 9. This Malagasy dealer in Antsirabe, known locally as "Papa Emeil," had a variety of rough and cut Madagascar gems. Photo by Brendan Laurs.

several very fine crystal clusters in February 1998, according to Dr. Pezzotta.

We briefly visited Milanoa, a small gem-trading town about 50 km south of Daraina. Apatite, which is heated to obtain its bright greenish blue color, reportedly comes from a primary deposit about 40 km southwest of Milanoa. Most of the sapphire traded in Milanoa comes from alluvial deposits in the Ambilobe area (sometimes identified as "Diego Suarez," after the city to the north). A dealer in Daraina reported that about 200 miners were active in this area, having recently returned from Ilakaka, where they could not obtain productive claims. Significant stones are occasionally recovered: We were shown an approximately 50 g gemmy dark blue sapphire crystal that was reportedly found in a river about 40 km west of Milanoa in early November 1999.

After returning to Antananarivo, we drove about three hours south on national highway 7 to Antsirabe, which is the traditional hub of the gem trade in Madagascar due to its proximity to abundant gem-bearing pegmatites. Most of the dealers we visited (see, e.g., figure 9) had rough and faceted stones from Ilakaka, as well as stocks of other gems such as amethyst, garnets, and multicolored tourmaline (probably liddicoatite). We visited several pegmatites in the central portion of the Sahatany Valley, which produces tourmaline (red and multicolored), beryl (morganite), and spodumene (kunzite), as well as the rare gem mineral rhodizite. Only one of these pegmatites was being actively mined. According to Dr. Pezzotta, these late Pan-African granitic pegmatites are hosted by marble, quartzite, and schist, and have been worked in shallow hand-dug pits and tunnels since the turn of the century. Gem production fell sharply after the mines in this part of the valley were nationalized in 1974. More recently, activity has slowed due to the migration of miners to Ilakaka. Our reconnaissance of the workings suggested that some of the pegmatites still hold significant potential for gem production.

For the journey to Ilakaka, I joined Tom Cushman of Allerton Cushman & Co., who was one of the first dealers to visit Ilakaka after sapphires were discovered there in 1998. We flew from Antananarivo to Tulear, and then drove about three hours northeast on national highway 7 to Ilakaka.

The Ilakaka gem deposits are hosted by conglomerate layers within the Paleozoic-Mesozoic Isalo Formation (part of the Karoo Supergroup), which covers an enormous portion of south and east Madagascar. Most of the mining is done in an area that measures about 30 × 65 km, but the gem-bearing region extends at least 30 km north and 100 km southwest of the town of Ilakaka. The miners hand dig pits—typically a few meters, although deeper pits are sometimes excavated (figure 10)—in the weathered sediments to reach the conglomerates, which are loaded into sacks and taken to the nearby stream for washing. The gems are hand picked from primitive sieves made by poking holes through sheet metal that is supported by a wooden frame. The stones are sold to Malagasy middlemen, who offer them to overseas buyers (mostly from Sri Lanka and Thailand) at a local central selling area called the Comptoir.

The sapphires range from near-colorless to pink, purple, and blue (figure 11). Within just two days, we noted several gem species besides sapphire: spinel (dark gray-blue to green-blue, and grayish pink), garnet (purplish red, red, yellow-orange), chrysoberyl (including cat's-eye and alexandrite), topaz (pale yellow or blue), tourmaline (dark yellow-green to red-brown or brownish pink), andalusite, kyanite, zircon (reddish brown and greenish brown), and quartz (colorless, smoky, and amethyst). All of these gem materials have been documented previously from this area (see, e.g., reports by H. A. Hänni in the Summer 1999 Gem News, p. 150, and F. Pezzotta, in *extraLapis* No. 17, 1999, p. 92). The sapphire rough typically ranged from 1 to 3 ct, with 10 ct considered large. Transparent pebbles of spinel, garnet, and chrysoberyl commonly weighed up to 25 ct.

According to Mr. Cushman, about 80% to 90% of the blue sapphires from Ilakaka need to be heated (to improve or even out their color); a somewhat lower proportion of pinks require heat treatment (to remove the purple component). As has been reported in the trade press, several buyers were disappointed initially with the

response of the sapphires to heat treatment: Over-dark blues did not get lighter with heating, and some of what appeared to be *geuda*-type sapphire did not alter to blue. None of the rough at the Comptoir showed any evidence of heat treatment, despite prior reports to the contrary (see, e.g., J. Henricus, "Mixing heated material with natural at mines," *Jewellery News Asia*, July 1999, p. 49). Although we could not confirm whether any sapphires are heat-treated within Madagascar, in Antananarivo I was offered faceted pink and blue sapphires that showed evidence of heating (i.e., discoid fractures surrounding inclusions). Zircon is heat-treated in Madagascar at relatively low temperatures to lighten the red-brown color to a more desirable pale orangy yellow. If heated too long, the stones will become overly pale.

At the June 2000 JCK show, Mr. Cushman provided a further update on the Ilakaka area. During a visit there in May 2000, he noted that there is a new mechanized mining operation just south of the Comptoir, on the opposite side of the Ilakaka River. Heavy equipment, including a large excavator, bulldozer, and two dump trucks, is being used in conjunction with a three-story-tall processing plant, with water supplied by from the Ilakaka River. The mining is being conducted by a Thai company (Société Mining Discovery), and all rough is sent directly to Bangkok. Mr. Cushman also stated that a major new mining area has developed about 60 km southwest of Ilakaka that shares its "boom town" atmosphere. According to Alexander Leuenberger of Larimar SARL in Antananarivo, this new mining area is located at Mahasoa.

Brendan M. Laurs
Senior Editor, Gems & Gemology

Figure 10. At Ilakaka, Madagascar, miners dig pits through the weathered sandstone to reach the productive gem-bearing conglomerate layers. At the time this photo was taken (December 1999), this was the largest hand-dug excavation at Ilakaka. Photo by Brendan Laurs.

Freshwater cultured "Kasumiga pearls," with Akoya cultured pearl nuclei. Frieden of Switzerland, a client of the SSEF Swiss Gemmological Institute, submitted three strands of attractive Japanese freshwater cultured pearls that was believed to be the product called Kasumiga, after the pearl-culturing region of Lake Kasumigaura, north of Tokyo. Kasumiga pearls are said to be grown in *Hyriopsis schlegeli* × *Anadonta plicata* hybrid mussels. Each of the 40-cm-long strands consisted of approximately 40 pearls, which ranged from 9 to 13 mm in diameter. The client had requested information about the presence or absence of a nucleus, the thickness of the nacre, and whether the overgrowth formed in freshwater or saltwater.

Figure 11. Sapphires in a range of colors have been recovered from Ilakaka. These samples weigh 1.42–4.76 ct; photo by Maha Tannous.

X-radiographs revealed the presence of two drill holes in most of the cultured pearls, at a random orientation to each other (figure 12). *Gems & Gemology* reported such features in Japanese freshwater cultured pearls nearly 40

years ago (see R. Crowningshield, "Fresh-water cultured pearls," Spring 1962, pp. 259–273).

With the client's permission, we ground away half of one cultured pearl and polished the surface (figure 13). The bead nucleus was covered by a very thin (0.2 mm) overgrowth of nacre, which was separated by a slight gap from a much thicker (>2 mm) layer of freshwater nacre (figure 14). An energy-dispersive X-ray fluorescence analysis of the aragonite at the pearl's surface showed an abundance of manganese: three times more than in average saltwater nacre. This confirmed the freshwater origin of the outer nacre layer. It appears, then, that drilled low-quality Akoya (saltwater) cultured pearls were used as bead material for these Kasumiga freshwater cultured pearls. The resulting freshwater cultured pearls have a remarkable diameter with thick nacre layers and appealing surface quality. *HAH*

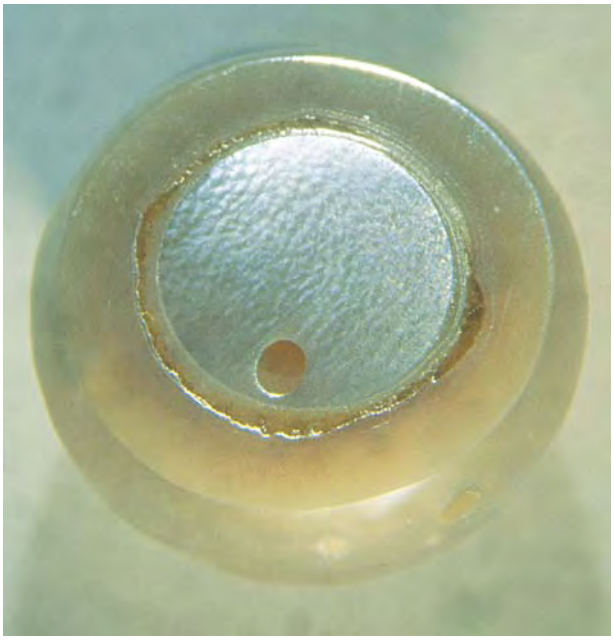

Figure 13. This 9.7 mm Kasumiga freshwater cultured pearl appears to have been nucleated by a nacre-covered shell bead (7 mm in diameter) that shows a normal drill hole. Photo by H. A. Hänni.

Trapiche ruby: An update. Trapiche rubies from Mong Hsu, Myanmar, consist of six transparent-to-translucent ruby sectors separated by translucent-to-opaque yellow or white planes that form a fixed six-rayed star. Many samples also reveal a hexagonal yellow, black, or red core (figure 15). The yellow or white "arms" of the six-rayed stars consist of ruby with a dense concentration of solid, liquid, or two-phase inclusions. The solid inclusions have been identified as calcite and dolomite (K. Schmetzer et al., "Trapiche rubies," *Gems & Gemology*, Winter 1996, pp. 242–250).

The chemical zoning in Mong Hsu trapiche rubies was examined by K. Schmetzer et al. ("Element mapping of trapiche rubies," *Journal of Gemmology*, Vol. 26, No. 5, 1999, pp. 289–301). From subsequent chemical and microscopic examinations, I. Sunagawa et al. ("Texture formation and element partitioning in trapiche ruby," *Journal of Crystal Growth*, Vol. 206, 1999, pp. 322–330) concluded that the arms formed first, during a period of dendritic growth. The transparent-to-translucent triangular or trapezoidal ruby sectors formed later, by layer-by-layer growth on smooth interfaces (figure 16).

Figure 12. Most of the cultured pearls in this X-radiograph of a strand of Japanese Kasumiga cultured pearls reveal the drill hole through the bead nucleus as an oblique line (the length of which depends on its inclination to the direction of observation) that ends at the thicker nacre layer. X-radiograph by H. A. Hänni.

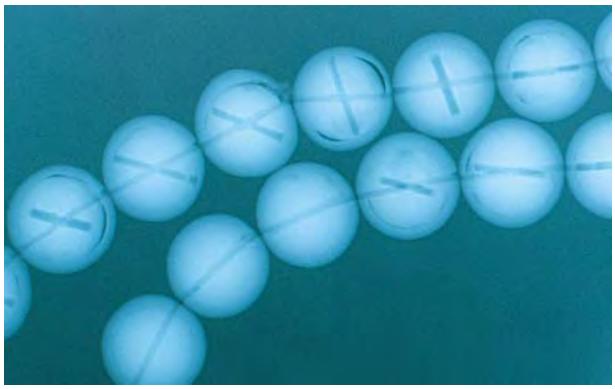

Figure 14. With magnification and reflected light, the two generations of nacre, separated by a gap, are clearly visible in the Kasumiga cultured pearl shown in figure 13. The relatively high manganese content of the outer layer proved that it formed in fresh water rather than salt water. Photo by H. A. Hänni.

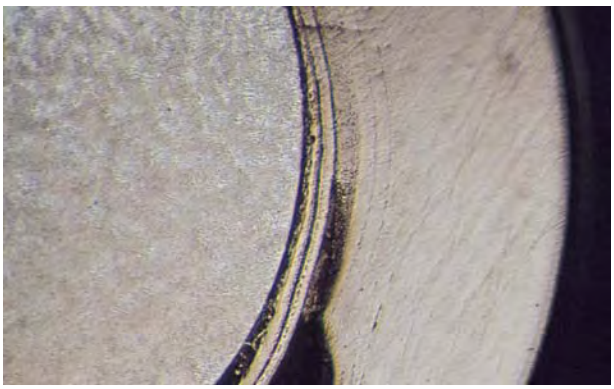

Although trace-element mapping has indicated chemical zoning (e.g., of chromium and titanium) in the six ruby sectors of some trapiche rubies, direct microscopic observation had not previously revealed growth zoning that might indicate the mechanism by which these regions formed. However, we recently observed distinct zoning in several trapiche rubies found by one contributor (DS) within parcels of Mong Hsu rough obtained at the gem market at Mae Sai, in northern Thailand.

The layer-by-layer growth pattern in the ruby sectors was clearly seen in polished slabs cut perpendicular to the c-axis of these crystals. In its simplest form, this growth zoning consists of sequential parallel ruby layers. In some samples (again, see figure 15), alternating red and dark violet-to-black layers were found, with layers of both colors oriented parallel to the hexagonal dipyramid ω (14 14 $\overline{28}$ 3). This crystal form is the commonly observed dominant growth plane in Mong Hsu rubies. The presence of this growth zoning confirms the sequential layer-by-layer growth mechanism for the ruby sectors of Mong Hsu trapiche rubies, as proposed by Sunagawa et al. (1999).

KS and
Dietmar Schwarz
Gübelin Gem Lab
Lucerne, Switzerland

Figure 15. This trapiche ruby from Mong Hsu, Myanmar, consists of a dark violet, almost black core, six white arms that widen toward the outer edge of the crystal, and six trapezoidal ruby sectors. In some of these transparent ruby sectors, a distinct red and dark violet color zoning parallel to dipyramidal growth planes was observed with magnification. The sample measures about 5.5 × 6 mm. Photo by K. Schmetzer.

Spinel from Ilakaka, Madagascar. As discussed in the "Update on Madagascar" entry above and in numerous other publications, this recently discovered mining area has become well known for its large production of blue and fancy-color sapphires and numerous other gems. Besides garnet, one of the most abundant of these other gem materials appears to be spinel.

To help characterize the gem spinels from Ilakaka, this editor studied 120 samples: 80 pebbles that ranged from 0.5 to 40 ct were selected from different parcels of mixed rough that were obtained from Ilakaka; and 40 faceted gems (0.2 to 4.0 ct) were selected from mixed parcels of corundum and spinel, all of which had been purchased in Ilakaka and faceted in Madagascar. The samples were separated into a total of five groups on the basis of their color. Roughly half were violet to grayish violet, purplish violet, or bluish violet (figure 17). Of the remaining half, about 30 were violetish blue to blue (figure 18), and about 20 were purple to reddish purple (figure 19, right). Another five samples were red, pink (figure 19, left), or orange, and the remaining five samples were greenish blue to bluish green (figure 17, inset).

Refractive indices, measured on all faceted samples, ranged from 1.716 to 1.719. Specific gravity values (measured hydrostatically) ranged from 3.59 to 3.64. Microscopic examination revealed the presence of birefringent mineral inclusions in about one-third of the spinels. When examined between crossed polarizers, most of the otherwise inclusion-free spinels showed weak anomalous double refraction.

Natural spinels typically have complex spectra that, in general, consist of the superimposed absorption bands of several basic types of spectra (see, e.g., J. E. Shigley and C. M. Stockton, "Cobalt-blue gem spinels," Spring 1984 *Gems & Gemology*, pp. 34–41; and K. Schmetzer et al., "Color of natural spinels, gahnospinels, and gahnites," *Neues Jahrbuch für Mineralogie Abhandlungen*, Vol. 162, No. 2, 1989, pp. 159–180). This is also the case for

Figure 16. In trapiche rubies, the arms develop by dendritic growth, and then the ruby sectors form by layer-by-layer growth. In some cases, (right), a core grows first by a different smooth-surface mechanism. Figure adapted with permission from Sunagawa et al. (1999).

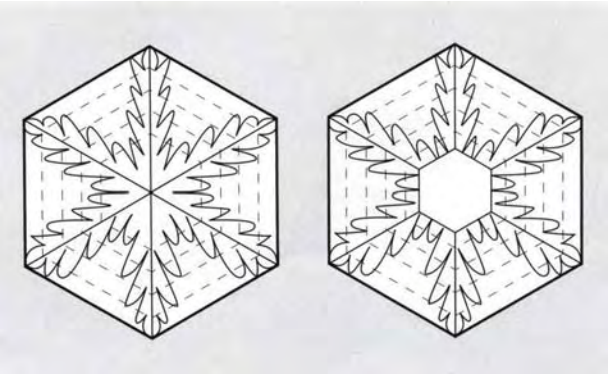

Figure 17. These three violet to purplish violet spinels from Ilakaka, Madagascar, are predominantly colored by iron; the samples weigh 1.30–1.67 ct. Inset: Two bluish green samples (1.21 and 0.78 ct), also colored by iron, represent spinel colors that have been seen only rarely in lots from Ilakaka. Photos by Maha Tannous.

Ilakaka spinels that are colored by iron or chromium, or by a combination of iron plus cobalt or iron plus chromium. A general scheme of the colors (and their causes) found thus far in Ilakaka spinels is given in figure 20.

Absorption spectra in the visible and UV range showed distinct features for the five groups. The largest (violet) group revealed spectra typical for spinels that are colored predominantly by iron. The violetish blue to blue samples showed the same features, plus absorption bands that have been assigned to cobalt in spinels; the most prominent was a band at 625 nm. Other cobalt-related bands overlap with iron bands, but the influence of cobalt on the color can be estimated by the intensity of the 625 nm absorption.

Figure 18. These three blue spinels from Ilakaka (0.99 to 2.09 ct) are colored by cobalt and iron. Photo by Maha Tannous.

The small group of greenish blue to bluish green samples again revealed a basic iron spectrum, which is superimposed by an absorption band at about 645 nm. This absorption band has been assigned to Fe^{2+}/Fe^{3+} charge transfer (see Schmetzer et al., 1989, above). The remaining two groups of purple to red or pink samples revealed a chromium spectrum, with absorption maxima at 543, 413, and 388 nm. A continuous series was observed from pink or red samples colored predominantly by chromium to violet samples colored predominantly by iron. Intermediate spinels (orange, reddish purple, or purple) exhibited an iron spectrum that was superimposed by chromium absorption bands of variable intensity.

The different color groups observed thus far in spinels from Ilakaka represent the full range of colors and spectral features observed in samples from other localities, such as Sri Lanka. *KS*

TREATMENTS

Unusual treated chalcedony. A number of small-volume gem and mineral dealers set up "shop" on small tables along the Interstate 10 corridor in Tucson, Arizona, during the Tucson gem shows each year in late January and early February. While the first impression might be that these goods are of questionable interest to the greater gem and jewelry community, closer inspection shows that there are some fascinating items to be found.

One such item was a translucent white oval cabochon with a large, well-centered, silvery gray metallic-looking dendritic plume formation (figure 21). The 26.87 ct cabochon measured 31.10 × 22.79 × 5.10 mm, and was represented as chalcedony with a dendritic formation composed of electrically induced metallic tin. It was a "one-only item" in a large group of obviously treated light blue-green translucent chalcedony cabochons that also contained electrically induced dendrites, but of elemental copper. We had encountered the latter dendrites

Figure 19. The pink spinel (1.36 ct) is predominantly colored by chromium, and the color of the purple sample (3.74 ct) is caused by a combination of chromium and iron. Photo by Maha Tannous.

in chalcedony on several prior occasions (see, e.g., Winter 1986 Gem News, p. 246). However, we had not previously examined a treated chalcedony with dendritic plumes represented as elemental tin, so we purchased this cabochon for testing and photography.

While standard gemological tests easily established that the cabochon was chalcedony, we turned to EDXRF analysis (by Sam Muhlmeister, of GIA's Research Department) to determine the chemical nature of the dendrites. This technique detected only silicon and tin. The strength of the tin peak, together with the metallic appearance of the dendritic plumes both macroscopically and microscopically, left no doubt that the dendrite formation was indeed composed of elemental tin.

This particular tin dendrite was probably produced by the same type of electrically stimulated chemical reaction sequence that is used to induce copper dendrites in chalcedony. G. W. Fischer provides step-by-step descriptions of the treatment processes used to form both copper and tin dendrites in porous translucent chalcedony in his book *Gemstone and Chemicals: How to Create Color and Inclusions* (self-published, 1991).

Figure 20. This schematic diagram shows the colors—and their causes—found in spinels from Ilakaka.

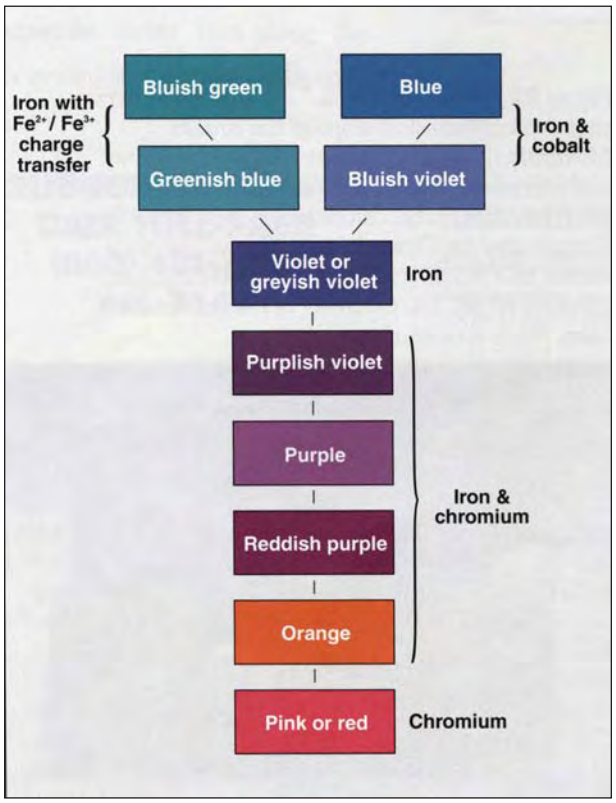

Figure 21. This 26.87 ct cabochon of chalcedony contains an electrochemically induced dendritic plume formation composed of elemental tin. Photo by Maha Tannous.

Induced copper dendrites in chalcedony are relatively attractive because of the color of the metal and the blue-green body color that the copper salt solution gives to the host chalcedony. However, the induced tin dendrites in the chalcedony we examined are a dull silvery gray, and the solution apparently does not produce an attractive color in the host either. It is probably this lack of visual appeal that has limited the production of chalcedony with induced tin dendrites.

SYNTHETICS AND SIMULANTS

Black diamond imitation. Black diamonds have become increasingly popular. Many manufacturers design jewelry that highlights them, often as large areas of melee. The main problem for the manufacturer is to make sure that the black diamonds are not treated or imitations. Beginning in late 1999, Franck Notari and Pierre-Yves Boillat of GemTechLab in Geneva, Switzerland, brought to the attention of this editor some unusual black diamond imitations. In the course of examining more than 17,000 black diamonds for jewelry manufacturers who specialize in this material, they separated out approximately 30 faceted samples (0.20 to 0.41 ct) because of their unusual luster (duller than is usually seen in black diamonds), uneven surface appearance, and luminescence excited by UV radiation (long- and short-wave, as described below). These samples also appeared slightly grayer than typical black diamonds (see, e.g., figure 22).

When examined with a 10× loupe or a binocular microscope, the material appeared inhomogeneous, with black shiny fragments of variable dimensions in a duller, lighter-color matrix. Most of the shiny fragments measured approximately 0.10 mm in maximum dimension. Although some were much smaller, a few reached nearly 1 mm. These fragments were relatively homogeneous in some samples, while in others they varied in

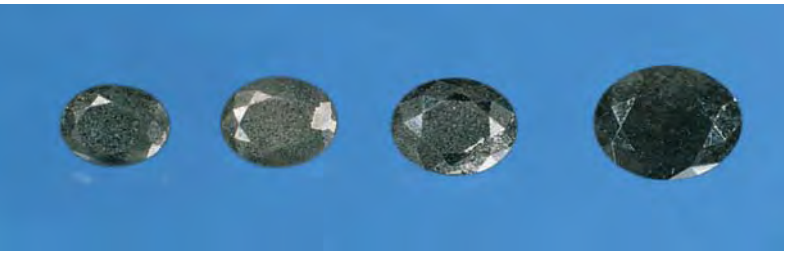

Figure 22. The three samples on the left are imitation black diamonds that are actually composed of diamond fragments in a metallic matrix; the 0.45 ct stone on the far right is a natural black diamond. From left to third right: 0.25 ct, Si-based matrix; 0.21 ct, Si-based matrix with some Rh recorded; 0.34 ct, Fe-based matrix. Photo by Alain Cossard.

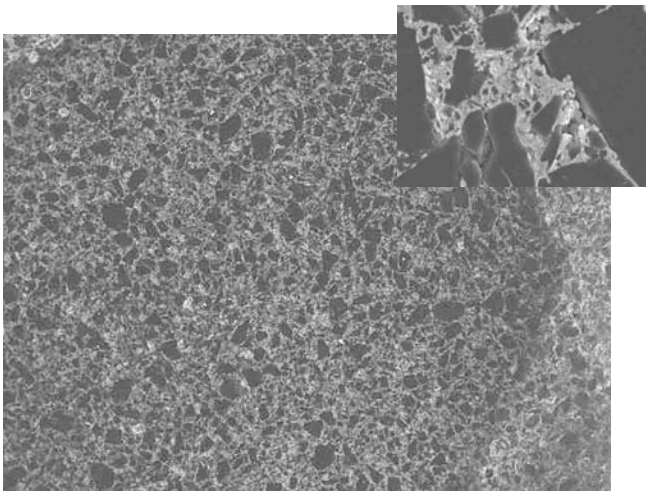

Figure 23. As seen with an SEM in this backscattered electron image (magnified 55×), the homogeneous dark areas are diamond and the lighter matrix is made of silicon, in this case with traces of rhodium. The inset (magnified 2300×) shows the "cauliflower" appearance of the matrix, contrasting with the sharp edges of the diamond fragments. Photos by Alain Barreau.

size by a factor of more than 10. Clearly, this material was not monocrystalline, as a natural faceted black diamond would be, but rather was a composite product that imitates black diamond. This composite nature was confirmed by the luminescence to long- and short-wave UV radiation, which revealed that the background was inert, but contained numerous tiny spots emitting various colors that corresponded to the fragments mentioned above. Some samples showed essentially the same fluorescence color in all the fragments; in others, the color varied greatly from grain to grain. Some grains even fluoresced more than one color.

Despite the inhomogeneous nature of these pieces, use of a carefully calibrated Digital Jemeter from Sarasota Instruments revealed approximate R.I. values of about 1.86 to 2.03. These values are consistent with the lower luster of these imitations compared to that of diamond (which has an R.I. of 2.42). The samples ranged in specific gravity from 3.04 to 3.52. Six samples were analyzed further at the University of Nantes. Laser Raman microspectrometry with a Jobin Yvon T64000 microprobe confirmed that the fragments were diamond, but the matrix gave no noticeable spectrum (perhaps because the surface condition was extremely poor). Secondary- and backscattered-electron images produced by a JEOL 5800 scanning electron microscope (SEM) showed shards of a material embedded in a matrix of higher atomic number (figure 23). At higher magnification (e.g., 2000×), the matrix had a "cauliflower" appearance and was often inhomogeneous. Microanalysis using an energy-dispersive spectrometer (with an "ultrathin" window) attached to the SEM confirmed that the shards contain carbon and no heavier elements.

The chemical composition of the matrix varied from sample to sample and, in some cases, within a sample. In one specimen, iron (Fe) and vanadium (V) dominated the composition (with traces of silicon and aluminum); in the other five, silicon (Si) was the main or only component. Among those five, two showed an admixture of rhodium (Rh) in variable amounts, one some Fe, and one was very inhomogeneous with some areas rich in Fe, V, and titanium, as well as traces of potassium, calcium, aluminum, chromium, tungsten, and molybdenum. This contributor believes that the rhodium probably is residual of plating applied to a silver setting while the stone was mounted. We were not

Figure 24. "Aurora Borealis," a 131 ct opal carving that depicts the north slope of the Brooks Mountain range in Alaska, took "Best of Show" and first place in the Carving division of the 2000 AGTA Cutting Edge competition. Fashioned from Oregon opal by Thomas Harth Ames, the piece stands 65.1 × 37.2 × 6.3 mm. Photo © 2000 John Parrish and AGTA. Courtesy of the American Gem Trade Association.

permitted to break a stone to check whether rhodium was present internally, or only on the surface.

Jean-Pierre Chalain of the SSEF Swiss Gemmological Laboratory informed us that he had seen two similar black diamond imitations in the summer of 1999. They were sent for study to Dr. Paul Spear of the De Beers DTC Research Centre in Maidenhead, United Kingdom. Dr. Spear established, by X-ray diffraction and chemical microanalysis, that these two samples consisted of diamond fragments in a matrix of iron-nickel or silicon. These conclusions are consistent with our findings.

Therefore, it appears that black diamond imitations, similar in concept but not all identical in chemical composition, have entered the gem market. They resemble "compacts"—abrasive materials made of small diamond particles that are cemented by a metal, generally cobalt or iron. One might wonder if this is a product engineered specifically as a gem simulant, or the by-product of a material developed for a specific industrial application. *EF*

ANNOUNCEMENTS

Tenth annual Cutting Edge awards. Judges chose 16 winners and five honorable mentions in this year's 10th annual Cutting Edge competition, sponsored by the American Gem Trade Association (AGTA) in Dallas, Texas, on April 29 and 30.

"Best of Show" and first place in Carving were awarded to "Aurora Borealis," a 131 ct rectangular opal carving fashioned by Thomas Harth Ames of Arvada, Colorado (figure 24). Other first-place awards were: Classic Gemstone—Allen Kleiman of Boulder, Colorado, for his 10.18 ct cushion-cut sapphire; Faceting—Joseph Krivanek of Alma, Colorado, for a 12.93 ct mixed square-cut rhodochrosite; New/Innovative/Combination—Thomas Trozzo of Culpeper, Virginia, for a 42.98 ct concave fancy-cut ametrine; Pairs & Suites—Stephen Avery of Lakewood, Colorado, for a 9.25 total carat weight "trishield" spessartite garnet pair; Objects of Art—Dalan Hargrave of San Antonio, Texas, for a scepter made of cat's-eye quartz, beryl, tourmaline, rose quartz, sunstone, peridot, and amethyst.

The competition was open to all colored gemstones of natural origin that were fashioned in North America by a professional lapidary artist. Entries were evaluated on the basis of design, quality of lapidary work, technique, quality and rarity of gem materials, and overall beauty. The winning gemstones were displayed at this year's JCK Show in Las Vegas, and the winners will be honored at the February 2001 AGTA Tucson GemFair.

The Dresden Green at the Smithsonian. The famous Dresden Green diamond will be on display for the first time in the United States, in the Harry Winston Gallery at the Smithsonian Institution's National Museum of Natural History, from October 2000 to January 2001. On loan from the Albertinum Museum, part of the Dresden State Museum, Germany, where it has resided since 1741, this approximately 41 ct diamond is the largest natural-color green diamond known. A full report on this diamond was published by R. E. Kane et al. in the Winter 1990 issue of *Gems & Gemology* (pp. 248–266). For more information, call the Museum at 202-357-2700.

Gem 2000. Presented by the Canadian Gemmological Association, Vancouver Community College, and the Vancouver Chapter of GIA Alumni and Associates, the Gem 2000 conference will be held October 20–22 in Vancouver. Several prominent industry figures will cover a variety of current topics in gemology. A variety of GIA Extension education classes will also take place before and during the conference, and an intensive six-day course on grading rough diamonds will be taught after the conference by John Louis Raath of Johannesburg, South Africa. For more information, visit www.giaalumni.bc.ca, or contact Donna Hawrelko at 604-926-2599 (phone), 604-926-7545 (fax), or e-mail donnahawrelko@hotmail.com.

Mineralientage München. The Munich Mineral Show 2000 will take place October 6–8, and will feature a special exhibit titled *Diamond—The Millennium Crystal*. In addition to 750 exhibitors and numerous collectors' showcases, the show will host a design competition in Unique Jewellery. For more information, fax 089-6135400, e-mail info@mineralientage.de, or visit http://mineralientage.de.

Gemstones at upcoming scientific meetings. These upcoming meetings will feature sections on gemstones:

• The 4th International Mineralogy and Museums Conference will take place in Melbourne, Australia, from December 3–7, 2000. The International Mineralogical Association Commission on Gem Materials will present a symposium in honor of Ralph Segnit on *Gems and Gem Materials*. Contact Dr. Bill Birch at 61-3-9270-5043 (fax), bbirch@mov.vic.gov.au (e-mail), or visit the Web site www.mov.vic.gov.au/mineralogy/mm4web/.

• *A Field Course on the Rare Element Pegmatites of Madagascar* will take participants to famous gem-bearing pegmatites on June 9–24, 2001. The itinerary will also include a brief visit to the Ilakaka alluvial gemstone deposit. Two days of scientific presentations in Antananarivo will round out the symposium. The meeting is being organized by the Museum of Natural History of Milan (Italy), the Department of Geology and Geophysics at the University of New Orleans, the Geological Survey at the Ministry of Energy and Mines in Antananarivo (Madagascar), and Pyramide Co., Antananarivo. A deposit and preregistration form are required; contact William B. "Skip" Simmons (e-mail wsimmons@uno.edu, or fax 504-280-7396).

Book Reviews

Susan B. Johnson & Jana E. Miyahira-Smith, Editors

PROCEEDINGS OF THE VIIth INTERNATIONAL KIMBERLITE CONFERENCE

Edited by J. J. Gurney, J. L. Gurney, M. D. Pascoe, and S. H. Richardson, 947 pp. in two volumes, illus., publ. by Red Roof Design, Cape Town, South Africa, 1999. US$150 (plus postage)

Since the First International Kimberlite Conference (IKC) was held in 1973 in Cape Town, South Africa, the world's leading authorities on the earth's upper mantle, the formation of kimberlites and natural diamonds, and the theoretical aspects of diamond exploration have gathered every four to five years to present the results of their research. Subsequent conferences were held in the United States (1977), France (1982), Australia (1986), Brazil (1991), and Russia (1995). In April 1998, the conference returned to Cape Town for its 25th anniversary meeting. This was the largest-ever IKC in number of delegates (over 600), extended abstracts submitted (361), and papers published in the two-volume IKC *Proceedings* (102). Each volume contains 51 papers, ordered alphabetically by the lead author's surname (rather than by subject area, as this reviewer would have preferred). Never before has so much new and exciting information appeared in the span between meetings.

No review of such a massive undertaking, with both applied and theoretical aspects, can do justice to it: Nevertheless, there are certain highlights. These include five review articles on: recent Canadian kimberlite discoveries (Carlson et al.), contrasting kimberlite emplacement in South Africa and Canada (Field and Scott Smith), crust-mantle coupling (Grutter et al.), tectonic aspects of the diamond-kimberlite connection (Helmstaedt and Harrap), and diamond formation in the earth's mantle (Navon). Of special interest to gemologists are the numerous contributions on specific new kimberlite discoveries worldwide in addition to Canada (e.g., Finland, Australia, and Brazil), and new details on the characteristics of rough diamonds from several localities (e.g., Yakutia and Jwaneng).

On the basis of these volumes, it is undeniable that major progress in all aspects of diamond and kimberlite geology has been made over the past few years. Furthermore, it is also clear that significant credit for much of this progress belongs to certain major international diamond producers such as De Beers, BHP Diamonds, and Alrosa. These corporations have laudably supported and encouraged such advances by supplying samples to many academics and research organizations and, for the first time, have enabled many of their scientists to present and publish articles on topics that heretofore would have been unthinkable. Yet there are still many loose ends and many differences of opinion on numerous topics, which ensures that the next IKC, scheduled to be held in Victoria, British Columbia, Canada, will be very interesting.

These IKC *Proceedings* volumes are well produced and very reasonably priced. They suffer only from the lack of an index. As a compendium of our present knowledge of kimberlites, the formation of diamonds, and related topics, they have no peer.

A. A. LEVINSON
University of Calgary
Calgary, Alberta, Canada

GEMS & JEWELRY APPRAISING, 2nd Edition

*By Anna M. Miller, 222 pp., illus., publ. by Gemstone Press, Woodstock, VT, 1999, US$39.95**

Eleven years after the first was published, this second edition of one of the original "how-to-be-an-appraiser" books does a sound job of updating and improving its predecessor.

Both editions follow the same format, as the author goes through the steps on how to become educated and affiliated, and how to set up an appraisal business. Chapters on appraisal procedures and the nature of value are followed by sections on value characteristics of individual varieties of gem materials, historical and specialty jewelry, carvings, and related personal property. The final chapters address the legal and ethical aspects of appraising, and the preparation of a professional appraisal report, with detailed examples. The appendix contains many helpful tables and charts, and the glossary complements the text well.

Especially welcome are the expanded and updated discussions of jade, pearls, period jewelry reproductions, ethnic jewelry, watches, ivory, and silver, along with a more extensive bibliography. New discussions of gemstone treatments and photography are important additions.

"Pie-in-the-sky" predictions of technological advances in appraising from the first edition are replaced by an excellent discussion on qualitative ranking and more down-to-earth listings of resources such as trading net-

This book is available for purchase through the GIA Bookstore, 5345 Armada Drive, Carlsbad, CA 92008. Telephone: (800) 421-7250, ext. 4200; outside the U.S. (760) 603-4200. Fax: (760) 603-4266.

works, helpful Web sites, and appraisal-related software.

Too many spelled-out numbers, a style carried forward from the first edition, make reading the text difficult. And in spite of an oblique reference to appraisal politics in the preface, the glaring omission of one of the major educational programs (listed in the first edition), and the inclusion of the author's own program without attribution, seems disingenuous. Minor errors, misdirected references, and misspellings of high-profile names (e.g., *Van Clef, Winstons*) detract from an otherwise well-edited book. The 83 black-and-white photographs and 23 line drawings, the majority of which come from the first edition, illustrate the material adequately.

Overall, this second edition of *Gem & Jewelry Appraising* is a good presentation of many of the business aspects that a professional jewelry appraiser will encounter. More than just a primer for novices, this book is also a quality resource for experienced jewelry appraisers.

CHARLES I. CARMONA
Guild Laboratories, Inc.
Los Angeles, California

1000 PHOTOS OF MINERALS AND FOSSILS

By Alain Eid, photography by Michel Viard, 127 pp., illus., publ. by Barron's Educational Series, Hauppauge, NY, 2000. US$24.95

This is the latest installment in the Barron's Educational "1000 Photos" series. Presented by the authors as an overview of gem cutting, mineral sources, metals, meteorites, and fossils, *1000 Photos* delivers only what its title promises, and little more.

The photos themselves are billed as the attraction of the book, and they are well made. In many instances, though, the photographer was given less than compelling subjects to work with, even by mineralogical standards. Moreover, the production quality of the book—including matte-like rather than glossy photographs and less-expensive, aromatic ink—deprives the photos of some of their impact and removes the desirable sheen that readers expect from a photo book.

1000 Photos is aimed at the home education and hobbyist demographic. As published, however, the book is probably suitable only for young students or the true neophyte hobbyist. The book's greatest shortcoming is a lack of any coherent organization or consistent theme. Portions of the book exposit outmoded conventions. The first sentence, "Only diamonds, rubies, sapphires, and emeralds can rightly be called precious stones," is off-putting to the gem enthusiast and is a strange introduction for what is supposed to be a mineral and fossil text. The italicized captions explaining the photos on each page, however, are more connected to the photos and more insightful than the body of the text. This might have been a more appealing book had the publisher limited its content to the photos and captions.

In sum, the photos in this book are worthwhile for a first discovery, but the book is weakened by a disappointing narrative and cheaper production values.

M. R. CAVENDISH
Cavendish of Avondale
Jacksonville, Florida

FIRE INTO ICE: CHARLES FIPKE AND THE GREAT DIAMOND HUNT

By Vernon Frolick, 354 pp., illus., publ. by Raincoast Books, Vancouver, 1999. US$21.95

In 1978, Canadian geologist Charles Fipke began a quest to find diamond-bearing kimberlite pipes beneath the tundra of Canada's Northwest Territories. He set out with little support and even less competition: The idea of Canadian diamonds was widely ridiculed, dismissed as a hoax. Thirteen years later, Fipke overcame the skepticism and the seemingly insurmountable odds by discovering the first Canadian diamonds. His claim eventually became the now-famous Ekati mine. But what drove him to pursue such an unlikely dream in the first place?

Fire Into Ice provides a wealth of insight into Fipke's complex character and intense personal drive. A rather lengthy background of the Fipke family leads up to a more telling description of Fipke's childhood in rural Canada, where he developed an aggressive spirit and an appreciation for the natural world. After completing his undergraduate work in geology in 1970, Fipke was sent by a major exploration company to the jungles of Western Papua, New Guinea. Prospecting for copper, Fipke frequently risked his life to obtain mineral samples. Another early assignment took him to Queensland, Australia, where he visited the opal fields of Lightning Ridge and got his first taste of gem mining. Throughout these and subsequent chapters set in the farthest reaches of southern Africa and South America, Fipke is portrayed as a compulsive explorer of minerals and cultures alike, one whose unorthodox methods often clashed with conventional wisdom.

Only the last quarter of *Fire Into Ice* is devoted to Fipke's Canadian exploits. Here the book presents an inside look at the risky world of geological exploration ventures, and how Fipke followed a trail of indicator minerals for more than 600 km to the source of the diamonds. Discussion of the diamond geology is light, and no maps are offered for this tale of discovery. In fact, illustrations for the entire book are limited to a handful of black-and-white photographs of Fipke and some of the localities from throughout his career.) With *Fire Into Ice*, Vernon Frolick has nevertheless created an absorbing account of the man who put Canadian diamonds on the map.

STUART D. OVERLIN
Gemological Institute of America
Carlsbad, California

Gemological ABSTRACTS

COLORED STONES AND ORGANIC MATERIALS

Characterisation of recent and fossil ivory. V. Rolandi, *Australian Gemmologist*, Vol. 20, No. 7, 1999, pp. 266–276.

This article begins with a brief historical overview of the use of ivory, and then examines the chemical, structural, and gemological properties of different types of ivory and ivory imitations. "Fossil" ivory comes from the preserved remains of mammoths, whereas present-day ivory sources include elephant, hippopotamus, babiroussa, wild boar, walrus, narwhal, and sperm whale. The article notes that mammoth ivory is not actually fossilized, since it is not altered by mineralization. Imitations include bone and vegetable "ivory" (i.e., hard seeds of certain palm trees). Curiously omitted are the seeds of the Doom palm (*Hyphaene thebaica*) of north and central Africa.

Diagnostic features are identified that will distinguish each type (e.g., hippo ivory is denser and of finer texture than elephant ivory). However, the value of easily determined physical features for studying ivory is variable. For example, specific gravity frequently can indicate the source of many ivories, but refractive index will only indicate that a specimen could be ivory. Other physical tests and gemological properties are not useful. Whereas visual examination with a microscope frequently enables discrimination of one type of ivory from another, in some cases it is extremely difficult (e.g., distinguishing elephant from mammoth ivory, particularly in small sizes).

This section is designed to provide as complete a record as practical of the recent literature on gems and gemology. Articles are selected for abstracting solely at the discretion of the section editor and his reviewers, and space limitations may require that we include only those articles that we feel will be of greatest interest to our readership.

Requests for reprints of articles abstracted must be addressed to the author or publisher of the original material.

The reviewer of each article is identified by his or her initials at the end of each abstract. Guest reviewers are identified by their full names. Opinions expressed in an abstract belong to the abstracter and in no way reflect the position of Gems & Gemology or GIA.

The inorganic and organic components differ among the various types of ivory, particularly in the amino acid contents of their collagen, and these are reflected in characteristic infrared spectra (which are illustrated). Amino acid differences were confirmed by biochemical analyses, which found higher hydroxyproline and hydroxylisine in elephant ivory than in mammoth ivory. Raman spectra provide complementary information to infrared: Often the weakest lines in the IR spectrum will be the strongest lines in the Raman spectrum. Notwithstanding the value of IR and Raman techniques for discriminating between look-alike ivories, they should always be used in conjunction with gemological properties and a detailed microscopic examination of the external surface of each specimen. *JEC*

Classification of the minerals of the tourmaline group. F. C. Hawthorne and D. J. Henry, *European Journal of Mineralogy*, Vol. 11, No. 2, 1999, pp. 201–215.

The variety and complexity of crystallographic sites and chemical elements in the tourmaline group [general formula $XY_3Z_6(T_6O_{18})(BO_3)_3V_3W$] results in the presence of numerous distinct species. Several tourmaline classification schemes have been proposed, but confusion on the nomenclature remains. This led the authors to propose a new working model based on chemistry and site occupancy; it is intended to facilitate continuing international research on tourmalines.

The following guidelines are used to develop the classification and assign species names: (1) The dominant *X* site element establishes whether the tourmaline belongs in the calcic, alkali, or vacant site group (e.g., liddicoatite, elbaite, and rossmanite, respectively); (2) the dominant anion in the *W* site determines the prefix "hydroxy-," "fluor-," or "oxy-" that is added to the species root name (e.g., fluor-elbaite); (3) in the *V* site, the dominant anion for most tourmalines is hydroxyl, (OH), except for the alkali tourmalines olenite and buergerite, for which O is prevalent; (4) *Y* site cations (Mg, Fe^{2+}, Li) define end-member compositions on three *W* site-based ternary diagrams in each of the three *X* site groups; and (5) *Z* site cations (Al, Cr^{3+}, Fe^{3+}) should be established as in step (4). Currently, there are 13 accepted tourmaline species, but the authors have defined 27 hypothetical end-member species that have yet to be found in nature.

The precision with which this system can be used depends on the level of chemical data available. Commonly used methods of tourmaline analysis, such as the electron microprobe, do not obtain data for light elements or oxidation states. Meaningful testing and further establishment of this classification scheme will require expensive and sophisticated analytical methods that account for all the variables of the tourmaline formula. Consequently, acceptance of this scheme must await a better understanding of tourmaline crystal chemistry. *JL*

Coloured gemstones have huge growth potential. *Mining in Southern Africa*, No. 3, 1999, pp. 1 *et passim*.

Southern and East Africa are the source of a significant amount of the world's colored gems. This article is a potpourri of short, but very informative, descriptions of important colored stone deposits in several African countries, with particular emphasis on those in the gem-rich Mozambique Orogenic Belt. This vast geologic formation extends at least 5,000 km from Sudan in the north, through East Africa and Mozambique, to Madagascar in the south.

Several gem minerals, and the mines that produce them, receive special recognition by virtue of their importance to world supply. Thus, the Sandawana mines in Zimbabwe, which have produced emeralds for nearly 40 years, are described. Although more than 50 kg of mixed grades are currently produced per month, only 4% have the necessary transparency and color to be faceted or cut *en cabochon*. Tanzanite, recovered exclusively from the Merelani Hill area of Tanzania, is considered the "gemstone find of the century"; at least one new major mining project is in the evaluation stage. Tourmaline from pegmatites in the Karibib-Usakos area of Namibia is believed to have great potential but, because the mining is artisanal (and consolidation of the industry under large companies has been resisted), at present there is a lack of regular production from this area.

Since colored gems usually have a relatively high specific gravity, dense-media separation is the recovery technique of choice, at least in larger automated operations. Two entries describe the operating conditions (e.g., particle size constraints), limitations, and advantages of modern dense-media separation plants and their use in southern African gem-mining operations. *MT*

A new pearl culture. D. Yonick, *Basel Magazine*, No. 3, June 1999, pp. 31–34.

Pearls are enjoying unprecedented popularity, yet the industry is faced with major changes and challenges. Of greatest significance is the prediction that China will dominate cultured pearl production in the 21st century, both in the saltwater and freshwater categories. Currently, China's greatest strength is in freshwater cultured pearls, with 1998 production of 800 tons. This is expected to double within five years. China is also producing tons (number unspecified) of saltwater Akoya cultured pearls, but the best of these are comparable only to medium-quality Japanese Akoya. In some cases, Chinese freshwater cultured pearls sell for 60%–70% less than comparable saltwater counterparts.

In Japan, the Akoya cultured pearl industry remains in crisis, stemming from the die-off of millions of oysters that started in 1996. This high mortality has resulted in a roughly 70% reduction in the amount produced, from about 18,000 kan before 1996 to about 5,000 kan currently (1 kan = 3.75 kg). It has caused a shortage in all sizes of

fine Akoyas, particularly in the 5–7 mm range. There are encouraging signs that development of a more resistant species of oyster, a cross between a Chinese breed and the Japanese Akoya, will be successful. Nevertheless, the Japanese pearl industry has been forced to restructure for the next four to five years, and it may never regain its previous dominance.

South Sea saltwater cultured pearls are also challenging the Japanese, with their white and black products having overtaken the Japanese Akoya. Australia and Tahiti are the main producing areas, with Indonesia and the Philippines becoming increasingly important. In terms of value, there are two-and-a-half times more South Sea than Akoya cultured pearls. Although in relatively small quantities, fine cultured pearls are coming from New Zealand (mabé cultured abalone pearls) and the U.S. (Tennessee freshwater cultured pearls). *JEM-S*

Pearls. *Jewellery News Asia*, No. 182, October 1999, pp. 47–48, 50, 52.

This collection of four short articles reviews several aspects of the pearl industry in Asia. In Indonesia, pearls are now being cultured in sizes above 12 mm; diameters up to 16 mm are not uncommon. Nevertheless, the future of the Indonesian pearling industry lies in upgrading quality (to obtain a whiter appearance), increasing yield, and maintaining the production of larger sizes. In Japan, expectations are for a 20% better harvest in 2000 compared to 1999 because of favorable weather during the summer of 1999 in the Akoya farming areas. Even so, the Akoya industry is still suffering from massive oyster mortality. Interestingly, China is importing larger quantities of cultured pearls despite its own enormous production of both freshwater and saltwater goods. However, analysis of customs statistics shows that cultured pearl exports from China are nine times greater than imports.

The saltwater cultured pearl industry, which comprises Akoyas and black and white South Sea cultured pearls, underwent a dramatic shift between 1994 and 1999. In 1994 it was valued at US$830 million, with Akoya cultured pearls dominating 66% of the total value (i.e., $550 million). In 1999, it was estimated that Akoyas would account for only 26.8% of a global market that had shrunk to $489 million. *JEM-S*

Philippine South Sea pearl industry moves towards the big league. L. Sanchez, *Jewellery News Asia*, No. 177, May 1999, pp. 72–73, 77.

In April 1999, the largest and most advanced cultured pearl farm in the Philippines was opened by Terramar Inc. The 5,000 hectare farm, with a staff of 200, is located at Shark's Fin Bay, Palawan Island. With its advanced technology in genetics, breeding, and cultivation, this farm is poised to push the Philippine pearl industry forward. The focus will be on expansion in quality, rather than quantity.

In late 1998, there were 23 cultured pearl farms in the Philippines, mostly on Palawan. The entire industry has taken a strong stance on environmental protection. The South Sea cultured pearl has been the country's national gem since 1996, and increased emphasis is being placed on promoting the Philippines as a source of quality cultured pearls. This goal is being fostered by the Philippine Association of Pearl Producers and Exporters (PAPPE), which has been successful in attracting international joint ventures, promoting the export of Philippine pearl products, and lobbying the government. *JEM-S*

Tantalizing turquoise. J. A. Harriss, *Smithsonian*, Vol. 30, No. 5, August 1999, pp. 70–78, 80.

A historical timeline on the use of turquoise, particularly in the Americas, weaves through this comprehensive article. Turquoise has held great fascination for many diverse cultures, ranging from the ancient Egyptians 5,500 years ago to the modern Navajo and Pueblo Indians of the southwestern U.S. Most U.S. mines are located in Arizona, New Mexico, Nevada, and Colorado. The article discusses these mines, past and present, including their colorful histories and their owners, production, and marketing channels. One profile depicts Douglas Magnus, a jewelry designer who in 1988 purchased a 50 acre area in the Cerrillos mining district of New Mexico that contains the famous Tiffany, Castilian, Alisa, and Council mines. He has since renamed the property the Millennium turquoise mine. In production since prehistoric times, the area had a strong resurgence from 1889 to 1910. The retail value of the turquoise mined during that interval is estimated at over $1 million. Magnus still collects turquoise pebbles in the old mine tunnels and uses them in his jewelry designs. Other renowned turquoise jewelry designers profiled in the article include Alvin Yellowhorse and Ray Tracey.

The article also discusses important turquoise collections held by the Smithsonian Institution in Washington, DC; the Turquoise Museum in Albuquerque, New Mexico; and the Millicent Rogers Museum in Taos, New Mexico. This museum overview encourages more exploration into this fascinating subject. *JEC*

Testing of copal resin and amber. Z. Qiu, B. Chen, and Y. Zhang, *Journal of Gems & Gemmology*, Vol. 1, No. 1, 1999, pp. 35–39 [in Chinese with English abstract].

The distinction between Kauri copal (from New Zealand) and amber is reviewed on the basis of the gemological properties, inclusions, and Fourier-transform infrared (FTIR) spectra of 25 specimens. The results demonstrate that copal can be distinguished from amber by testing with alcohol and by FTIR spectroscopy. A drop of alcohol on the surface of Kauri copal will cause the area tested to lose transparency within 30 seconds, but amber is unaffected. The use of specific gravity, refractive indices, and inclusions to make this separation must be done with caution. *RAH*

DIAMONDS

Argyle, Australien: Größte Diamantmine der Welt [Argyle, Australia: The world's largest diamond mine]. D. Pardon, *Lapis*, Vol. 24, No. 4, 1999, pp. 13–21 [in German].

This article provides comprehensive information on diamond mining at the Argyle mine, situated in the desert landscape of the West Kimberleys about 1,000 km (650 miles) west of Darwin, Australia. The diamond-bearing "Argyle Kimberlite No. 1" was discovered on October 2, 1979; the host rock was subsequently identified as lamproite. Diamond production started in 1982. Today, Argyle is the largest source of diamonds worldwide (1998 production was about 39 million carats). By autumn 1997, mining had turned the lamproite pipe into a valley 2 km long, with some 150 m of the original 530 m of lamproite still to be excavated. Open-pit mining will continue until at least 2002; the exact mining procedures, and amount of annual production, after that date are uncertain.

The author provides details on the mining and ore-processing methods, the qualities and colors of the diamonds, and historical production data. The world-famous pink-to-red diamonds are discussed, as are the difficult working conditions and the mine's relationship with the local population. Seventeen excellent photographs show the mine and the huge machinery used for excavation, along with rough diamonds (including a beautiful red crystal and the two largest pieces of rough found to date, a 42.6 ct "whitish" diamond and a 41.7 ct yellow) and some cut pink diamonds. *RT*

Confocal microscopy of color center distributions in diamond. J. Martin, W. Grebner, W. Sigle, and R. Wannemacher, *Journal of Luminescence*, Vol. 83–84, 1999, pp. 493–497.

The fluorescence bands at 637 nm and 575 nm in diamonds have been attributed to nitrogen-vacancy (NV) complexes caused by irradiation and annealing. Presently, the most widely accepted models show the 637 nm center to be negatively charged (NV^-) and the 575 nm center to be neutral (NV^0). A 1996 study by Y. Mita, which was based on a large number of samples that were homogeneously irradiated and annealed, showed that the 637 nm fluorescence is diminished when a diamond is exposed to a relatively high neutron irradiation dosage, while the 575 nm fluorescence appears abruptly at a certain dosage and then increases. The present study describes small type 1b synthetic diamond crystals (precise number not indicated) that were irradiated by a focused electron beam, annealed, and then imaged across the irradiated surface. A comparison of the 575 nm and 637 nm fluorescence profiles across the irradiated surface did not reveal any reduction in the 637 nm center corresponding to an increase in the 575 nm center with increasing irradiation dosage, which contradicts the earlier results reported by Mita. The asymmetry of the concentration profile for the 575 nm center suggests that other properties of the crystal may influence the strength of this center. *TB*

Current problems in diamond: Towards a quantitative understanding. G. Davies, *Physica B*, Vol. 273–274, 1999, pp. 15–23.

This article reviews recent work and current knowledge of the point defects in diamond. Point defects occur at the atomic level when the arrangement of carbon atoms is disrupted by the presence of foreign atoms (e.g., nitrogen, boron, or transition metals such as nickel and cobalt), by vacancies (atoms missing from normal positions), or by interstitials (atoms displaced to locations between normal positions). These defects are important because they can influence the physical properties of diamond. In gemology, the spectral features associated with point defects are important in helping distinguish natural, treated, and synthetic diamonds.

Characterization of point defects is carried out by careful measurements using several spectroscopic techniques. Studies of synthetic diamonds doped with foreign atoms, of diamonds with particular isotopic compositions, and of diamonds before and after exposure to ionizing radiation, all provide new information on various point defects. This includes their structure, as well as their rates of production, conversion to one another, or destruction. Although some point defects are well known, others are poorly understood and are the subject of current research. Data on the main point defects in diamond, and citations to relevant literature, are provided.

JES

De Beers as sightholder and major polished dealer. *Mazal U'Bracha*, Vol. 15, No. 112, July–August 1999, pp. 20 *et passim*.

Although the name *De Beers* has been associated almost exclusively with rough diamonds, for the past 34 years it has operated the little-known Polished Diamond Division (PDD), a sightholder in its own right. Best recognized as the Antwerp-headquartered sightholder Diatrada, PDD competes in all aspects of the polished diamond market. The division receives its rough diamonds in the same manner as other sightholders, and buys some rough for polishing on the open market. The PDD cuts its rough in its own factories or on contract, buys polished stones on the open market to satisfy its needs, and sells its production directly to jewelry manufacturers or retailers. Today it is one of the world's largest polished diamond manufacturers, with its own or contract factories in at least six countries and annual polished sales estimated at $120–$150 million. Clearly, De Beers—through its PDD subsidiary—competes with other De Beers sightholders and is a major polished dealer.

The question arises as to the motive for such a division. According to Jeremy Richdale, head of the PDD, the

motivation is to collect information and gain a better understanding of the polished diamond market. This can only be done by conducting business in the same manner as other sightholders. The sentiment is that "you cannot fix the price of rough if you don't know correctly the price of polished." De Beers wants to ensure that sight boxes are profitable and that sightholders are not losing money in the long run. The long-term purpose of the PDD is to provide information as a service to the main body of De Beers, and to educate the company in the broader sense about polished diamonds. *Phil York*

Diamonds and accompanying minerals from the Arkhangelsk kimberlite[s], Russia. T. V. Possoukhova, G. P. Kudryavtseva, and V. K. Garanin, in C. J. Stanley et al., Eds., *Mineral Deposits: Processes to Processing*, Proceedings of the 5th Biennial SGA Meeting and the 10th Quadrennial IAGOD Symposium, London, August 22–25, 1999, Balkema/Rotterdam/Brookfield, 1999, pp. 667–670.

A study of more than 200 diamond crystals—as well as garnet, spinel, ilmenite, pyroxene, and olivine—from three kimberlite fields in the Arkhangelsk diamondiferous province is reported. The characteristics of the diamonds and their accompanying minerals differ from one field to another, according to the depth of formation of the parent kimberlite.

More than 50% of the diamonds examined from the Lomonosov deposit (Zolotitskoye field) were of gem quality; most were rhombododecahedra, some showing a blue luminescence. The main feature of diamonds from the Verkhotinskoye field is the presence of fragments derived from larger crystals (i.e., >4 mm), which indicates the existence there of larger diamonds. The Kepinskoye field is characterized by smaller quantities of diamonds, all <0.5 mm in size and mostly as fragments of distorted crystals with an irregular appearance. The diamond potential of the kimberlites in the Arkhangelsk diamondiferous province decreases toward the east. *RAH*

A diamond trilogy: Superplumes, supercontinents, and supernovae. S. E. Haggerty, *Science*, Vol. 285, No. 5429, August 6, 1999, pp. 851–860.

This ambitious review article integrates the various occurrences and origins of natural diamonds in the universe, the formation of kimberlites and related rocks that originate in the mantle, and the emplacement of these diamond-containing rocks into ancient (>1.6 billion years old) cratons on the earth's surface. A major theme is that diamond is an extraordinary time capsule of astrophysical and geodynamic events that extend from the far reaches of space to the earth's deep interior. Diamonds have formed in (1) presolar *supernovae* (the explosions of dying stars) by carbon vapor deposition, (2) asteroid impacts by shock metamorphism, and (3) the earth's mantle from fluids and melts. In 1990, great quantities of microdiamonds (the largest is 100 microns) were reported for the first time in metamorphic crustal rocks from Kazakhstan, and later from Norway and China. These microdiamonds are the products of ultra-high-pressure metamorphism during the periods of major continent-continent collisions that produced the Eurasian *supercontinent*.

Gem-quality diamonds are formed only in the mantle. The general consensus is that mantle diamonds formed in one of two types of rocks: peridotites (P-type) from primordial carbon, or eclogites (E-type) from carbon originally on the earth's surface. Here the author takes the controversial position that the carbon in E-type diamonds is also primordial. With respect to kimberlite and related rocks that bring diamonds to the earth's surface, it is argued that these rocks form at depths of at least 410 km (because some mineral inclusions within diamonds formed at such depths), and possibly in the lower mantle (660 to 2,900 km). They rise to the surface in *superplumes*, large bodies of magma ascending into the crust from as deep as the core-mantle boundary. Superplumes are uncommon global events, but they have been correlated with periods of major kimberlite emplacements, for example 80–120 million years ago. *AAL*

Diamonds in volcaniclastic komatiite from French Guiana. R. Capdevila, N. Arndt, J. Letendre, and J.-F. Sauvage. *Nature*, Vol. 399, No. 6735, June 3, 1999, pp. 456–458.

Diamonds were first documented in the Dachine region of French Guiana in 1982. Further exploration revealed a new type of primary diamond occurrence in the area. The host rock is komatiite (now altered to a talc schist), an unusual type of ultramafic volcanic rock. Its chemical composition (particularly some trace elements) and origin as part of an island-arc sequence are unlike those of kimberlite and lamproite, which are found in stable cratonic settings. Like kimberlite and lamproite, however, the komatiite formed at depths of greater than 150 km, where diamond is stable, and rapidly transported the diamonds to the surface.

The komatiite host rock at Dachine is at least 5 km long and 350–1,100 m wide, making this a potentially very large deposit. On the basis of sampling to date, microdiamonds predominate, although larger diamonds (>1 mm) are locally abundant. The largest diamond recovered is ~4.6 mm in diameter. The grade reaches 4 ct/m^3 in alluvium overlying mineralized bedrock, though neither the quality nor value of the stones is stated. This discovery has exploration implications for Canada, South Africa, Norway, and other countries in which komatiitic volcanic rocks are known. *AAL*

Hennig and Bettonville joint venture: "The Visag Option." C. Even-Zohar, *Mazal U'Bracha*, Vol. 15, No. 109, March–April 1999, pp. 38 *et passim*.

For those sightholders and manufacturers of diamonds who are finding it difficult to cut certain goods and still stay profitable, the solution may be "The Visag Option."

Visag, as the harbor city of Vishakhapatnam is known, is located in one of India's poorest regions, on the east coast a few hundred kilometers south of Calcutta. It is also a "free export processing zone," where import and export operations are very efficient. Worldwide Diamond Manufactures Pvt. Ltd., a joint venture between I. Hennig and Bettonville, has opened a state-of-the-art plant there that offers a subcontracting service for diamond cutting, especially of better goods typical of Israel, Belgium, and South Africa. The joint venture concentrates on the 2 grainer (0.50 ct) range, as distinct from the small diamonds typically cut in India. The success of this operation can be related directly to its labor costs ($60–$75 per month), which are significantly lower than those in other parts of India.

Visag represents a new concept in the diamond industry. I Hennig, a CSO broker, now considers itself a specialized diamond consultancy. Although its main function remains that of a diamond broker, this new role permits and encourages diversification into complementary services, such as diamond manufacturing on a contract basis (but not into diamond marketing, as this would conflict with the interests of its core CSO clients). For Bettonville, the world's major manufacturer and supplier of diamond industry equipment, it is an opportunity to become a consumer of its own products. For both partners, it is an opportunity to gain manufacturing experience that will be useful in understanding the problems of their respective core clients. The ideological and philosophical change illustrated by this joint venture is a harbinger of things to come in the rapidly changing traditions of the diamond industry. *Phil York*

New tool for diamond separation. *Mining Journal, London*, Vol. 333, No. 8554, October 22, 1999, p. 327.

Deb Tech, De Beers's technical division, has developed a more accurate method for separating diamond ore components with different densities by using magnetic fluids. Such fluids, which were developed by NASA in the 1960s, have a unique property in that their apparent density changes when they are exposed to a uniform magnetic field. Ferrohydrostatic separation (FHS) allows the separation of materials with specific gravities within 0.02 of each other; a proprietary DebTech system monitors the fluid to adjust for changes induced, for example, by temperature. A prototype has recently been tested successfully, and De Beers hopes to use this separation system on its oceangoing mining vessels. *MLJ*

Optoelectronic unit for the detection of diamonds by Raman light scattering. O. A. Gudaev, I. F. Kanaev, V. I. Paterikin, I. N. Kupriyanov, and A. F. Tirmyaev, *Journal of Mining Science*, Vol. 34, No. 6, 1998, pp. 561–564.

In today's highly automated processing plants, crushed kimberlite or lamproite ore concentrate is passed through an X-ray beam, causing the diamonds to fluoresce. Photosensors trigger a directed jet of air that separates the diamonds from the ore. However, this technique has certain limitations, as some diamonds do not fluoresce strongly enough to trigger the device. Further, some nondiamondiferous components of the ore also fluoresce strongly, requiring an additional separation procedure.

An experimental technique based on Raman light scattering (RS) offers the potential to overcome the deficiencies of the X-ray excitation method. A narrow-band He-Ne laser (λ = 632.8 nm) produces an RS band in all diamonds and is particularly intense in high-quality diamonds (for reasons not explained in the article). In addition, a general luminescence is produced in diamonds that is variable in intensity and spectral composition. By means of dedicated photoelectron multipliers (one each for the RS and luminescence spectra) and an electronic comparison circuit, it is possible to identify diamonds rapidly, to the exclusion of other ore components; in practice, the diamonds could then be separated by a directed jet of air. Laboratory tests on 100 diamonds of all types and qualities, and on 40 typical diamond-bearing rocks, were successful. *Phil York*

Russian gem diamond production forecast to reach $2.2 billion by 2005. S. Oulin, *Mazal U'Bracha*, Vol. 15, No. 113, September 1999, pp. 71–73.

Projections for the Russian diamond industry, including both the mining and polishing sectors, are extremely promising in the eyes of the author, the vice president of Alrosa. This company currently mines 98% of Russia's diamonds, all in Yakutia (Sakha). This article highlights several facts that are not widely known about the Russian diamond industry, such as:

- The industry directly employs about 50,000 workers, mostly in mining.
- Of the approximately US$700 million of polished goods that are manufactured annually, 97% are exported.
- More than 150 diamond polishing companies are registered, but only about 60 are currently active.
- These domestic polishing companies have priority in purchasing rough, for which they pay 2%–3% below world prices.
- There are 13 major jewelry manufacturing factories; diamond jewelry accounts for 25% of the locally manufactured jewelry.

In the mining sector, Russia presently produces about 20% of the world's diamonds by value—about US$1.4 billion, second only to Botswana. There are proven diamond reserves for 40–50 years, with predicted resources that are 2.5 times the proven reserves. The forecast calls for the Russian diamond industry to generate $2.2 billion in 2005, mostly realized by a significant increase in rough diamond production. The forecast is more likely to become a reality with large infusions of capital, for which Alrosa has gone to the world's financial markets. *AAL*

GEM LOCALITIES

Characterisation of emeralds from the Delbegetey deposit, Kazakhstan. E. V. Gavrilenko and B. Calvo Pérez, In C. J. Stanley et al., Eds., *Mineral Deposits: Processes to Processing*, Proceedings of the 5th Biennial SGA Meeting and the 10th Quadrennial IAGOD Symposium, London, August 22–25, 1999, Balkema/Rotterdam/Brookfield, 1999, pp. 1097–1100.

A study of the properties and composition of 12 emeralds and green beryls from the Delbegetey deposit is reported, and comparisons are made both with emeralds from elsewhere in the world and with synthetic emeralds. The Delbegetey emeralds have a saturated bluish green hue, with n_ε = 1.558–1.562, n_ω = 1.566–1.570, and a density of 2.65 g/cm^3. These refractive index and density values are low in comparison with those of other natural emeralds and beryls; in fact, they are typical of the values for flux-grown synthetic emeralds. Averaged electron microprobe analysis values for 11 emeralds are tabulated: 0.02–1.23 wt.% Cr_2O_3, 0.01–0.19 wt.% V_2O_3, and low Na, Mg, and Fe. Primary fluid inclusions have unusual liquid-to-vapor ratios of 50:50 to 90:10; emeralds from other deposits generally have a greater abundance of the liquid phase.

This deposit is genetically associated with a granite intrusion. Unlike other deposits, which tend to be associated with metamorphic rocks and/or intrusive ultrabasic rocks rich in Cr, Delbegetey is hosted by sedimentary rocks. The source of the Cr to color the emeralds is unresolved. *RAH*

Emeralds in the Eastern Cordillera of Colombia: Two tectonic settings for one mineralization. Y. Branquet, B. Laumonier, A. Cheilletz, and G. Giuliani, *Geology*, Vol. 27, No. 7, July 1999, pp. 597–600.

The two major emerald-producing areas in the Eastern Cordillera of Colombia are the Western Zone (which contains Muzo and Coscuez) and the Eastern Zone (which contains Chivor and Gachalá), about 100 km north and 75 km northeast, respectively, of Bogotá. Recent work has shown that all the Eastern Cordilleran emerald deposits formed from hydrothermal fluids that originated from the dissolution of evaporite deposits and the metasomatism of other associated sedimentary rocks. The authors propose that the two zones formed at different times and in distinctly different tectonic settings.

Emeralds in the Western Zone are found in hydrothermal breccias or carbonate-pyrite veins, and the deposits are folded and broken by compressional faults. The deposits are located in structural traps along regional tear faults, which suggests that emerald mineralization was contemporaneous with regional compressional development of the Eastern Cordillera mountains about 38–32 million years ago.

Eastern Zone emerald mineralization occurred along centimeter-scale extensional faults, meter-scale extensional fractures injected with hydrothermal breccia, and a prominent set of parallel extensional fractures filled with carbonate and pyrite. These emerald deposits, classified as stratiform, appear to be associated with extensional deformation that occurred about 65 million years ago.

The rocks that host these deposits were subsequently folded by the compressional events mentioned above.

This study points out the diversity of geologic environments in which Colombian emeralds can form. Since the currently exploited emerald deposits in Colombia are being exhausted, a good understanding of the geology associated with the deposits will aid prospectors. *JL*

Lavra da Sapo—derzeit fündigste Turmalin-Mine in Minais Gerais/Brasilien [Lavra da Sapo—Currently the most productive tourmaline mine in Minas Gerais/Brazil]. G. Steger, *Lapis*, Vol. 24, No. 3, 1999, pp. 26–29 [in German].

This article describes the gem-bearing pegmatites of the Lavra da Sapo mine, near Goiabera, about 130 km (80 miles) east of Governador Valadares, Minas Gerais. The author visited this underground mine in November 1998. Access to the mine is difficult because of the poor roads, which turn to mud during the rainy season. During four and a half years of mining, about 250 m of tunnels have been excavated under difficult working conditions (heat, dust, and constant danger of flooding). The mine has produced about 70 tons of "crocodile quartz," 20 tons of "window quartz," and 10 tons of citrine. In addition, morganite (amount not specified) and some goshenite, aquamarine, dravite, schorl, and herderite have been recovered. Of greatest interest, though, are the spectacular elbaite tourmalines, which have been found in many colors and sizes, up to 1 m and larger. The article contains a sketch map of the tunnels, along with photos of the mining operation and of some of the beautiful tourmaline specimens it has produced. *RT*

On the nature of colouring of gem clinohumites from Kukhilal (the south-western Pamirs). L. V. Nickolskaya, S. S. Rudenko, M. V. Zamoryanskaya, and A. V. Shchukarev, *Proceedings of the Russian Mineralogical Society*, Vol. 128, No. 2, 1999, pp. 93–99 [in Russian with English abstract].

Platy specimens of yellow-to-brown gem-quality clinohumite [$(Mg,Fe^{2+})_9(SiO_4)_4(F,OH)_2$] were investigated by optical microscopy, electron microprobe, cathodoluminescence, and X-ray photoelectronic spectroscopy in order to interpret their optical absorption spectra. The main chromophores, as shown by electron microprobe lie in the ranges Ti = 0.95%–1.5%, Fe = 0.05%–0.15%, and Mn = 0.01%–0.02%; the latter was detected in "honey"-colored specimens. Titanium enters the Mg sites, forming the charge-transfer pairs $Ti^{3+}_{M(3)} \rightarrow Ti^{4+}_{M(3)}$, which mainly cause the yellow-to-brown clinohumite color. The Fe^{2+} chromophore, which can also form pairs with charge transition following the scheme $Fe^{2+}_{M(2)} \rightarrow Ti^{4+}_{M(3)}$ and $Fe^{2+}_{M(1)} \rightarrow Fe^{3+}_{M(2)}$, appears in spectra taken in certain non-{001} orientations but does not have any significant influence on coloring.

The color, however, is influenced considerably by the orientation effect, which determines the clinohumite's pleochroism. *RAH*

Fluid inclusion characteristics of sapphires from Thailand. B. Srithai and A. H. Rankin, in C. J. Stanley et al., Eds., *Mineral Deposits: Processes to Processing*, Proceedings of the 5th Biennial SGA Meeting and the 10th Quadrennial IAGOD Symposium, London, August 22–25, 1999, Balkema/Rotterdam/Brookfield, 1999, pp. 107–111.

Three main types of fluid inclusions occur in Bo Ploi sapphires: (1) vapor-rich CO_2 with a density up to about 0.86 g/cm^3; (2) multiphase inclusions with several daughter minerals, hypersaline brine, and a CO_2-rich vapor phase; and (3) (silicate?)-melt inclusions with immobile vapor bubbles in an isotropic/weakly anisotropic phase of low relief. The bubbles move when heated to >800°C. These results suggest a magmatic source for these sapphires (but they did not form as phenocrysts within the basalts that brought them to the surface). *RAH*

Pyrope from Yunnan province, China. W. Zhang, *Journal of Gems & Gemmology*, Vol. 1, No. 2, 1999, pp. 22–24 [in Chinese with English abstract].

The geologic occurrence, gemological properties, and chemical features of pyrope garnet from Yunnan, China, are described, as is the economic importance of this material. The garnets are relatively large and of attractive color, with few imperfections. They are found in weathered Neogene basaltic breccia pipes along with gem-quality chrome diopside. Data are presented for R.I., density, color, and selected chemical components (Al, Mg, Fe, and Cr). The red color is caused by chromium. On the basis of Cr content, three categories of pyrope were recognized: chromium-bearing pyrope, low-chromium pyrope, and pyrope.

This garnet, which has enjoyed a positive market response over the past decade, is mainly faceted as ovals in various sizes (from 3 × 5 mm to 10 × 12 mm). Some of the jewelry products are exported to Hong Kong, the U.S., and Japan. *Taijin Lu*

Rare earth elements in corundum-bearing metasomatic and related rocks of the eastern Pamirs. E. N. Terekhov, V. A. Kruglov, and V. I. Levitskii, *Geochemistry International*, Vol. 37, No. 3, 1999, pp. 202–212.

Corundum-bearing rocks containing ruby, sapphire, and pink sapphire are found in the Kukurt gemstone field, in the Pamir Mountains of southern Tajikistan. The authors used rare-earth-element (REE) data and other geochemical characteristics of rocks in this region to study the processes and conditions of corundum formation.

This research, and related work by other scientists, suggests that the oldest rocks in the Kukurt area underwent a major metamorphic event more than 500 million years (m.y.) ago. Corundum mineralization occurred much more recently, about 20 m.y. ago, during the formation of the Himalayas. Most of the corundum occurrences are related to linear geologic structures such as shear zones and lithologic contacts; they are found in several different rock types, mainly marble and gneiss.

According to the authors, geochemical enrichments in REE, Al, Ti, and several trace elements—as well as the association of minerals rich in Cl, B, and F in the corundum-bearing rocks—suggest that gem corundum mineralization was caused by through-flowing volatile-rich fluids that possibly originated in a deep-seated mantle source. Fluid movement was facilitated by the active deformation associated with mountain-building events. Since these events were regional in character, other commercially viable corundum deposits may be found through the application of these models to geologically similar areas in the high mountain ranges of Central Asia. *JL*

Ruby mineralization in southwest Madagascar. A. Mercier, M. Rakotondrazafy, and B. Ravolomiandrinarivo, *Gondwana Research*, Vol. 2, No. 3, 1999, pp. 433–438.

The primary ruby deposits in the Ejeda-Fotadrevo area in southwest Madagascar are closely associated with basic to ultrabasic complexes within the high-grade metamorphic terrain of the Precambrian Vohibory unit. Ruby is recovered from amphibolite and anorthosite veins within these complexes. Petrographic data and pressure-temperature estimates indicate that the ruby-bearing rocks crystallized under granulite-facies conditions of 750°–850°C and 9–11.5 kbar.

These Malagasy ruby deposits have many similarities with those of East Africa, particularly Tanzania, which indicates a similar geologic setting. This suggests that ruby formation in both these areas resulted from the same mineralizing event while Madagascar was still attached to East Africa. *RAH*

The ruby mines of Mogok. T. Waltham, *Geology Today*, Vol. 15, No. 4, 1999, pp. 143–149.

This timely article is an update on mining methods and production statistics for the Mogok ruby mining area in Myanmar. There are now more than 1,000 mines in the Mogok Stone Tract (a zone about 20 km wide and 5 km long between the Kin and Yeni Rivers), most of which are small and labor intensive but appropriate for the region. There are about 500 mines each in *byon* (gem-bearing alluvial sediments) and bedrock. Together, the mines produce over 100,000 carats (20 kg) of rubies annually, as well as three times that amount in other colored gems—predominantly sapphires and spinels, but also topaz, peridot, and tourmaline, among others.

The vast majority of the gems are still recovered from byon, which can be up to 50 m thick on floors of the Mogok and Kyatpyin Valleys, by the same primitive methods developed centuries ago. Most production comes from

twilons (round, unlined shafts about 15 m deep) or *lebins* (square shafts lined with a bamboo framework that go down as far as 30 m). A few large and relatively modern open-pit mines are operating in byon, one of which (Shwepyiaye) is 300 m across and has reached a depth of 30 m. This mine produces only about 25 carats of ruby from the 100 tonnes of gravels processed daily. At primary deposits (i.e., *loodwins*), tunnels follow calcite veins that are typically 2–3 m wide. Deep loodwins (up to 300 m) operate intermittently, in part because of flooding during the monsoon season.

The gem markets are functioning essentially in the same traditional manner, with most of the trading conducted by women in open-air markets. The most obvious change in the past 40 years has been the formation of the Myanma Gems Enterprise in Yangon; this successful operation sells most of the output from government-owned mines, and reportedly all of the large stones.

KSM

Sapphire and ruby in Australia. B. J. Neville and F. von Gnielinski, *Queensland Government Mining Journal*, Vol. 100, No. 1171, June 1999, pp. 6–12.

Sapphires, predominantly medium to dark blue but also in other colors (e.g., green and parti-color), have been mined in eastern Australia for more than 100 years. Most have come from two major fields: Anakie in Queensland, and New England in New South Wales. The sapphires are alluvial, derived from the erosion of alkali volcanic rocks (basalt lavas, pyroclastics, and volcaniclastics) of Tertiary and Quaternary age. They are similar in many ways (including gemological properties) to sapphires from Thailand, Cambodia, Nigeria, and China, which also are associated with alkali volcanic rocks of similar ages.

The gem properties of Australian sapphires are typical for sapphire, with a broad range of refractive index (n_ε = 1.761–1.765, n_ω = 1.769–1.774) and specific gravity (3.97–4.02) values. The diaphaneity varies from transparent to opaque. Most stones exhibit a strong 450 nm iron-related absorption band with a spectroscope, and most are inert to both long- and short-wave UV radiation. Australian sapphires are characterized by their inclusions (e.g., pyrochlore, ilmenite, and spinel), chemistry (high iron content), and strong growth zoning and color banding. Nearly all are heat treated to improve clarity and color. The average size of faceted Australian sapphires is under 2 ct. The largest recorded rough sapphire, which weighed 4,180 ct, was carved into a 3,294 ct bust of Dr. Martin Luther King, Jr.

Although numerous alluvial occurrences of ruby have been reported in Australia, gem-quality material is rare, and none of these deposits has ever been economic. The first discovery with significant potential was within gneiss in the Harts Range (Northern Territory). However, mining ceased after only minor production of mostly low-grade cabochon material.

Sapphire mining in Australia was minor and sporadic from the 1880s until the early 1960s, except for a few favorable periods—such as immediately preceding World War I, when there was strong demand from Germany and Imperial Russia. Demand for sapphires increased in the 1960s and, with the arrival of buyers from Thailand, there was unprecedented activity in the Anakie and New England fields. Mining reached its peak in the mid-1970s, making Australia a major world producer. Since then, the Australian sapphire industry has declined because of the depletion of known resources, increased costs, and difficult land access. The situation has been further exacerbated by the discovery in recent years of important deposits in countries that have lower mining costs, mainly Madagascar, Tanzania, and Nigeria. Since 1998, sapphire mining in Australia has effectively ceased, and the industry faces an uncertain future. *KSM*

JEWELRY MANUFACTURING

Getting the lead out. S. Wade, *American Jewelry Manufacturer*, Vol. 44, No. 4, April 1999, pp. 32–35, 37.

The health and environmental hazards of many chemicals and heavy metals has prompted U.S. manufacturers to eliminate such materials from their work environment. Accordingly, many jewelry manufacturers have started using lead-free alloys when casting white metals. Doing so is not always as easy as it sounds, because lead-free alternatives lack the pouring fluidity of leaded alloys, which can lead to casting problems.

This article offers many suggestions that will help manufacturers make the transition away from leaded alloys. The first and most basic is simply to ask metals suppliers for advice based on the job that is planned; specific alloys may be recommended for certain types of casting. Also included are suggestions for dealing with high casting temperatures, porosity, and finishing. The transition to lead-free alloys will be easier if it is researched and well planned. *JEM-S*

Unshrouding the mystery of invisibly set gemstones. G. Roskin, *Jewelers' Circular Keystone*, Vol. 170, No. 8, August 1999, pp. 84–88, 90.

Originally popular during the Art Deco movement, which dominated the 1920s and 1930s, invisibly set jewelry returned boldly to the market in the 1990s. Characterized as "a ribbon of gemstones," the style is designed to show only the gems and none of the metal mounting. Although several jewelers claimed that they had perfected invisibly set jewelry, this technique became synonymous with the firm of Van Cleef & Arpels.

In 1929, jeweler Jacques-Albert Algier patented a method of holding a gem in place without metal showing by cutting a groove in the pavilion of the stone and sliding it along rails of precious metal. In December 1933, Van Cleef & Arpels filed their patent for an invisible setting, which they called *serti mysterieux* ("mystery setting"). Using crude saw blades of silk that were coated

with diamond powder, precise grooves were carved on opposite sides of each gem. Many gems were broken during the grooving process. Some important pieces used hundreds of gems and required months to construct.

Due to changing tastes and designs in the 1950s, the style practically vanished. Since the 1980s, however, there has been a resurgence of invisibly set jewelry. Leading the way was Robert Bruce Bielka, a Certified Master Bench Jeweler, who invented "Jeweled Mesh for Jewelry." Using hexagonally faceted gems notched and set into individual hidden fasteners, Bielka has found a way to add flowing movement to his pieces of invisibly set jewelry. Thanks to new titanium, ceramic, and laser saws, cutting the grooves has become cheaper and faster (with less breakage). Some jewelers are also trying newer, faster techniques to create invisibly set jewelry. With in-place casting, for example, diamonds are placed in the wax and the jewelry is cast with the diamonds in place.

Most invisibly set jewelry involves diamond or corundum gemstones ranging from 1.4 to 3.5 mm. Repairing or sizing invisibly set jewelry from any era can be extremely difficult. *Paige Tullos*

JEWELRY RETAILING

Antique-cut diamonds stage a comeback. *Jewellery News Asia*, No. 181, September 1999, pp. 292, 294, 296.

The jewelry industry has witnessed a renewed interest in antique-cut diamonds. Some in the industry attribute this to a sentimentality for what is old as we start the new millennium. Some younger consumers also see past eras as romantic, and movies such as *Titanic* have increased interest in antiques and antique-inspired designs. Although the trend has yet to gain acceptance in some countries (such as Japan), designers in the U.S. and Europe have enjoyed increased demand for antique styles. The old-cut diamonds are also desired for replacement stones in antique jewelry pieces that need repair.

Particular interest is being shown in the following antique cuts: rose, bead, old European, old mine, and briolette. Briolettes have the added advantage of being able to conceal small inclusions better than the modern round brilliant, and so medium-clarity stones tend to look clean. The supply of diamond rough suitable for rose cuts, meanwhile, has not been able to keep up with demand. One reason is that trilliants and higher-domed rose cuts are produced from the same types of rough; suppliers may add a premium to such goods. Some manufacturers in India are catering to this niche market. *JEM-S*

Making your transition to an Internet economy. J. S. Diamond, *Jewelers' Circular Keystone*, Vol. 170, No. 10, October 1999, pp. 146 *et passim*.

The impact of the Internet on jewelry retailing can no longer be ignored. Online jewelry sales totaled roughly $102 million in 1999, and they are expected to double in *each* of the next five years. Yet few independent jewelers are selling directly on the Internet for a variety of reasons, such as the perceived expense of setting up, maintaining, and advertising a Web site. However, 54% of jewelers do use the Internet for business purposes other than selling—mainly, buying merchandise, locating new suppliers, researching competitors, and viewing industry Web sites.

The 20% of jewelry retailers who do use the Internet for selling employ three approaches: (1) providing a virtual brochure to build an image and credibility for the store, (2) selling online at fixed prices, and (3) selling through online auctions.

There are numerous other potentially lucrative ways, requiring relatively little time or money, in which the Internet can be used in the retail jewelry business. Some examples include: (1) e-mail marketing, that is, sending direct mail, personal notes, or newsletters about upcoming special sales or events to customers who indicate they would welcome such information; (2) setting up an unobtrusive "information-only" Web site; (3) posting jewelry images with price and product information, along with a toll-free phone number, on the information-only Web site; (4) publicizing the online address, such as in Yellow Pages advertising, to attract customers because only a small portion of retail jewelry store Web sites are listed by search engines; and (5) offering an e-mail occasion-reminder service (e.g., for birthdays and anniversaries) to interested customers. *JY*

PRECIOUS METALS

Gold production history of the United States. J. R. Craig and J. D. Rimstidt, *Ore Geology Reviews*, Vol. 13, No. 6, 1999, pp. 407–464.

This remarkably complete and interesting report compiles historical data (mainly from government sources) on gold discoveries, commercial production, and prices in the U.S. Undocumented production by Native Americans could not be quantified, although descriptions of major discoveries in the 17th and 18th centuries are presented. Detailed records for each gold-producing state are given for 1800 to 1995, as are short histories of gold explorations and strikes. Reports of gold occurrences in non-producing states are also listed.

Since 1800, 24 states in the U.S. have produced a total of more than 420 million troy ounces. California, Nevada, and South Dakota are the largest producers. During the first half of the 19th century, gold production was about 40,000 ounces/year. After the California gold rush, production rose to 2 million ounces/year, and it exceeded 4 million ounces/year shortly after 1900. Production declined to about 2 million ounces/year in the 1920s and 1930s, and to below 1 million ounces/year during World War II. Today, however, the U.S. produces more than 10 million ounces per year.

The recent production pattern has followed two important changes in gold economics and recovery. When

the U.S. went off the gold standard, the price per ounce rose from $41.51 in 1969 to over $300 in 1979. These high prices made the mining of relatively low-grade lode deposits (in terms of gold recovered per ton of ore) profitable. The growing use of the cyanidization method of gold recovery made the large-scale mining of such deposits even more feasible. As a result, the recovery grade has decreased by almost an order of magnitude since the mid-1970s. *JL*

Platinum: Synonymous with the highest quality diamonds together creating luxury jewelry. Platinum Guild and Johnson Matthey Ltd., *Mazal U'Bracha*, Vol. 15, No. 112, 1999, pp. 61–63.

The global promotion of platinum jewelry to consumer markets has increased greatly in the past few years, and platinum's success can be judged by the fact that it now surpasses gold jewelry in the high-end luxury market. The increase is largely attributed to greater sales in China and the U.S., abetted by a general increase in consumer demand for white metal, including white gold.

In 1998, China and the U.S. consumed 26% and 9%, respectively, of the platinum used in jewelry worldwide. Five years ago, both of these countries were insignificant consumers of platinum jewelry. In China, platinum advertising has been concentrated on young consumers, with retail sales dominated by simple, lightweight rings and neckchains. The focus in the U.S., meanwhile, is on the upscale bridal market and platinum accessories.

The mainstay of the platinum jewelry industry is Japan, which accounted for 54% of the world's platinum jewelry consumption in 1998 (1.29 million ounces out of a world consumption of 2.37 million ounces). Even with Japan's economic downturn and the sharp fall in luxury spending in 1998, unit sales of platinum jewelry fell only by 3%, whereas unit sales of gold items declined by 15%. Sales of platinum accessories (necklaces, bracelets, and earrings) were particularly strong, offsetting declines in the ring sector.

The platinum jewelry market in Europe is relatively small (approximately 7% of world consumption), with Germany, the U.K., and Switzerland the primary consumers; in Switzerland, watchmakers are major users of platinum. The future expansion of the platinum jewelry market will likely be in China and the U.S., which—not incidentally—are the two major centers for platinum jewelry fabrication. *AAL*

SYNTHETICS AND SIMULANTS

Fake gems pose threat to the industry. *Mining in Southern Africa*, No. 3, 1999, p. 27.

Fake uncut gems, either in massive form or as imitations of crystals, are appearing in increasing quantities in southern Africa. Two basic variations are currently encountered: (1) synthetics, some with imitation matrices; and (2) natural minerals that have been modified (e.g., by grinding to change morphology) or radically enhanced (e.g., with dyes) to pass as substitutes for more valuable gem materials. Earlier attempts at gem fraud concentrated on fake emeralds, which were usually externally dyed, morphologically modified quartz crystals or green feldspar. Today, fakes of other gems such as ruby, sapphire, tourmaline, aquamarine, amethyst, and tanzanite also are encountered.

It is likely that this problem will continue to grow, because imitations will continue to improve, especially with the advances that have been made in molding technology. Clever composites will undoubtedly replace formerly crude replicas. The best protection against such hoaxes is the well-trained gemologist, with shrewd microscopic skills and a knowledge of the morphology of different natural gem materials. *AMB*

Silica transport and growth of high-temperature crystalline quartz in supercritical aqueous fluids. V. S. Balitsky, L. V. Balitskaya, H. Ivasaki, and F. Ivasaki, *Geochemistry International*, Vol. 37, No. 5, 1999, pp. 391–396.

Silica (SiO_2) has many crystal structure phases, or polymorphs. The particular phase depends on the temperature and pressure conditions of the growth environment. The best-known example is the phase transition of low-temperature quartz (α-quartz) to high-temperature quartz (β-quartz) at 573°C.

The authors carried out the first experimental investigation of the growth and morphology of gem-quality high-temperature synthetic quartz, with particular emphasis on silica transport in supercritical aqueous fluids at different temperatures (580°–1100°C) and pressures (0.2–5 kilobars). They used aqueous solutions containing low concentrations (0.01–1 wt.%) of NaOH, K_2CO_3, NaCl, NH_4F, HF, and other compounds to change the pH from 1 to 12. In some experiments, an oxidant ($LiNO_3$) was added to solutions; oxides of those metals that most often occur as impurities in quartz (Al, P, Ti, Fe, Ge, and Be) also were added to the charge. The resulting high-temperature quartz crystals had hexagonal prismatic $\{10\bar{1}0\}$ and hexagonal bipyramidal $\{10\bar{1}1\}$ faces. The introduction of trace amounts of Fe and Ti into the solutions resulted in the formation of violet-pink in these quartz crystals. [*Abstracter's note:* GIA Research has received several of the violet-pink high-temperature quartz crystals for examination. The crystals have many fractures and inclusions; the largest measures 60 × 12 × 12 mm.] *Taijin Lu*

TREATMENTS

Colour changes produced in natural brown diamonds by high-pressure, high-temperature treatment. A. T. Collins, H. Kanda, and H. Kitawaki, *Diamond and Related Materials*, Vol. 9, No. 2, 2000, pp. 113–122.

The authors report and discuss spectral results for 14 natural brown diamonds (rough and polished) that they

HPHT-treated at 60 kbar and 1,700°–1,800°C for five hours, and for three (originally brown) yellow-green (two faceted) and green (one rough) diamonds that had been HPHT-treated by NovaDiamond of Provo, Utah, at 60 kbar and 2,025°C for approximately 30 minutes. Mid-infrared and visible–to–near-infrared absorption spectroscopy, together with low-temperature photoluminescence spectroscopy, were used to explore changes to the optical centers caused by the HPHT treatment.

One low-nitrogen sample treated by the authors changed from brown to pale yellow-brown, and the remainder became less brown and more yellow. The visible spectra of two diamonds before and after treatment showed reduction of the broad bands associated with plastic deformation that produce the brownish color, and distinct growth of the H3 center (503 nm) that both contributes to the yellow color and produces green "transmission" luminescence to visible light. The visible spectra of the commercially processed diamonds showed strong absorption at this center and also at the H2 center (a negatively charged state of the H3; 985 nm), as well as a weak sharp peak at 637 nm. In one of the commercially treated diamonds, the absorption at the H2 center was strong enough to cause some green bodycolor in the diamond. Luminescence spectra before HPHT treatment showed three peaks: 415 nm (N3), 491 nm, and 503 nm (H3). After treatment, the N3 center was somewhat stronger, the 491 nm peak was gone, and the H3 center was much stronger.

After summarizing previous work regarding the aggregation of nitrogen in diamond, the effects of radiation damage on aggregation, and the various infrared and visible centers associated with the different forms of nitrogen, the authors propose a model for the changes caused by the HPHT process. Annealing partially heals the plastic deformation, reducing the brown coloration and releasing vacancies and interstitial carbon atoms into the diamond. In a diamond with little or no nitrogen, these two defects "cancel" each other, resulting in a reduction of brown color (e.g., as in brown type IIa GE POL diamonds). In diamonds with nitrogen, vacancies are trapped at nitrogen aggregates, leading to the large increase in absorption by the H3 center. Higher annealing temperatures cause some nitrogen aggregates to break up as well, resulting in the formation of NV centers (637 nm) and the H2 center.

The paper includes a postscript describing observations before and after commercial HPHT treatment of two diamonds, one brown and one pale yellow ("Cape") stone, by NovaDiamond. The brown diamond reacted similarly to the NovaDiamond samples described above. The resulting color was yellow-green, and it showed green luminescence to visible light. The Cape diamond showed no plastic deformation before treatment, and the visible spectrum after treatment showed rising absorption toward shorter wavelengths, but no H3 or H2 centers. The resulting color was saturated yellow without green "transmission" luminescence. *PRB*

Identification of GE POL diamonds: A second step. J.-P. Chalain, E. Fritsch, and H. A. Hänni, *Journal of Gemmology*, Vol. 27, No. 2, 2000, pp. 73–78.

The authors studied 10 untreated (seven colorless, three brown) type IIa diamonds and five GE POL diamonds. On the basis of their results, they tentatively propose that GE POL diamonds can be identified using a two-step process. The first step is to determine whether the sample is type IIa; this was done by the authors using the new SSEF Type IIa Diamond Spotter, which is based on the transparency of these diamonds to short-wave ultraviolet radiation. The second step is to look for subtle luminescence features related to N-V centers in type IIa diamonds with a Raman spectrometer. When 514 nm laser excitation was used, all five of the GE POL diamonds analyzed (at room temperature) showed a luminescence peak at 3760 cm^{-1} (corresponding to 637 nm), whereas none of the seven untreated D-color type IIa diamonds showed this feature. The authors also noted the presence of 637 nm luminescence in all three of the untreated brown diamonds studied, and suggest that the presence of N-V centers in near-colorless diamonds is probably indicative of GE POL treatment. *Brendan M. Laurs*

MISCELLANEOUS

Diamonds aren't forever. *GemKey Magazine*, Vol. 2, No. 3, March/April 2000, p. 18.

When the engagement of a Pennsylvania couple was called off, the bride-to-be returned the $17,000 engagement ring. Subsequently, the couple became engaged a second time, and again the prospective groom broke it off. However, on this occasion the woman refused to return the ring. The ensuing dispute was settled by the Pennsylvania Supreme Court, which ruled that in the state of Pennsylvania, an engagement ring is a "conditional gift" and must be returned. *AAL*

The gang that loves glitter. P. Annin and J. B. Rhine, *Newsweek*, Vol. 134, No. 10, September 6, 1999, pp. 32–33.

Big-time jewelry thefts by a shadowy group of South American gangs are an escalating problem in the U.S. Although commonly referred to as "the Colombians," members come from at least five Latin American nations. The gangs consist of an estimated 2,000 thieves organized in teams of 20–30 individuals who are usually based in major cities such as Miami, New York, Chicago, and Los Angeles. However, they also move around the country, targeting gem and jewelry salespeople where they are most vulnerable: on the road. The gangs use sophisticated surveillance techniques and a repertoire of diversionary and distraction tactics.

This article describes how the thieves terrorize members of the U.S. gem and jewelry trade, particularly traveling sales representatives who carry real jewelry rather than photographs or simulants. Increasingly, violence is being used, which has resulted in 281 jewelry industry

deaths since 1984. While the FBI continues its efforts, police in the affected cities are working with the trade to alleviate the escalating problem. *AAL*

How to choose a colored gem lab. R. B. Drucker, *Jewelers Circular Keystone*, Vol. 170, No. 10, October 1999, pp. 130–132, 134.

A listing of several prominent colored gemstone laboratories is presented, along with a description of the services they offer. Each of the laboratories provides gemstone identification and a determination of both authenticity and enhancement. However, other specialized services—country-of-origin determination, the type and level of enhancement, pearl analysis, and appraisals—are not offered by all the laboratories. These capabilities are mainly a reflection of their equipment and the expertise of their staffs. Hence, jewelers should investigate the services of each laboratory and select the one that best suits their needs.

Readers are forewarned that even the major labs occasionally struggle with the identification of certain features or attributes of some colored stones. Results may be inconclusive, or conflicting reports may be received when the stone is submitted to different laboratories. In the case of important stones, a second authoritative opinion is appropriate. *AMB*

Visual clarity is the key to great jewelry slides. S. Meltzer, *The Crafts Report*, Vol. 35, No. 279, July 1999, pp. 36–37.

When jewelry images are captured on slides for the purpose of judging, the most essential aspect is image clarity. If the image does not convey the subject to the jury, other factors such as lighting, sharpness, or composition will have little impact. Five tips for achieving visual clarity when photographing crafts in general, but jewelry in particular, are:

1. Ensure that the images convey all the specific elements of an object (e.g., shoes have heels, cups have handles).
2. Keep areas of similar colors or tones separate on three-dimensional pieces. Try to move the camera and/or the lighting until one of the areas becomes lighter or darker, thereby separating the distinct areas.
3. When photographing several items, separate pieces of similar color and tone so they won't appear to be the same object.
4. Pay particular attention to the background color. The background must not distract the eye from the subject, and it must be compatible with the jewelry's colors, or lack of color.
5. Keep it simple. Jewelry looks best on plain, simple backgrounds. *MT*

The wild side of De Beers. *Australia's Paydirt*, Vol. 1, No. 48, March 1999, pp. 50, 54.

"Sustainable utilization of resources" is the slogan for De Beers's wildlife conservation policy, an aspect of the world diamond leader that is essentially unknown to most of the world. De Beers is now the largest supplier of live game animals to game reserves and game ranches throughout South Africa. The company acquired land in the 1880s to secure sites (known as "floors") on which diamond-bearing kimberlite ore could be spread out and left to weather, a common form of early diamond recovery. De Beers has since decided to protect game on such properties, where hunting is prohibited.

De Beers's Rooipoort Nature Reserve and Benfontein Ranch were declared natural heritage sites in 1985 and 1989, respectively. Rooipoort is home to antelope, giraffe, small mammals, and bird life, including the only pure Cape ostrich flock in existence. The Venetia Limpopo Nature Reserve, established in 1990, is adjacent to the Venetia diamond mine and hosts many species of plains game. Ecological and behavioral studies are being conducted on the aardwolf, springbok, springhare, black-footed cat, tortoise, sparrow-weaver, and elephant. A project to breed disease-free buffalo, now in its seventh year, is a joint enterprise between De Beers and the kwaZulu Natal Parks Board. This project is expected to have important conservation and economic benefits for wildlife. *MT*

continued from page 97

yellow in the color separations process to restore the *actual* color of the synthetic emeralds. With some films and lighting conditions, rubies turn orange, blue sapphires become tanzanites, and demantoid garnets resemble peridots. In all of these cases, we routinely correct the colors.

With regard to these particular color-change garnet photos, Ms. Tannous had indeed photographed the stone in both lighting conditions and a number of orientations. But the areas of extinction were so strong in the slide taken with incandescent light that even with color correction we did not feel we could give our readers a good representation of the color change. The editors made the decision to color correct a duplicate of the image seen with fluorescent light to show how the overall color appearance changed while other variables were held constant. We worked with the color separator, gemstone in hand, through several proofs to obtain what we felt was the closest match possible to the actual appearance in the different lighting conditions.

Our color photos are not always representative of the color in the original transparency or print. Instead, they are the best representation possible of the *actual* gem material.

Alice S. Keller
Editor